SYNTHESIS AND ANALYSIS OF Al2O3, ZnO, GO NANO PARTICLE ENHANCED DEIONIZED WATER AS A HEAT TRANSFER FLUID

S M Abul Fatha Rifat	**201636045**
MD. Rafsan Jamil	**201736016**
Prattay Saha	**201736033**

Military Institute of Science and Technology (MIST)

Department of Industrial and Production Engineering

Mirpur Cantonment, Mirpur, Dhaka - 1216

Date of submission (24 March, 2021)

SYNTHESIS AND ANALYSIS OF Al2O3, ZnO, GO NANO PARTICLE ENHANCED DEIONIZED WATER AS A HEAT TRANSFER FLUID

by

S M Abul Fatha Rifat **201636045**

MD. Rafsan Jamil **201736016**

Prattay Saha **201736033**

A Thesis

Submitted to the

Department of Industrial & Production Engineering

In Partial Fulfillment of the

Requirements for the Degree

of

BACHELOR OF SCIENCE IN INDUSTRIAL & PRODUCTION ENGINEERING

Military Institute of Science and Technology (MIST)

Department of Industrial and Production Engineering

Mirpur Cantonment, Mirpur, Dhaka-1216

CERTIFICATE OF APPROVAL

The thesis entitled as **"Al2O3, ZnO, GO Nano Particle Enhanced Heat Transfer Deionized Water Fluid"** submitted by the following students have been accepted as satisfactory in partial fulfillment of the requirement for the degree of B.Sc. in Industrial and Production Engineering on **24 March, 2021**.

S M Abul Fatha Rifat	**201636045**
MD. Rafsan Jamil	**201736016**
Prattay Saha	**201736033**

Name of the Supervisor

Dr. Muammer Din Arif
Assistant Professor
Department of Industrial and Production Engineering
Military Institute of Science and Technology
Dhaka-1208, Bangladesh

Name of the Examiner

Dr. Abdullahil Kafy
Assistant Professor

Muzahid Khan
Lecturer

Department of Industrial and Production Engineering

Military Institute of Science and Technology

DECLARATION OF CANDIDATE

It is hereby declared that this thesis or any part of it has not been submitted elsewhere for the award of any degree or diploma.

S M Abul Fatha Rifat	**201636045**
MD. Rafsan Jamil	**201736016**
Prattay Saha	**201736033**

ACKNOWLEDGEMENT

Our thesis would be incomplete without thanking some people. We would like to acknowledge the people who helped and supported us throughout the report writing process. First and foremost, we would like to convey sincere gratitude to our thesis supervisor, Assistant Professor**, Dr. Muammer Din Arif**. He has helped us in developing and clarifying our concepts on thesis by providing us their valued teaching. We also express our heartful gratitude to **Dr. Gafur sir** for his selfless guidance and support in BCSIR labs. We would also like to pay solemn gratitude to all the persons who provided us with the necessary information. Finally, we would like to thank our classmates for their continuous support and encouragement.

Authors

ABSTRACT

Metal is a very good thing to get a good heat transfer, when we shift into nanoparticle making nanofluid, we found that nanofluid have tremendous thermal properties for enhancing the heat transfer coefficient. We have prepared different nanofluid samples at different volume concentration of alumina (.1g, .2g,.3g,.4g,.5g), Zinc Oxide concentration of (.1g,.2g,.3g,.4g), graphene Oxide concentration of (.1g,.3g,.5g) by magnetic stirring and use deionized water as a base fluid. We disperse the nanofluid by ultrasonication. We measure the heat coefficient in a vertical shell and tube and in the heat exchanger copper tube is used. Viscosity data is taken from HAAKE machine which model no is D-78227.Our experiment is done under the laminar condition. We found that our heat transfer coefficient is increasing of nanofluids. Graphene nanofluid gives the best heat transfer coefficient. We also use linear regression, SVR model to predict the heat coefficient.

TABLE OF CONTENTS

Topic **Page No.**

CERTIFICATE OF APPROVAL ii
DECLARATION OF CANDIDATE iv
ABSTRACT vi
TABLE OF CONTENTS vii
LIST OF TABLES xi
LIST OF FIGURES xii
NOMENCLATURE xvi
Chapter 1 ..... - 1 -
INTRODUCTION ..... - 1 -
1.1. Background ..... - 1 -
1.2. Nanofluid Concept ..... - 2 -
1.2.1. Introduction ..... - 2 -
1.2.2. Particle Material and Base Fluid ..... - 2 -
1.2.3. Particle Size ..... - 3 -
1.2.4. Particle Shape ..... - 3 -
1.3. Thermal Conductivity of Nanofluids ..... - 3 -
1.4. Research Goals and Objectives: ..... - 5 -
1.5. Future-Scope: ..... - 5 -
Chapter 2 ..... - 6 -

Literature review ..... - 6 -
2.1. Introduction..... - 6 -
2.2. Heat Transfer Enhancement ..... - 6 -
2.2.1. Application of CuO (Copper Oxide) Nano-particles ..... - 6 -
2.2.2. Application of ZnO(Zinc Oxide):..... - 10 -
2.2.3. Application of CNT and GO (Graphene Oxide): ..... - 10 -
2.2.4. Application of titanium dioxide: ..... - 11 -
2.2.5. Application of Metal Oxide mixtures: ..... - 12 -
2.2.6. Application of Hybrid Nanofluid:..... - 13 -
2.2.7. Application of Aluminum Oxide:..... - 13 -
2.3. Summary ..... - 15 -
Chapter 3..... - 16 -
Methodology ..... - 16 -
3.1 Overview..... - 16 -
3.2. Experimental tools:..... - 16 -
3.3 Required chemicals: ..... - 16 -
3.4 Other component detail: ..... - 17 -
3.5 Preparation of nanofluids:..... - 19 -
3.6 Dispersibility test: ..... - 19 -
3.7 Ultrasonication:..... - 20 -
3.8 Measuring the Heat Transfer Co-efficient:..... - 21 -
3.9 Viscosity Measurement: ..... - 23 -
Chapter 4..... - 24 -
Result and Discussion ..... - 24 -
4.1.1. Heat Transfer Coefficient Measurement of Alumina Solution:..... - 24 -
4.1.1.2 0.1% alumina solution: ..... - 24 -
4.1.1.3 0.2% Alumina Solution:..... - 30 -
4.1.1.4 0.3% Alumina Solution:..... - 36 -
4.1.1.5 0.4% Alumina Solution:..... - 42 -

4.1.1.6. 0.5% Alumina Solution:..... - 48 -
4.1.1.7. Heat Transfer Co-efficient of Alumina Solution:..... - 54 -
4.1.2. Heat Transfer Coefficient Measurement of Zinc Oxide Solution:.. - 55 -
4.1.2.1. 0.1% Zinc Oxide Solution..... - 55 -
4.1.2.2 0.2% Zinc Oxide Solution:..... - 61 -
4.1.2.3. 0.3% Zinc Oxide Solution:..... - 67 -
4.1.2.4. 0.4% Zinc Oxide solution: ..... - 72 -
4.1.2.5. Heat Transfer Coefficient of Zinc Oxide Solution: ..... - 79 -
4.1.3. Heat Transfer Coefficient Measurement Of Graphene Oxide Solution: ..... - 79 -
4.1.3.1. 0.1% Graphene Oxide Solution: ..... - 79 -
4.1.3.2 0.3% Graphene Oxide Solution: ..... - 85 -
4.1.3.3. 0.5% Graphene Oxide Solution: ..... - 91 -
4.1.3.4. Heat Transfer Coefficient Of Graphene Oxide Solution:..... - 97 -
4.2.1. Viscosity measurement of Alumina Solution:..... - 98 -
4.2.1.1. 0.1% Alumina Solution :..... - 98 -
4.2.1.2. 0.2% Alumina Solution:..... - 101 -
4.2.1.3. 0.3% Alumina Solution:..... - 105 -
4.2.1.4. 0.5% Alumina Solution:..... - 108 -
4.2.1.4. Viscosity Properties of Alumina Solution: ..... - 112 -
4.2.2. Viscosity measurement of Zinc Oxide Solution:..... - 113 -
4.2.2.1. 0.1% Zinc Solution:..... - 113 -
4.2.2.2. 0.2% Zinc Solution:..... - 117 -
4.2.2.3. 0.3% Zinc Solution:..... - 120 -
4.2.2.4. 0.4% Zinc Solution:..... - 124 -
4.2.2.5. Viscosity Properties of Zinc Oxide Solution: ..... - 128 -
4.2.3. Viscosity measurement of Graphene Oxide Solution: ..... - 129 -
4.2.3.1. 0.1% Graphene Oxide Solution: ..... - 129 -
4.2.3.2. 0.3% Graphene Oxide Solution: ..... - 132 -

4.2.3.3. 0.5% Graphene Oxide Solution: ..... - 135 -
4.3. Overall result in Heat Transfer Co-efficient: ..... - 139 -
4.4. Limitations: ..... - 140 -
Chapter 5 ..... - 141 -
Conclusion ..... - 141 -
References ..... - 142 -

LIST OF TABLES

Table No.	Table Title	Page No.
Table 1.1	**Conductivity values for different solids and liquids (metallic and non-metallic)**	4

LIST OF FIGURES

Figure No.	Figure Title	Page No.
Fig.3.1	Magnetic stirrer with hot plate	17
Fig.3.2	Micro Oven	18
Fig.3.3	Stirring Operation	19
Fig.3.4	0.2% Alumina Solution after a day.	19
Fig.3.5	During Ultrasonication	20
Fig.3.6	Ultrasonication Device	20
Fig.3.7	Experimental setup for the measurement of forced convective heat transfer coefficient of nanofluids.	21
Fig.3.8	Heat Transfer Coefficient Measuring Machine	22
Fig.3.9	K-type thermocouple	22
Fig.3.10	Viscosity Measuring Machine	23
Fig.4.1	Fitted Line Plot for 0.1% Alumina Solution.	26
Fig.4.2	Residual Plots for 0.1% Alumina Solution	28
Fig.4.3	Support Vector Regression Model by using ML for 0.1% Alumina Solution	30
Fig.4.4	Simple Linear Regression Model by using ML for 0.1% Alumina Solution	30
Fig.4.5	Fitted Line Plot for 0.2% Alumina Solution.	32
Fig.4.6	Residual Plots for 0.2% Alumina Solution	34
Fig.4.7	Support Vector Regression Model by using ML for 0.2% Alumina Solution	36
Fig.4.8	Simple Linear Regression Model by using ML for 0.2% Alumina Solution	36
Fig.4.9	Fitted Line Plot for 0.3% Alumina Solution.	38
Fig.4.10	Residual Plots for 0.3% Alumina Solution	40

Fig no	Figure Title	page no
Fig.4.11	Support Vector Regression Model by using ML for 0.3% Alumina Solution	42
Fig.4.12	Support Vector Regression Model by using ML for 0.3% Alumina Solution	42
Fig.4.13	Fitted Line Plot for 0.4% Alumina Solution.	44
Fig.4.14	Residual Plots for 0.4% Alumina Solution	46
Fig.4.15	Support Vector Regression Model by using ML for 0.4% Alumina Solution	48
Fig.4.16	Simple Linear Regression Model by using ML for 0.4% Alumina Solution	48
Fig.4.17	Fitted Line Plot for 0.5% Alumina Solution.	50
Fig.4.18	Residual Plots for 0.5% Alumina Solution	52
Fig.4.19	Support Vector Regression Model by using ML for 0.5% Alumina Solution	54
Fig.4.20	Simple Linear Regression Model by using ML for 0.5% Alumina Solution	54
Fig.4.21	Heat Transfer Co-efficient Bar-chart of Alumina Solution	55
Fig.4.22	Fitted Line Plot for 0.1% Zinc Oxide Solution.	57
Fig.4.23	Residual Plots for 0.1% Zinc Oxide Solution	59
Fig.4.24	Support Vector Regression Model by using ML for 0.1% Zinc Oxide Solution	61
Fig.4.25	Simple Linear Regression Model by using ML for 0.1% Zinc Oxide Solution	61
Fig.4.26	Fitted Line Plot for 0.2% Zinc Oxide Solution.	63

Fig.4.27	Residual Plots for 0.2% Zinc Oxide Solution	65
Fig.4.28	Support Vector Regression Model by using ML for 0.2% Zinc Oxide Solution	67
Fig.4.29	Simple Linear Regression Model by using ML for 0.2% Zinc Oxide Solution	68
Fig.4.30	Fitted Line Plot for 0.3% Zinc Oxide Solution.	70
Fig.4.31	Residual Plots for 0.3% Zinc Oxide Solution	72
Fig.4.32	Support Vector Regression Model by using ML for 0.3% Zinc Oxide Solution	73
Fig.4.33	Simple Linear Regression Model by using ML for 0.3% Zinc Oxide Solution	73
Fig.4.34	Fitted Line Plot for 0.4% Zinc Oxide Solution.	75
Fig.4.35	Residual Plots for 0.4% Zinc Oxide Solution	77
Fig.4.36	Support Vector Regression Model by using ML for 0.4% Zinc Oxide Solution	79
Fig.4.37	Simple Linear Regression Model by using ML for 0.4% Zinc Oxide Solution	79
Fig.4.38	Heat Transfer Co-efficient Bar-chart of ZnO Solution	80
Fig.4.39	Fitted Line Plot for 0.1% Graphene Solution.	82
Fig.4.40	Residual Plots for 0.1% Graphene Solution	84
Fig.4.41	Support Vector Regression Model by using ML for 0.1% Graphene Solution	85
Fig.4.42	Simple Linear Regression Model by using ML for 0.1% Graphene Solution	86
Fig.4.43	Fitted Line Plot for 0.3% Graphene Solution.	88
Fig.4.44	Residual Plots for 0.3% Graphene Solution	90
Fig.4.45	Simple Linear Regression Model by using ML for 0.3% Graphene Solution	91
Fig.4.46	Support Vector Regression Model by using ML for 0.3% Graphene Solution	92

Fig.4.47	Fitted Line Plot for 0.5% Graphene Solution.	94
Fig.4.48	Residual Plots for 0.5% Graphene Solution	96
Fig.4.49	Support Vector Regression Model by using ML for 0.5% Graphene Solution	97
Fig.4.50	Simple Linear Regression Model by using ML for 0.5% Graphene Solution	97
Fig.4.51	Heat Transfer Co-efficient Bar-chart of Graphene Solution	98
Fig.4.52	Residual Plots for 0.1% Alumina Solution	99
Fig.4.53	Fitted Line Plot for 0.1% Alumina Solution	101
Fig.4.54	Residual Plots for 0.2% Alumina Solution	103
Fig.4.55	Fitted Line Plot for 0.2% Alumina Solution	105
Fig.4.56	Residual Plots for 0.3% Alumina Solution	106
Fig.4.57	Fitted Line Plot for 0.3% Alumina Solution	108
Fig.4.58	Residual Plots for 0.5% Alumina Solution	110
Fig.4.59	Fitted Line Plot for 0.5% Alumina Solution	112
Fig.4.60	Viscosity Bar-chart of Alumina Solution	113
Fig.4.61	Residual Plots for 0.1% Zinc Oxide Solution	115
Fig.4.62	Fitted Line Plot for 0.1% Zinc Oxide Solution	117
Fig.4.63	Residual Plots for 0.2% Zinc Oxide Solution	118
Fig.4.64	Fitted Line Plot for 0.2% Zinc Oxide Solution	120
Fig.4.65	Residual Plots for 0.3% Zinc Oxide Solution	122
Fig.4.66	Fitted Line Plot for 0.3% Zinc Oxide Solution	124
Fig.4.67	Residual Plots for 0.1% Zinc Oxide Solution	126
Fig.4.68	Fitted Line Plot for 0.4% Zinc Oxide Solution	128
Fig.4.69	Viscosity Bar-chart of ZnO Solution	129
Fig.4.70	Residual Plots for 0.1% Graphene Solution	130
Fig.4.71	Residual Plots for 0.3% Graphene Solution	134
Fig.4.72	Residual Plots for 0.5% Alumina Solution	136
Fig.4.73	Viscosity Bar-chart of Graphene Solution	139
Fig.4.74	Overall result in Heat Transfer Co-efficient	140

NOMENCLATURE

Symbol	Description
NP	Nano particle
D	Diameter
L	Length
Δ	Difference
ρ	Density
Cp	Specific heat
μ	Viscosity
f	Friction factor
V	Volume concentration

CHAPTER 1

INTRODUCTION

1.1. Background

In the past decade technology has made a revolutionary change of all sector of industry. To achieve better results by minimizing losses increases efficiency by adding new properties. Researchers have discovered the benefit of nanotechnology in their respective field. Heat transfer is also an important issue that has taken into account for most present industrial processes. Traditional coolants like water, oils and ethylene glycol have limitations regarding to increasing the heat transfer capability. These liquids have constant values for their thermo-physical properties. So, for improving their heat transfer features has to be done through the device, that is to say, through augmenting the heat exchange area or the flow rates of coolants. As a result, nanotechnology has appeared as an option to fix heat exchange transfer demands at industrial scale. So, there is a growing thought that considers this demand can be fulfilled through the usage of nanofluids. Nanofluids are homogeneous mixtures of solids and liquids when these solid particles are smaller than 100 nm. These added solid particles are supposed to improve thermophysical properties and heat transfer behavior of its base fluid. Moreover, as was said, traditional coolants are an option to be improved from thermo-physical view point in order to cover the needs of refrigeration in electronic systems; because of that, nanofluids are expected to fill this gap. We use nanoparticle to enhance heat transfer of a system in this research work with production, characterization and validation by experiments.

1.2. Nanofluid Concept

1.2.1. Introduction

The idea of suspending nanoparticles in a base liquid for improving thermal conductivity has been proposed recently and such suspension of nanoparticles in a base fluid is called a nanofluid. Mainly, the nanofluid consists of two parts: nanoparticle and base fluid.
The main important parameters affect nanofluids behaviors are particle size, concentration and shape, nanoparticle material, base fluid nature & pH-value of dilution.
Due to their small size, nanoparticles fluidize easily inside the base fluid, and as a consequence, clogging of channels and erosion in channel walls are no longer a problem. It is even possible to use nanofluids in microchannels. When it comes to the stability of the suspension, it was shown that sedimentation of particles can be prevented by utilizing proper dispersants.

1.2.2. Particle Material and Base Fluid

Many different particle materials are used for nanofluid preparation. Al2O3, CuO, TiO2, SiC, TiC, Ag, Au, Cu, and Fe nanoparticles are frequently used in nanofluid research. Carbon nanotubes are also utilized due to their extremely high thermal conductivity in the longitudinal (axial) direction. Base fluids mostly used in the preparation of nanofluids are the common working fluids of heat transfer applications; such as, water, ethylene glycol and engine oil. In order to improve the stability of nanoparticles inside the base fluid, some additives are added to the mixture in small amounts.

1.2.3. Particle Size

Nanoparticles used in nanofluid preparation usually have diameters below 100 nm. Particles as small as 10 nm have been used in nanofluid research. When particles are not spherical but rod or tube-shaped, the diameter is still below 100 nm, but the length of the particles may be on the order of micrometers. It should also be noted that due to the clustering phenomenon, particles may form clusters with sizes on the order of micrometers.

1.2.4. Particle Shape

Spherical particles are mostly used in nanofluids. However, rod-shaped, tube-shaped and disk-shaped nanoparticles are also used. On the other hand, the clusters formed by nanoparticles may have fractal-like shapes.

1.3. Thermal Conductivity of Nanofluids

The thermal conductivity of nanofluids shows that high enhancements of thermal conductivity can be achieved by using nanofluids. It is possible to obtain thermal conductivity enhancements larger than 20% at a particle volume fraction smaller than 5%. Such enhancement values exceed the predictions of theoretical models developed for suspensions with larger particles. This is considered as an indication of the presence of additional thermal transport enhancement mechanisms of nanofluids.

Enhancement of thermal conductivity is because of the enormous thermal conductivity of solid particles, which usually are hundred or even thousand times larger than traditional base fluids, as can be seen in Table 1.

Table 1.1 Conductivity values for different solids and liquids (metallic and non-metallic)

Solid / Liquids	Material	Thermal Conductivity (W/mK)
Metallic solids	silver	429
	copper	401
	Aluminum	237
Non-metallic solids	Diamond	3300
	Carbon nanotubes	3000
	Silicon	1458
	Alumina (Al2O3)	40
Metallic liquids	Sodium @644K	72.3
Non-metallic liquids	Water	0.613
	Ethylene glycol	0.253
	Engine oil	0.145

1.4. Research Goals and Objectives:

This thesis is about preparation, stability analysis, characterization and subsequent experimental validation of experimental thermal properties like thermal conductivity and viscosity of nanofluid coolant. In addition to the evaluation of different nanofluids behavior tested in a test section, which simulates a microelectronic pipe. The aim of this thesis is to measure thermal conductivity and viscosity of nanofluids in a small microtube in order to evaluate their heat transfer performance based on different criteria. The objectives of this research project are given below:

- To prepare a working convective heat transfer nanofluids composed of Al2O3, ZnO, GO using base fluid deionized water.
- To characterize the NF and examine its morphology
- To see the dispersibility of our prepared nanofluid
- To measure the Heat coefficient of the nanofluid
- To see the viscosity property of our nanofluid
- To predict the heat coefficient of nanofluid with different algorithm

1.5. Future-Scope:

- To prepare a working convective heat transfer nanofluids composed of Al2O3, ZnO, GO using base fluid deionized water.
- To characterize the NF and examine its morphology
- To see the dispersibility of our prepared nanofluid
- To measure the Heat coefficient of the nanofluid
- To see the viscosity property of our nanofluid
- To predict the heat coefficient of nanofluid with different algorithm

CHAPTER 2

Literature review

2.1. Introduction

The exhaustive literature review of similar studies helped to grasp the advances in the field and to identify research gaps for the current work. By examining the strengths and weaknesses of existing research, we can thus make sure we adopt the most appropriate methods, data sources and analytical techniques for your own work.

2.2. Heat Transfer Enhancement

In our present world, nanofluid has played a great role for enhancing heat transfer. Once we used metals for enhancing heat transfer, but using nanofluid is a great revolution in that field. That is why people are doing a lot of research to get a better thermal conductivity, thermal stability & viscosity.

2.2.1. Application of CuO (Copper Oxide) Nano-particles

(Senthilraja & Vijayakumar 2013*)* had discussed the convective heat transfer coefficient of a CuO/water nanofluid in this paper. For this experiment, they used a double pipe parallel flow heat exchanger. The nanofluid was prepared by dispersing CuO (27nm) particles in deionized water. In the result section, we can see that the convective heat transfer coefficient increased with an increasing Reynolds number and also the Nusselt number increased with an increasing Reynolds number.

(Jesumathy et al., 2011) had discussed the studies conducted on phase transition times, heat fraction as well as heat transfer characteristics of paraffin wax as phase change material (PCM)

embedded with CuO nanoparticles. The experimental setup consists of a cylindrical tube, a high temperature bath, a low temperature bath, an electrical heating rod, K-type thermocouples, HP data logger and a Pentium III PC. It was found that nanoparticles enhanced PCM is best suited in concentric double pipe heat storage system because it achieves the best performance with no subcooling during discharge. The heat transfer coefficient during solidification was increased about 78% for the maximum flow rate with 10 wt% copper oxide enhanced PCM than pure paraffin wax. The paper provides a strategy for achieving high thermal conductivity and good heat storage properties by addition of small amount copper oxide nanoparticles to pure paraffin wax in PCM systems.

(Manimaran et al., 2012) had discussed the preparation of Copper oxide nanofluid by single-step wet chemical precipitation method. They used deionized water as base fluid. The particles were characterized by X-ray Diffraction (XRD) for structural determination. X-ray Fluorescence (XRF) was carried out using the Bruker. The thermo gravimetric analysis was carried out to confirm the thermal stability of the nanoparticle and it showed the thermo gravimetric analysis image of the copper oxide sample. The thermal conductivity of CuO nanofluid was measured using a KD2 Pro thermal property analyzer. The average size of the nanoparticle was found to be 20 nm which is calculated using De-Scherrer formula.

(Meenakshi & Sudhan2015) had synthesized three different concentrations 1%, 3% and 5% of copper oxide nanofluids. These synthesized nanofluids were characterized by Fourier transform infrared spectroscopy (FT-IR), transmission electron microscope (TEM), energy dispersive spectroscopy (EDS) and x-ray diffraction (XRD) techniques. From the FT-IR analysis of the synthesized nanofluids the structure of the copper oxide nanofluids was ascertained. TEM analysis was observed that the copper oxide particles are spherical in shape. The XRD analysis carried out on the copper oxide nanoparticles showed the crystalline nanometric phases of copper oxide nanoparticles. Viscosity increases by increasing the particle volume concentration of nanofluids. The average kinetic energy or energy of motion of the nanoparticles increases with temperature and hence the rate at which heat is transferred in the nanofluid also increases.

Hence it could be concluded that the copper oxide nanofluids prepared can be effectively used as coolants for automobile and heat transfer applications.

(Joseph et al., 2019) had discussed on developing of nano-CuO coating by using the sol-gel dip coating technique for heat transfer enhancement of a stainless steel. Morphological and structural characteristics of the coating, all are taken by using the SEM and X-Ray Diffraction apparatus. The heat transfer coefficient increased with an increase in porosity, roughness and decrease in wettability of the boiling surface. The CuO sol was the most notable specification impacting the heat transfer coefficient while sintering temperature was the least notable specification.

Mainly, their focus was on sol-gel derived nano structured CuO film to augment the pool boiling heat transfer coefficient. There is a decrease in grain size together with an increase in porosity, roughness and hydrophobicity which was found to enhance the boiling heat transfer rate. There is a decent increase in porosity, and an increase in contact angle of the nano-CuO coated boiling surface makes a tenfold increase in nucleation site density which in turn favored higher heat transfer coefficient values. The evaluated model using ANOVA revealed that the molar concentration had the highest influence in enhancing the heat transfer coefficient followed by dipping time and sintering temperature.

(Jesumathy et al., 2012) had discussed that paraffin wax has low thermal conductivity and not able to provide good output on enhancing energy storage applications. That's why some methods have been conducted to enhance heat transfer properties in the PCMs, including impregnations of porous material, dispersion of high thermal conductivity particles in the PCM, and placing the metal structure in PCM. Besides, the addition of copper oxide nanoparticles into the paraffin wax augments not only the conduction but also the natural convection very beneficially in synthesis and in paraffin wax.

(Luna et al., 2015) had discussed on measuring the forced convective heat transfer coefficient of low volume fraction CuO-PVA nanofluids under laminar flow and a constant heat flux condition by using a vertical shell-and-tube heat exchanger and XRD and SEM synthesizes CuO nanoparticles through chemical route and by their characterization. Generally, metal or metal oxide significantly ameliorate the thermal conductivity of the nanofluid and increased the coefficients of conduction and convection but Copper oxide nanofluid shows the ameliorated thermal stability and thermal conductivity when we went onto the comparing with other fluids. Besides, it could be beneficial for versatile heat transfer and thermal applications to get a vital development in the area of nanofluid or nanogel heat transfer.

(Luna et al., 2015) had discussed the preparation of CuO-PVA nanofluids using the two-step technique. One was using Copper oxide nanoparticles (CuO-NPs) by chemical precipitation method and another one was by dispersing CuO NPs in 4 wt% PVA solution using ultrasonication and magnetic stirring. The highly pure, crystalline and nanosized samples were showed by the X-ray diffraction (XRD) pattern of CuO-NPs. The thermal stability and weight loss of the CuO NPs were studied by using Thermogravimetric Analysis (TGA) and Differential Thermal Analysis (DTA). There, we got an increase in the concentration of nanofluid by showing the experimental result and also from the viscosity data, we got that the viscosity of nanofluids increases with an increase in concentration and decreases with an increase in temperature. We got a highly crystalline, pure and nanosized sample from chemical precipitation method. CuO-PVA nanofluid prepared in this experiment was very much satisfactory for convective heat transfer and fluid flow and also can be successfully done for heat transfer management systems in industrial applications.

(Zhou, 2003) had discussed the heat transfer characteristics of copper nanofluids with and without acoustic cavitation were investigated experimentally. The effects of such factors as acoustical parameters, nanofluid concentration and fluid subcooling on heat transfer enhancement around a heated horizontal copper tube were discussed in detail. The results indicated that the copper nanoparticles and acoustic cavitation had profound and significant influence on heat transport in the fluid. The addition of copper nanoparticles did not change the dependence of heat transfer on acoustic cavitation and fluid subcooling. The mechanism of heat transfer enhancement of the nanofluids was analyzed. Here The objective was to investigate the effects of acoustical parameters, nanofluid concentration and fluid subcooling on heat transfer characteristics around a heated horizontal copper tube. The results of this study will provide a better mechanism understanding of heat transfer enhancement of the nanofluids and hence accelerate its practical application.

(Sheikholeslami & Sadoughi, 2018) had discussed the impact of melting heat transfer on nanofluid heat transfer enhancement in presence of magnetic field was simulated. Innovative numerical approach is utilized namely CVFEM. KKL model was taken into account to obtain properties of CuO- water nanofluid. Roles of melting parameter, CuO-water volume fraction, Hartmann and Rayleigh numbers were demonstrated in outputs. Results depicted that temperature gradient augments with rise of melting parameter and Rayleigh number. Nusselt number detracts with rise

of Lorentz forces. At higher concentrations, nanofluid had greater merit to be used for heat transfer enhancement.

This intends of this paper was to report the impact of melting heat transfer on free convection of ferrofluid in presence of Lorentz forces. CVFEM is selected to find the outputs.

(Sheikholeslami et al., 2014) had discussed that Magnetic field effect on CuO–water nanofluid flow and heat transfer in an enclosure which was heated from below was investigated. Lattice Boltzmann method was applied to solve the governing equations. The effective thermal conductivity and viscosity of nanofluid are calculated by KKL (Koo–Klein strewer–Li) correlation. In this model effect of Brownian motion on the effective thermal conductivity was considered. Effect of active parameter such as: Hartmann number, heat source length, nano particle volume fraction and Rayleigh number son the flow and heat transfer characteristics had been examined. The result reveal that the enhancement in heat transfer increased as Hartmann number and heat source length increase but it decreased with increase of Rayleigh number. Also, it can be found that effect of Hartmann number and heat source length was more pronounced at high Rayleigh number.

2.2.2. Application of ZnO(Zinc Oxide):

(Yang et al.,2019) had found that Zinc oxide as a nanoparticle to get the better thermal performance of SAE 50 engine oil. Besides, SAE 50 engine oil played a great role as a base fluid to get better thermal stability.

The thermal conductivity of this coolant was based on temperature and volume fraction. The better thermal performance, we get at higher temperatures. But, the overall better thermal performance of conductivity and stability, we find at a particular point of temperature and volume fraction.

2.2.3. Application of CNT and GO (Graphene Oxide):

(Park & Kim 2013) had studied the heat-transfer enhancing utility of the heat pipe in a solar collector, the present work attempted to improve nanoparticle dispersion stability by means of a chemical reformation process wherein nanofluid is formulated with hydroxyl radicals combined with oxidized multi-walled CNTs (MWCNTs). Experiments entailing measurements of thermal conductivity and viscosity in distilled

water as functions of temperature were carried out to determine the best nanoparticle mixture ratio. The thermal conductivity increased with the increasing volumetric ratio of the oxidized MWCNTs and with increasing temperature. The viscosity also increased, slowly, until its concentration reached 0.01%, and then steeply increased, and was lower at high temperature.
Here the length of the carbon nanotube particle influences the thermal conductivity of nanofluids: that is, particles of longer length offer a superior, and excellent, thermal conductivity increase effect.

(Fares et all,2020) experimental investigated the effects of graphene nanofluids on the convective heat transfer in a vertical shell and tube heat exchanger. Graphene flakes were prepared using graphite foam that is derived from sugar as a raw material. The prepared Graphene flakes have been characterized using scanning electron microscopy, X-ray diffraction, atomic force microscopy, and Raman spectroscopy. The graphene nanofluid has been used in the tube side of the heat exchanger to enhance its heat transfer performance. Different parameters such as nanofluids' concentration, flow rate and inlet temperature were studied and their effects on heat transfer coefficient and thermal efficiencies are discussed. The results show that using of graphene/water nanofluids enhances the thermal performance of the vertical shell and tube heat exchanger. A maximum increase in the heat transfer coefficient of 29% was achieved using 0.2% graphene/water nanofluids. Furthermore, the mean thermal efficiency of the heat exchanger was enhanced by 13.7% by using graphene/ water nanofluid.

2.2.4. Application of titanium dioxide:

(He et al., 2006) have found that TiO2 nanofluids with different particle (agglomerate) sizes and concentrations are formulated and measured for their static thermal conductivity. The nanofluids were then measured for their heat transfer and flow behavior upon flowing upward through a vertical pipe in both the laminar and turbulent flow regimes. Addition of nanoparticles into the base liquid enhances the thermal conduction. Rheological measurements show that the shear viscosity of nanofluids decreases first with increasing shear rate, and then approaches a constant at a shear rate greater than _100 s_1. Given the flow Reynolds number and particle size, the convective heat transfer coefficient increases with nanoparticle concentration in both the laminar and turbulent flow regimes and the effect of particle concentration seems to be more considerable in the turbulent flow regime. The results also show that the pressure drop of the nanofluid flows was very close to that of the base liquid flows for a given Reynolds

number.

Here the small effect of particle size on the convective heat transfer coefficient could be due to particle migration. Also, some deviation occurs at high Reynolds numbers possibly due to the entrance effect. More work was clearly required to validate various explanations put forward for the marginal effect of particle size and deviation from the theory for the pressure drop at relatively high Reynolds numbers

2.2.5. Application of Metal Oxide mixtures:

(Abu-Nada et al., 2008) had found that Heat transfer enhancement in horizontal annuli using nanofluids was investigated. Water-based nanofluid containing various volume fractions of Cu, Ag, Al2O3 and TiO2 nanoparticles were used. For high values of Rayleigh number and high L/D ratio, nanoparticles with high thermal conductivity cause significant enhancement of heat transfer characteristics. On the other hand, for intermediate values of Rayleigh number, nanoparticles with low thermal conductivity cause a reduction in heat transfer. For Ra=103 and Ra=105 the addition of Al2O3 nanoparticles improves heat transfer nanoparticles with low thermal conductivity cause a reduction in heat transfer.

Here the Problem is only one half of the annulus was simulated. The annulus between the two cylinders was filled with water based nanofluid.

This paper had been found that the two nanoparticles of Aluminum Oxide and Copper Oxide are used and water plays as a role of the base fluid. The used of Al2O3 gave a great output and enhances more thermal conductivity than Copper Oxide. Dispersion of the Nanoparticles of Aluminum Oxide and Copper Oxide into the water actually augments the heat transfer coefficient by increasing the flow rate of the fluid and by using the high concentrated nanoparticles. Water, ethylene glycol & oil were the traditional heat transfer fluids. But they were actually immanently poor-performing heat transfer fluids. It could be better to use the metallic liquid as a base fluid for better enhancement of heat transfer (Naseema et al., 2017).

(Zamzamian et al., 2010) had discussed that, nanofluids of aluminum oxide and copper oxide were prepared in ethylene glycol separately. A double pipe and plate heat exchangers were used to calculate the effect of forced convective heat transfer coefficient in turbulent flow. In both heat exchangers, heat transfer was considerably enhanced for nanofluids compared to the base fluid. In double pipe heat exchanger, this enhancement was maximally 26% for 1.0% weight aluminum oxide in ethylene glycol and 37% for 1.0% weight copper oxide in ethylene glycol. In the plate heat exchanger, these figures were 38% and 49%, respectively.

However, both theoretical and experimental data suggest that homogenously dispersed and stabilized

nanoparticles enhance the forced convective heat transfer coefficient of the base fluid significantly. The greatest and smallest increased in this experiment were 49% and 3%, respectively.

This paper investigated that laminar flow heat transfer enhancement in circular tube utilizing different nanofluids including Al2O3 (20 nm), CuO (50 nm), and Cu (25 nm) nanoparticles in water and the result was satisfactory. They used a stabilizer, a dispersant, a surface activator, and an ultrasonic vibrator to produce suitable nanofluid. The experimental system designed for this study consisted of a flow loop containing several sections such as temperature, pressure and flow rate measuring units, heating and cooling sections, and a flow controlling system. Again, they used 10 k-type thermocouples in the setup. They found nanofluids that contain metal nanoparticles (Cu/water) show more enhancement compared to oxide nanofluids (Al2O3/water and CuO/water). Also, CuO/water nanofluid presents less enhancement in heat transfer coefficient at the same Peclet number and nanoparticle concentration. It is related to large particle size and high viscosity CuO and high thermal conductivity of Cu nanofluid.
From this paper we came to know that the nanofluids convective heat transfer coefficient enhancement is not only due to the increase of thermal conductivity but also other factors such as nanofluid viscosity, dispersion, chaotic movement of nanoparticles, Brownian motion, particle migration, fluctuation, and interaction between particles especially in high Peclet numbers (Heris et al., 2010).

2.2.6. Application of Hybrid Nanofluid:

(Bhattad et al., 2019) had found that the different combinations of Al2O3 hybrid nanofluids (Al2O3– SiC, Al2O3–AlN, Al2O3–MgO, Al2O3–CuO and Al2O3–MWCNT) can have better performence as a coolant. Among them, Al2O3–MWCNT gives a great thermal enhancing performance and gave a better output as a coolant. This paper had been investigated that bio-lubricants such as vegetable oil, paraffin oil and SAE oil which is reliable, durable & efficient was used as a base fluid and the thermal properties of the bio-lubricants are enhanced by the inclusion of Cu–Zn (50:50) hybrid nanoparticle. There, we got an enhancement in thermal conductivity of the hybrid nanofluids with an increase in volume concentrations in all type of oils. Among the oils, we get a better result by using vegetable oil. It showed less thermal stability but the thermal conductivity's great by using vegetable oil (Kumar et al., 2016).

2.2.7. Application of Aluminum Oxide:

(Salari et al., 2016) had discussed that Nanofluids are prepared by dispersing the alumina nanoparticles into the deionized water. For more details and better results, the experiment had been operated by two

phases. First one is called short-time study, mainly focused on enhancing the heat transfer coefficient of nanofluids and increased by increasing the heat and mass fluxes and concentration of nanofluids as well and also by decreasing the nanoparticle size.
Another one is called the extended study, mainly focused on enhancing the heat transfer coefficient of nanofluids by using the parameters of the roughness of the surface, lower contact angle, the number of nucleation sites.

This paper had been found that they experimentally investigate the natural convection behavior of Nanoparticle Enhanced Ionic Liquid (NEILs) formulating with spherical and whiskers Al2O3 nanoparticles into N-butyl-N-methyl pyrrolidinium bis{(trifluoromethyl)sulfonyl} imide, ([C4mpyrr][NTf2]) ionic liquid. They used Pycnometer to measure the density of base IL and NEILs. The results showed that the density of base IL and NEILs decreases with temperature within the measured temperature 283–343 and so the NEILs has higher density compared to the base IL because of high density Al2O3 nanoparticles. Again, all of the thermo physical properties increase with nanoparticles concentration. The measured effective density of NEILs correlates well with the calculated data by mixing theory. Viscosity of NEILs is highly temperature dependent and higher than the base IL.
The relative change of effective thermo physical properties was not fully responsible for the degradation of the natural convection of NEILs. In addition to thermo physical properties, particle–fluid interaction and clustering of nanoparticles also play a role in degrading the natural convection heat transfer (Paul et al., 2014).

(Nguyen et al., 2006) had investigated that the heat transfer behavior of a typical liquid cooling system by replacing the base fluid, which is distilled water, by a nanofluid that is composed of distilled water and Al2O3 nanoparticles for two different particle average diameters and various volume concentrations. The experimental liquid cooling system is relatively simple and consists of a closed fluidic circuit. They also used several k- type thermocouples to monitor the fluid temperature. Experimental results showed that a nanofluid with 36 nm particle size provides higher convective heat transfer coefficients than the ones given by nanofluid with 47 nm particles. Data obtained also clearly showed that the inclusion of nanoparticles into distilled water has produced a considerable enhancement of the cooling convective heat transfer coefficient. For a particular particle volume concentration of 6.8%, the heat transfer coefficient has been found to increase as much as 40% compared to that of the base fluid.
The result also showed that an increase of particle volume con-centration has produced a clear decrease of the heated block temperature.

(Noie et al., 2009) had found that they combined two mentioned techniques for heat transfer enhancement. Nanofluids of aqueous Al2O3 nanoparticles suspensions were prepared in various volume concentration of

1–3% and used in a TPCT (Two-phase closed) as working media. In the present study, Al2O3 nanoparticles were dispersed in distillate water by ultra-sonication without using any dispersant or stabilizer to pre-vent any possible changes of chemical properties of the nanofluid due to presence of additions. The result was satisfactory and they found that Nanofluids in all concentration showed better thermal performance than pure water. They improved efficiency of the TPCT up to 14.7%. Temperature distributions on the TPCT were lower level using nanofluid compared to pure water. Temperature differences between the evaporator and condenser sections with nanofluids were less that pure water, i.e., thermal resistance of the TPCT when charged with nanofluids was less.

2.3. Summary

Above all the discussions we found that CuO and Al2O3 nanoparticle are commonly used to enhance the heat transfer, they have better thermal properties which increases heat transfer coefficient compare to water or other fluids. Graphene and CNT is a hybrid nanofluid which have superior thermal properties to enhance the heat transfer coefficient. Heat transfer coefficient can be increase upto 29% by graphene.Here we will work with Alumina (Al2O3), Zinc Oxide (ZnO) and Graphene (GO).

CHAPTER 3

Methodology

3.1 Overview

This chapter presents the methods to be applied in the current research study. This chapter gives a brief description of the experimental setup, workpiece material and the measuring equipment that have been used in the experiments. Section 3.3 describes about the preparation of nanoparticles. Section 3.4 gives a detailed explanation of preparation of nanofluid. Section 3.5 gives a discussion of properties of Nanofluid.

3.2. Experimental tools:

We used a Reservoir shell, thermocouple for measuring the heat transfer coefficient. For measuring the viscosity, we use a HAAKE machine which model no is D-78227, ultrasonication machine is used for dispersion.

3.3 Required chemicals:

- Alumina (Al2O3)
- Zinc Oxide (ZnO)
- Graphene (GO)

3.3.1 Chemical component detail:

3.3.1.1 Al2O3:

Al2O3 is the main component of alumina nano fluid. It is small diameter of the particle (2-10 nm). It has high specific surface area.It has high defectiveness of the material surface. Grinding powder alumina particles of a nanometer level which size is less than Zero Micrometer. It has a good thermal conductivity and good heat transfer coefficient.

3.3.1.2 ZnO:

Zinc oxide nanoparticles are nanoparticles of zinc oxide (ZnO) that have diameters less than 100 nanometers. They have a large surface area relative to their size and high catalytic activity. The exact physical and chemical properties of zinc oxide nanoparticles depend on the different ways they are synthesized.

3.3.1.3 GO:

It has superior heat transfer capability. is a compound of carbon, oxygen, and hydrogen in variable ratios. It is a 2-dimensional, single layer of graphite, made of 6 carbon molecules join with others to form a perfect hexagonal lattice-shaped structure. Graphene is 2D single layer of graphite.

3.4 Other component detail:

3.4.1 Magnetic stirrer with hot plate:

A magnetic stirrer with hot plate is used for preparing nanofluid. It takes four hours for completing the nanofluid.

Fig 3.1; Magnetic stirrer with hot plate

3.4.2 Oven:

For making hot water to measure the heat coefficient we need oven. Di ionized water which we use as a base fluid were heated up to 100 degree Celsius and kept in the oven.

Fig.3.2: Micro Oven

3.5 Preparation of nanofluids:

We made 12 types of nanofluids of three nanoparticles with different concentration, Alumina (Al2O3) (.1g,.2g,.3g,.4g,.5g), Zinc Oxide (ZnO) (.1g,.2g,.3g,.4g), Graphene oxide (GO) (.1g,.3g,.5g). We take di- ionized water as a base fluid.

First of all, we take a biker with 250ml deionized water and mix up it with the appropriate concentration of nanoparticles and then put the biker on stirrer machine for stirring operation with a help of a magnet which takes 4 hours to prepare nanofluid. After 4 hours the nanofluid got prepared. Then we take pictures of that fluid after 5 Minutes, 10 minutes, 20 minutes and 40 minutes and after a day. We follow the same procedure to make the nanofluids of all concentration of the nanoparticles.

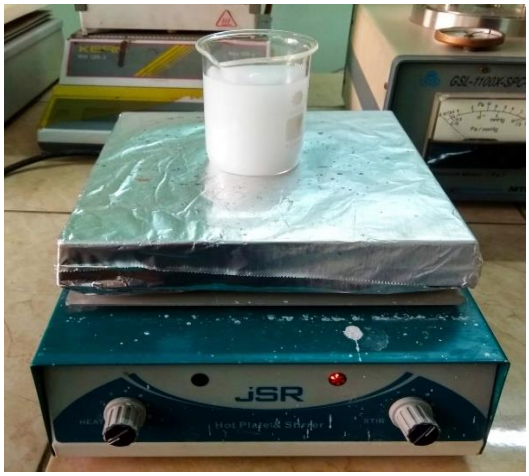

Fig 3.3: Stirring Operation

3.6 Dispersibility test:

To see the dispersion of the nanofluids we took pictures of the prepared nanofluids after certain time period. We found that .2% Al2O3, .3% Zinc Oxide and .1g Graphene shows the best dispersion among the all concentration of Alumina, Zinc Oxide and Graphene nanofluids .

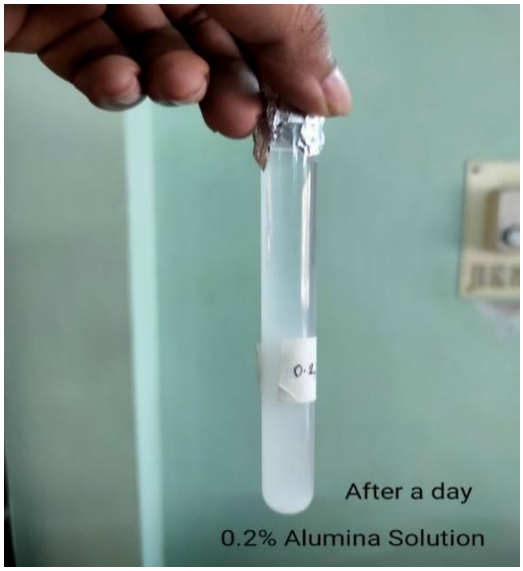

Figure 3.4: 0.2% Alumina Solution after a day.

3.7 Ultrasonication:

Before measuring the heat transfer coefficient, we do Ultrasonication bath of all the nanofluids to see the proper dispersion. Ultrasonication is used to disperse the nanofluids in base fluids b using ultrasonic wave.

Ultrasonication can be defined as the process which using sound energy at a very high frequency to break particle agglomerates apart by implosion and expansion of bubbles and by cavitation. The device used for Ultrasonication is shown in figure:

Figure3.5: During Ultrasonication

Figure 3.6: Ultrasonication Device

3.8 Measuring the Heat Transfer Co-efficient:

The setup which we used in this experiment for calculating the convective heat transfer coefficient is shown schematically in Figure. Our experimental setup consists of a reservoir shell of 350 ml volume, which contain hot water (100°C) in a stagnant condition. To store the nanofluid a syringe was placed. A constant heat flux condition was maintained. The spiral tube which is made from smooth copper tube with 0.44mm outer diameter, 0.15 mm thickness and 0.29 mm inner diameter and a heat exchange length of 68.58 cm was incorporated into the shell. A centrifugal pump (Espa Ref. XVM8 03F15T) was used to circulate the nanofluids and base fluid through the test section. The fluids took heat from the hot water and then passed away from the tube. nano fluids passed from the tube were collected in a beaker. To reduce the heat loss from the system the test section is perfectly insulated by using glass wool. The K- type thermocouples are used to measure the temperature at the shell and outlet side tube.

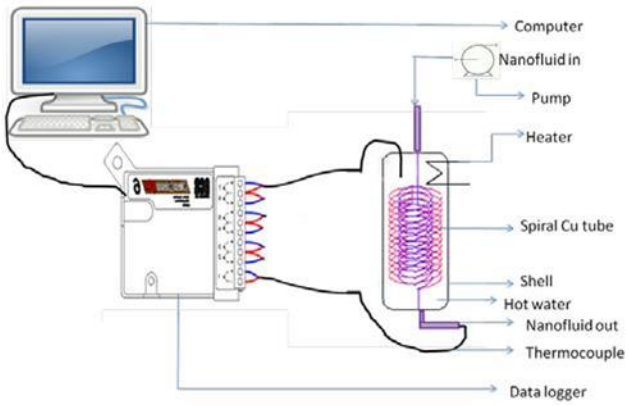

Figure 3.7: Experimental setup for the measurement of forced convective heat transfer coefficient of nanofluids.

Figure3.8: Heat Transfer Coefficient Measuring Machine

Figure3.9: K-type thermocouple

3.9 Viscosity Measurement:

For measuring the viscosity, we use HAAKE machine which model no is D-78227 which is shown in this figure. First of all, we disperse all of our nanofluid by ultrasonication. Then we clean the necessary machine parts and pass the nanofluid into that machine, the machine is connected to a computer. We monitor all of our data from the computer.

Figure3.10: Viscosity Measuring Machine

CHAPTER 4

RESULT AND DISCUSSION

4.1.1. Heat Transfer Coefficient Measurement of Alumina Solution:

4.1.1.2 0.1% alumina solution:

For 0.1% Alumina Solution,

Here,

m= 0.34, S=4178J/kg-K,

$\Delta\theta$= 84.4-81.9= 2.5

ΔT= 81.9-57.8= 24.1

A= 0.10075 m2

Now, h1= $(mS\Delta\theta)/(A\Delta T)$

= (0.35*4178*2.5)/(.1*24.1)

= 1516.91 W/(m2-K)

Similarly,

h2= 1511.49	h11= 1571.28
h3= 1499.423	h12= 1558.99
h4= 1521.64	h13= 1561.4
h5= 1509.23	h14= 1570.46
h6= 1529.6	h15= 1599.45
h7= 1540.03	h16= 1611
h8= 1542.51	h17= 1585.75

h9= 1548.047 h18= 1594.57

h10= 1550.63 h19= 1600.588

h20= 1601.77

h mean= 1556.238 W/(m2-K)

We take the dataset for 0.1% Alumina Solution and make our predictions by using a regression model. There we also apply other models to predict, but the regression fits most. That's why we make a detailed analysis of this. The precise result of the prediction model gives below:

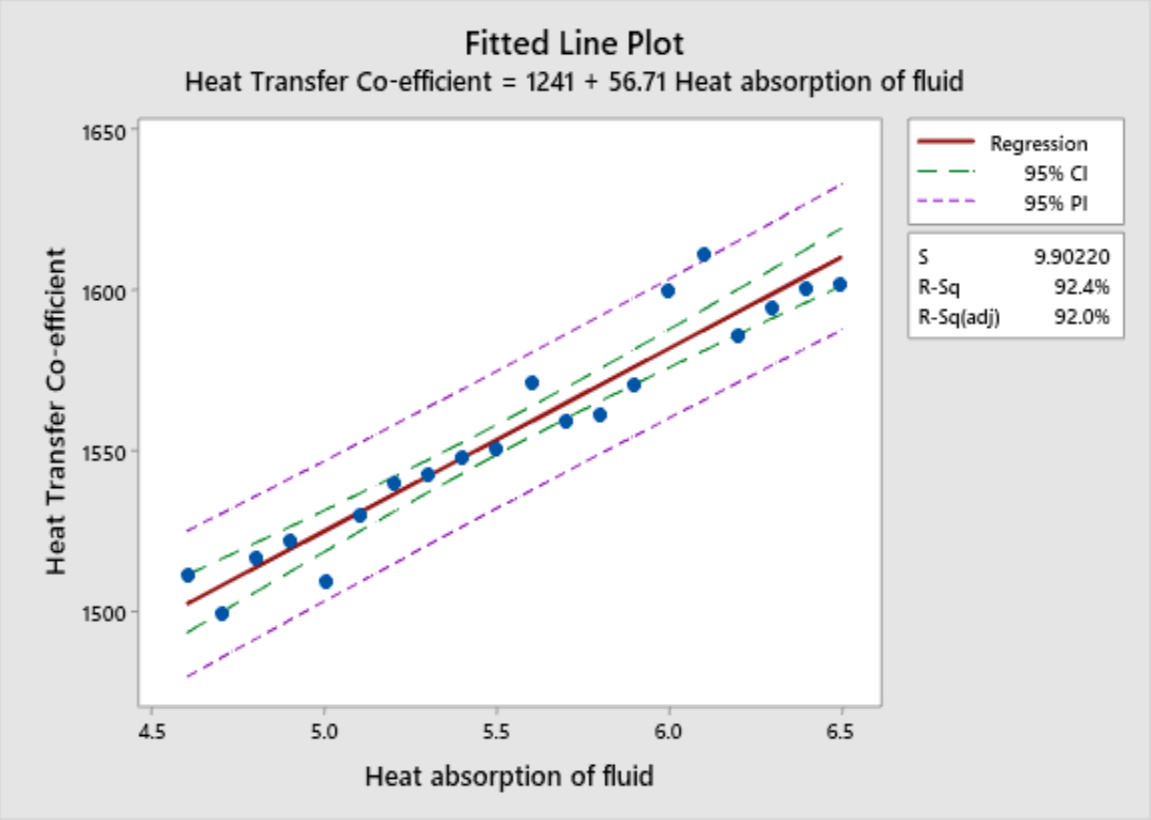

Figure 4.1: Fitted Line Plot for 0.1% Alumina Solution.

From the above figure, we get a fitted line plot to make our prediction using the Regression model, which gives us a relationship equation between the Heat Transfer Coefficient and the Heat absorption of fluid.

Regression Equation

Heat Transfer Co-efficient = 1241.5 + 56.71 Heat absorption of fluid

Coefficients

Term	Coef	SE Coef	T-Value	P-Value	VIF
Constant	1241.5	21.4	57.94	0.000	
Heat absorption of fluid	56.71	3.84	14.77	0.000	1.00

Analysis of Variance

Source	DF	Adj SS	Adj MS	F-Value	P-Value
Regression	1	21390	21390.1	218.15	0.000
Heat absorption of fluid	1	21390	21390.1	218.15	0.000
Error	18	1765	98.1		
Total	19	23155			

From the variance analysis result, we notice from the P-Value, which is equal to 0 & the F-value, which is larger than the F critical value that indicates Heat absorption of fluid, creates a significant impact on the regression model.

Durbin-Watson Statistic

Durbin-Watson Statistic	1.80007

From the Durbin-Watson Statistics, we get the value equal to 1.8, which shows that the Heat Transfer Co-efficient has maintained a decent relationship with the increasing heat absorption of fluid.

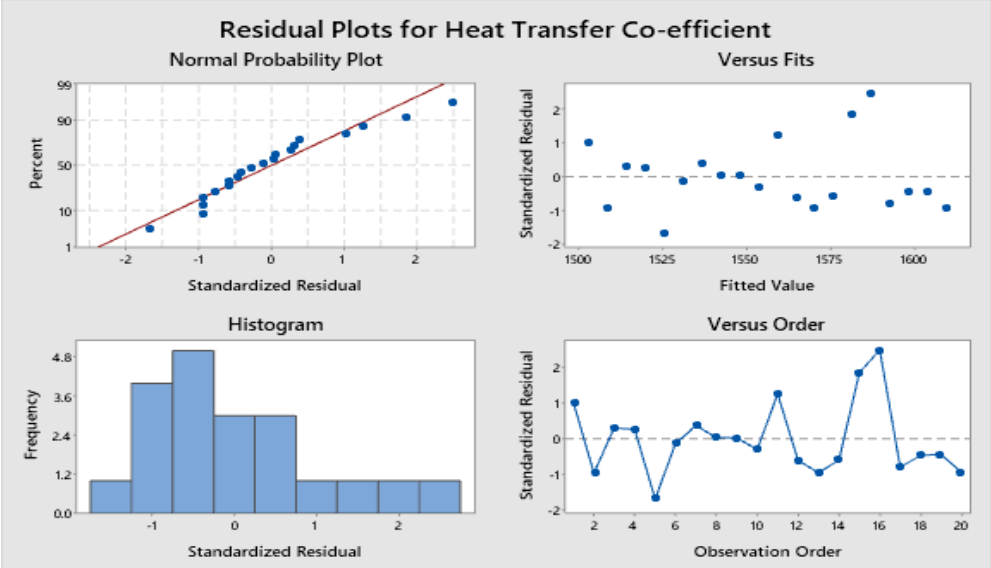

Figure 4.2: Residual Plots for 0.1% Alumina Solution

From the plots above, we get:

Fits and Diagnostics for Unusual Observations

Obs	Heat Transfer Co-efficient	Fit	Resid	Std Resid	
16	1611.00	1587.43	23.57	2.50	R

R Large residual

Model Summary

S	R-sq	R-sq(adj)	R-sq(pred)
9.90220	92.38%	91.95%	90.59%

We observe that there isn't much variation between the predicted line and the residual plot's observation data. That's why we get our satisfied R-sq value.

Then analyze more on ML algorithms and apply the Simple Linear Regression Model & Support Vector Regression to get a more accurate prediction model. For SVR, we get an accuracy of 88.17% and for SVR, we get an accuracy of 93.96%

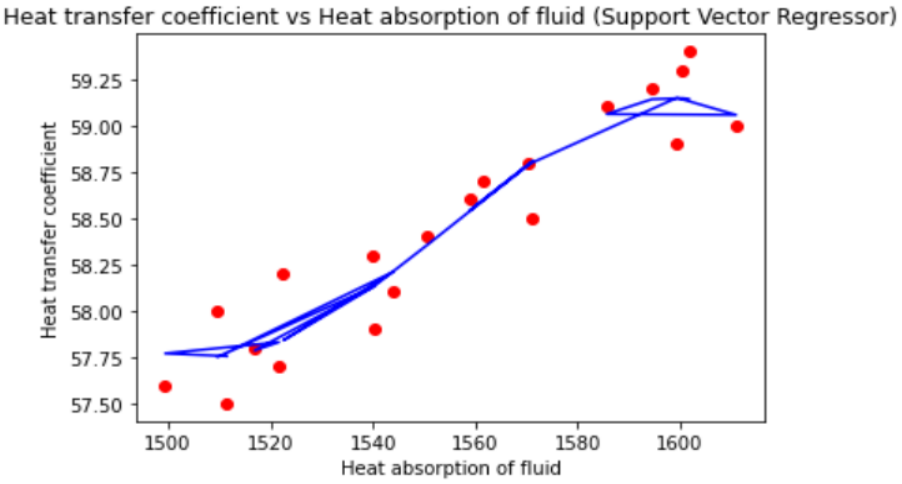


```
Accuracy: 88.16834485800459
```

.

Figure 4.3: Support Vector Regression Model by using ML for 0.1% Alumina Solution

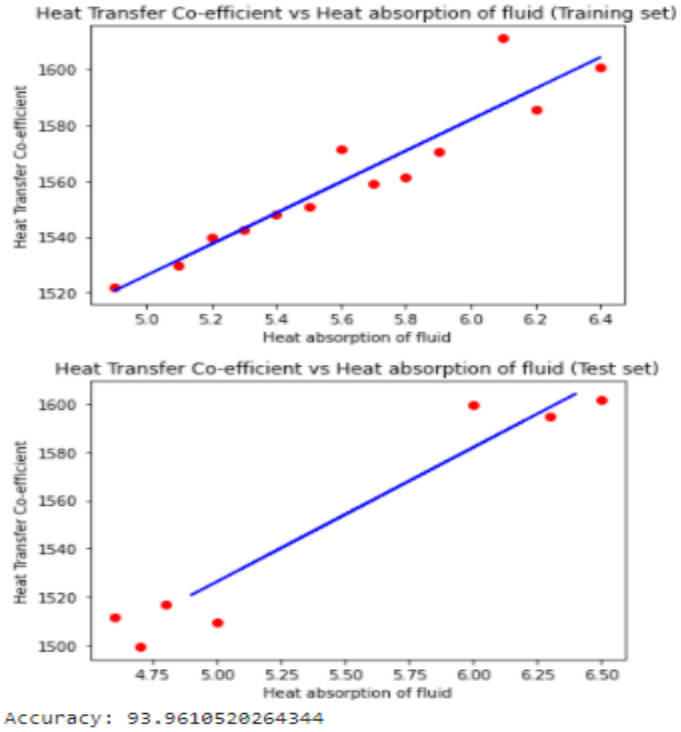


```
Accuracy: 93.9610520264344
```

Figure 4.4: Simple Linear Regression Model by using ML for 0.1% Alumina Solution

From the model, we observe that we get a good prediction model by using the Simple Linear Regression Model, and there we get the observation datasets that are so close to our predicted line.

4.1.1.3 0.2% Alumina Solution:

0.2% Alumina Solution

For 0.2% Alumina Solution,

Here,

m= 0.35, S= 4178J/kg-K,

$\Delta\theta$= 80.9-79.5= 1.4

ΔT= 10.5

A= 0.10075 m2

Now, h1= $mS\Delta\theta/(A\Delta T)$

= 1935.22 W/(m2-K)

Similarly,

h2=1855.14	h11= 1950.14
h3= 1851.56	h12= 1980.38
h4= 1844.26	h13= 1968.85
h5= 1836.22	h14= 2012.67
h6= 1850.68	h15= 2035.65
h7= 1878.74	h16= 2067.47
h8= 1890.63	h17= 2090.32

h9= 1909.83

h10= 1934.51

h18= 2073.54

h19= 2120.68

h20= 2140.65

h (mean)= 1961.357 W/(m2-K)

Similarly,

We take the dataset for 0.2% Alumina Solution and make our predictions by using a regression model. There we also apply other models to predict, but the regression fits most. That's why we make a detailed analysis of this. The precise result of the prediction model gives below:

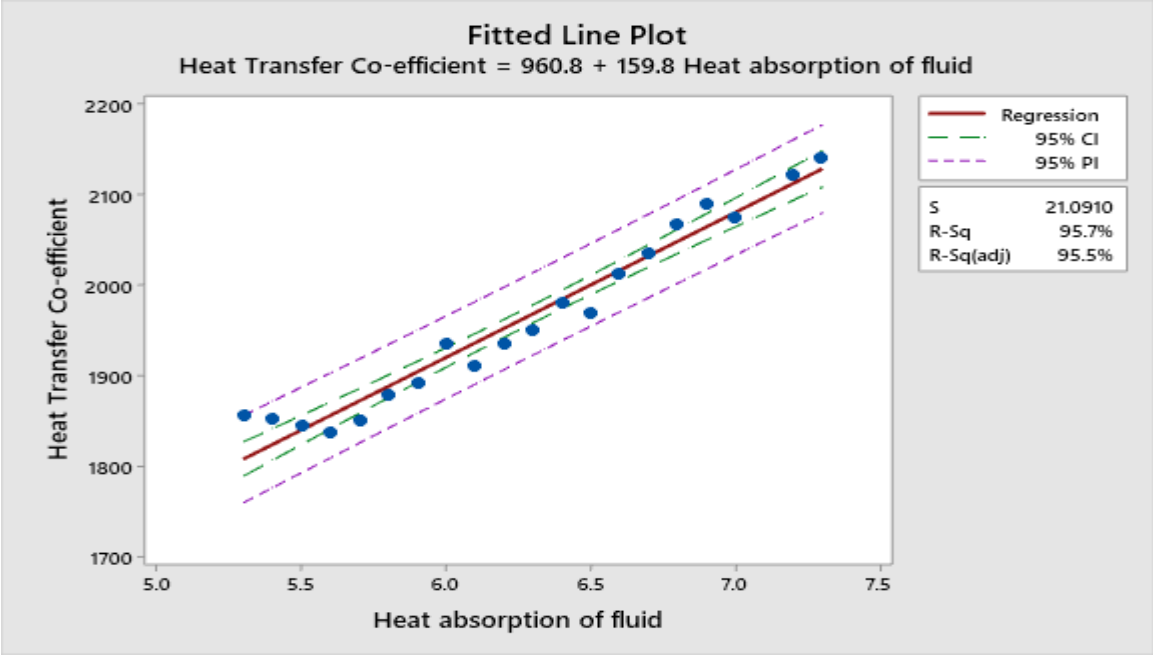

Figure 4.5: Fitted Line Plot for 0.2% Alumina Solution.

From the above figure, we get a fitted line plot to make our prediction using the Regression model. It gives us a relationship equation between the Heat Transfer Coefficient and the Heat absorption of fluid.

Regression Equation

Heat Transfer Co-efficient = 960.8 + 159.83 Heat absorption of fluid

Coefficients

Term	Coef	SE Coef	T-Value	P-Value	VIF
Constant	960.8	50.0	19.21	0.000	
Heat absorption of fluid	159.83	7.96	20.09	0.000	1.00

Analysis of Variance

Source	DF	Adj SS	Adj MS	F-Value	P-Value
Regression	1	179540	179540	403.61	0.000
Heat absorption of fluid	1	179540	179540	403.61	0.000
Error	18	8007	445		
Total	19	187547			

From the variance analysis result, we notice from the P-Value, which is equal to 0 & the F-value, which is larger than the F critical value that indicates Heat absorption of fluid, creates a significant impact on the regression model.

Durbin-Watson Statistic

Durbin-Watson Statistic = 0.958455

From the Durbin-Watson Statistics, we get a value equal to 0.96, which shows that the Heat Transfer Coefficient has maintained a strong relationship with the increasing heat absorption of fluid.

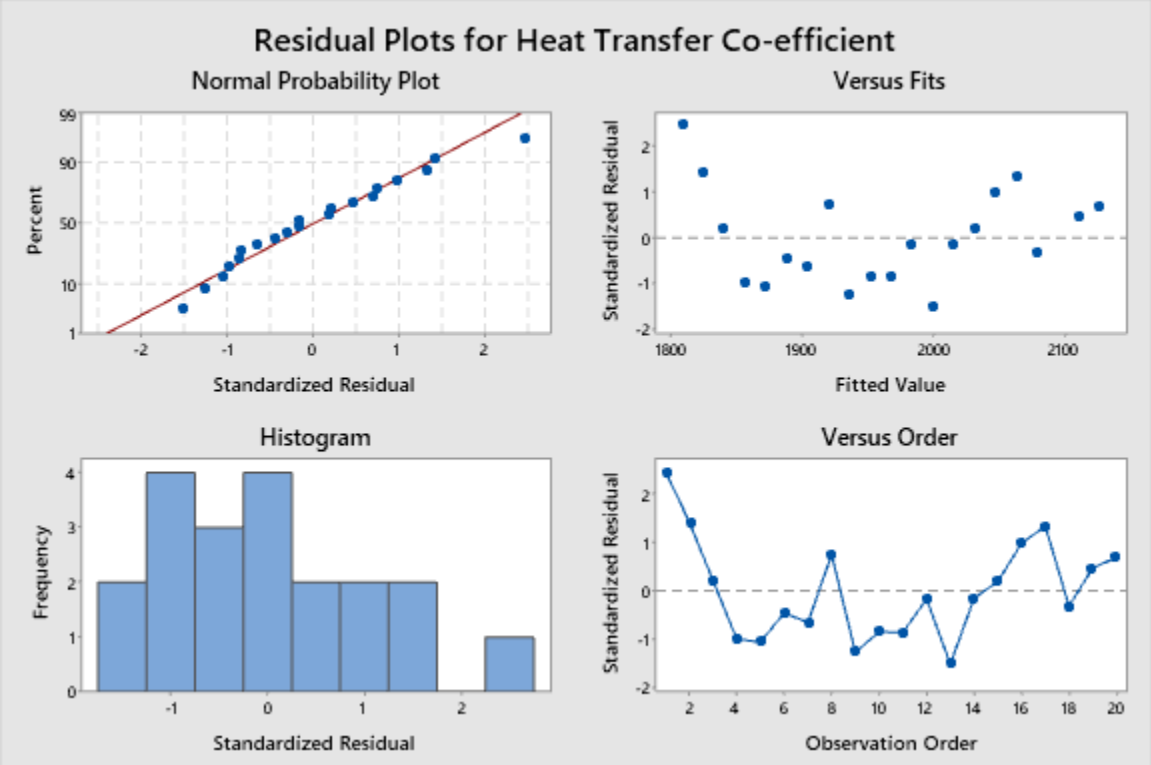

Figure 4.6: Residual Plots for 0.2% Alumina Solution

From the plots above. we get:

Fits and Diagnostics for Unusual Observations

Obs	Heat Transfer Co-efficient	Fit	Resid	Std Resid	
1	1855.14	1807.92	47.22	2.47	R

R Large residual

Model Summary

S	R-sq	R-sq(adj)	R-sq(pred)
21.0910	95.73%	95.49%	94.47%

We observe that there isn't much variation between the predicted line and the residual plot's observation data. That's why we get our satisfied R-sq value.

Then analyze more on ML algorithms and apply the Simple Linear Regression Model & Support Vector Regression to get a more accurate prediction model. For SVR, we get an accuracy of 95.68% & for SLR, and we get an accuracy of 92.55%.

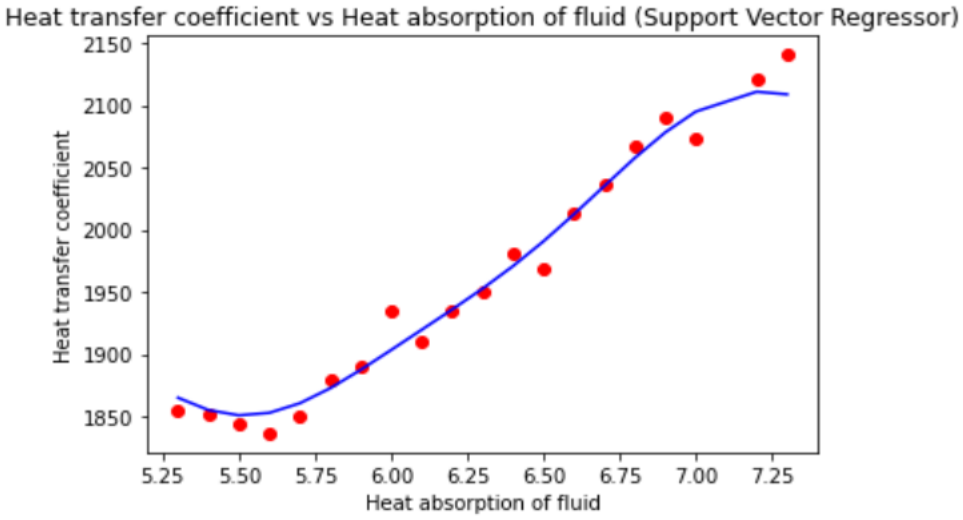

Figure 4.7: Support Vector Regression Model by using ML for 0.2% Alumina Solution

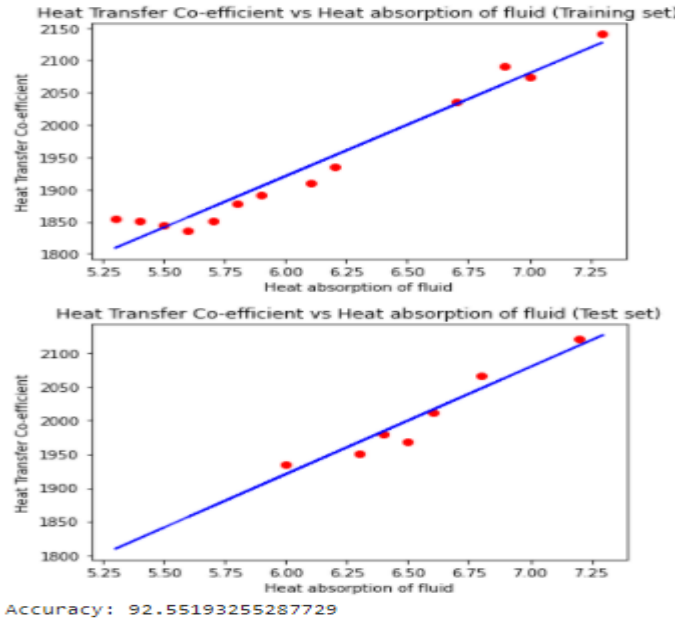

Figure 4.8: Simple Linear Regression Model by using ML for 0.2% Alumina Solution

We observe that we get a good prediction model by using the Support Vector Regression from those models. Though SLR gives a good prediction, and we get the observation datasets are so close to our predicted line in both cases, but in SVR, observation datasets are closer.

4.1.1.4 0.3% Alumina Solution:

For 0.3% Alumina Solution,

Here,

m= 0.35, S= 4178J/kg-K,

$\Delta\theta$= 1.6

ΔT= 9.8

A= 0.10075 m2

Now, h1= (mS$\Delta\theta$)(/AΔT)

= 2369.656 W/m2-K

Similarly,

h2= 2250.43	h11= 2450.76
h3= 2225.67	h12= 2490.52
h4= 2245.13	h13= 2519.24
h5= 2259.83	h14= 2512.36
h6= 2269.91	h15= 2619.72
h7= 2278.61	h16= 2589.32
h8= 2282.47	h17= 2610.62
h9= 2399.67	h18= 2649.14

h10= 2419.49 h19= 2672.61

h20= 2701.39

h (mean) = 2440.827 W/m2-K

We take the dataset for 0.3% Alumina Solution and make our predictions by using a regression model. There we also apply other models to predict, but the regression fits most. That's why we make a detailed analysis of this.

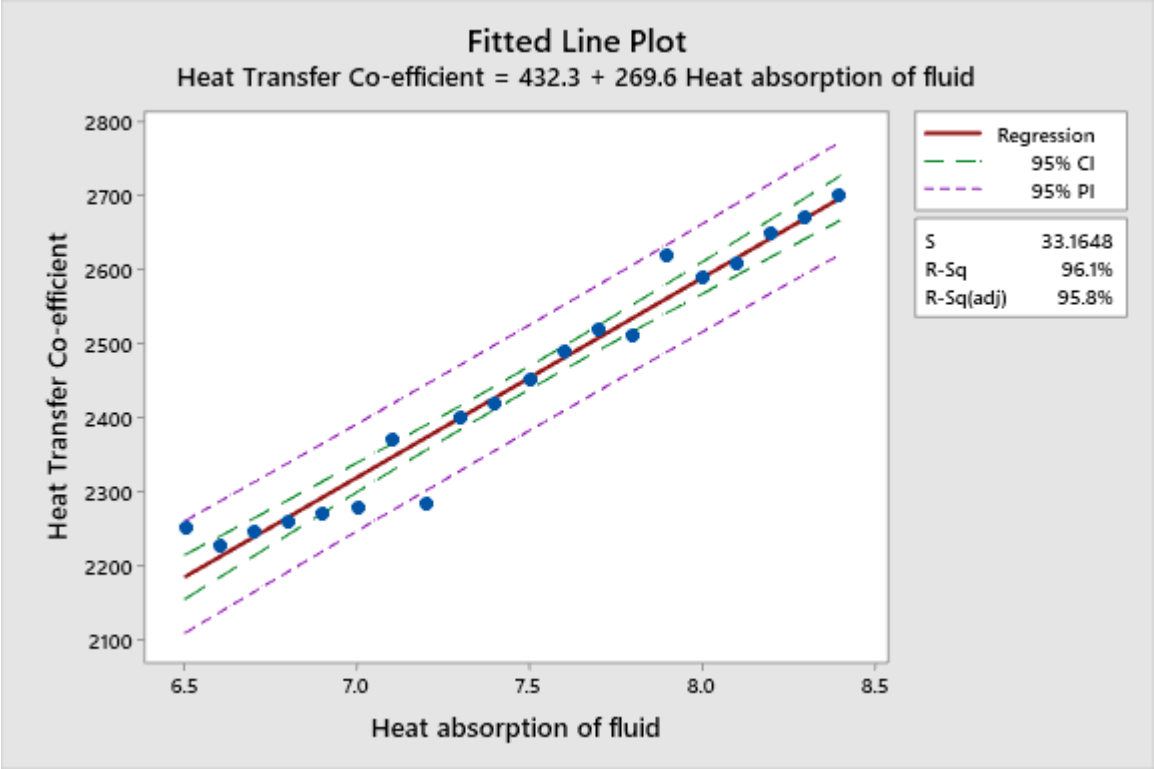

Figure 4.9: Fitted Line Plot for 0.3% Alumina Solution.

From the above figure, we get a fitted line plot for our prediction using the regression model. It gives us a relationship equation between the Heat Transfer Coefficient and the Heat absorption of fluid.

Regression Equation

Heat Transfer Co-efficient = 432.3 + 269.6 Heat absorption of fluid

Coefficients

Term	Coef	SE Coef	T-Value	P-Value	VIF
Constant	432.3	96.1	4.50	0.000	
Heat absorption of fluid	269.6	12.9	20.96	0.000	1.00

Analysis of Variance

Source	DF	Adj SS	Adj MS	F-Value	P-Value
Regression	1	483347	483347	439.44	0.000
Heat absorption of fluid	1	483347	483347	439.44	0.000
Error	18	19798	1100		
Total	19	503146			

From the variance analysis result, we notice from the P-Value, which is equal to 0 & the F-value, which is larger than the F critical value that indicates Heat absorption of fluid, creates a significant impact on the regression model.

Durbin-Watson Statistic

Durbin-Watson Statistic = 2.02533

From the Durbin-Watson Statistics, we get the value equal to 2.02, which shows that the Heat Transfer Co-efficient has maintained a decent relationship with the increasing heat absorption of fluid.

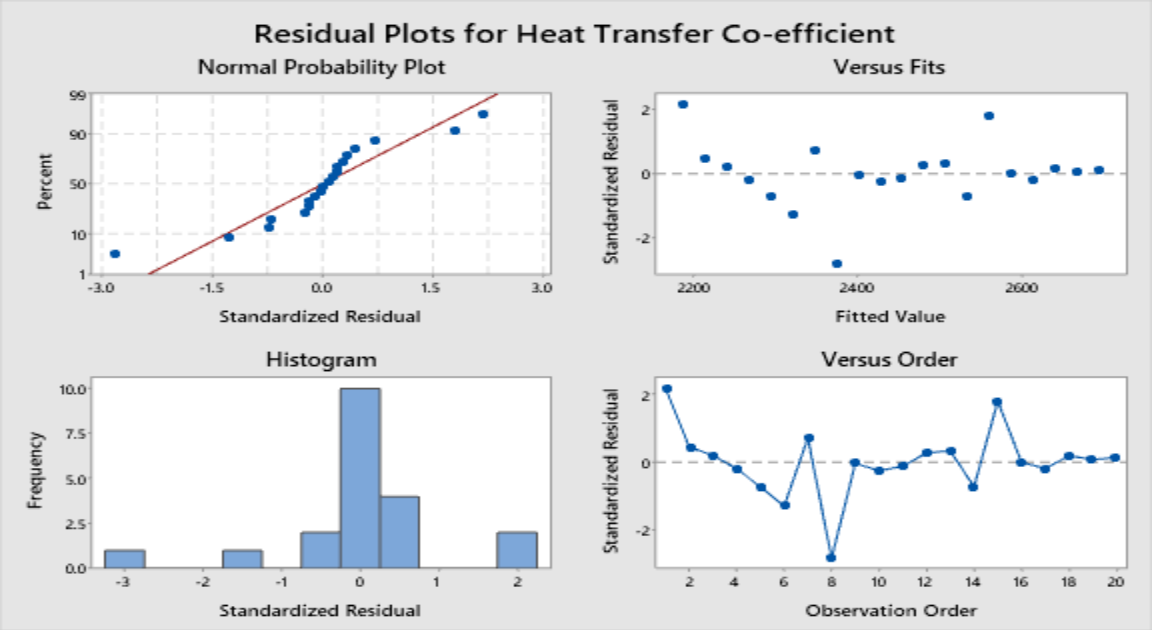

Figure 4.10: Residual Plots for 0.3% Alumina Solution

From the plot above. we get:

Fits and Diagnostics for Unusual Observations

Obs	Heat Transfer Co-efficient	Fit	Resid	Std Resid	
1	2250.4	2184.7	65.7	2.20	R
8	2282.5	2373.4	-91.0	-2.83	R

R Large residual

Model Summary

S	R-sq	R-sq(adj)	R-sq(pred)
33.1648	96.07%	95.85%	95.14%

We observe that there isn't much variation between the predicted line and the residual plot's observation data. That's why we get our satisfied R-sq value.

Then analyze more on ML algorithms and apply the Simple Linear Regression Model & Support Vector Regression to get a more accurate prediction model. For SVR, we get an accuracy is 96.02% & for SLR, we get an accuracy is 89.17%.

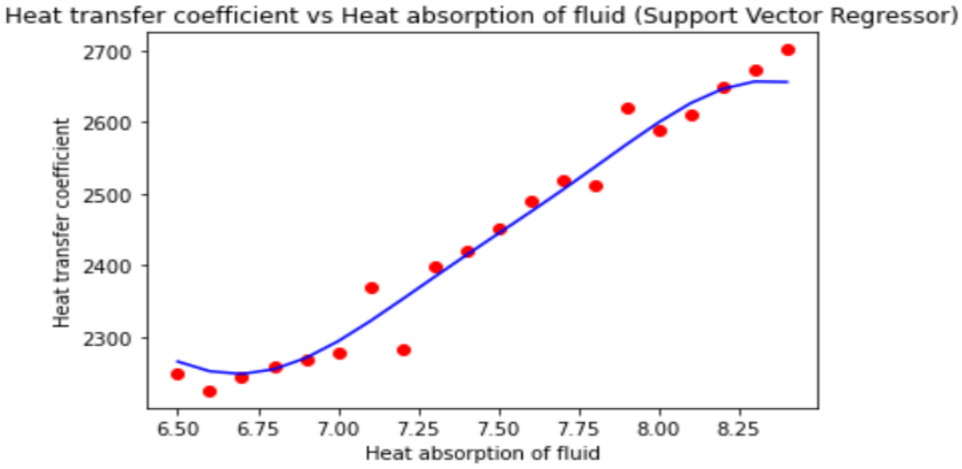


```
Accuracy: 96.02560977540384
```

Figure 4.11: Support Vector Regression Model by using ML for 0.3% Alumina Solution

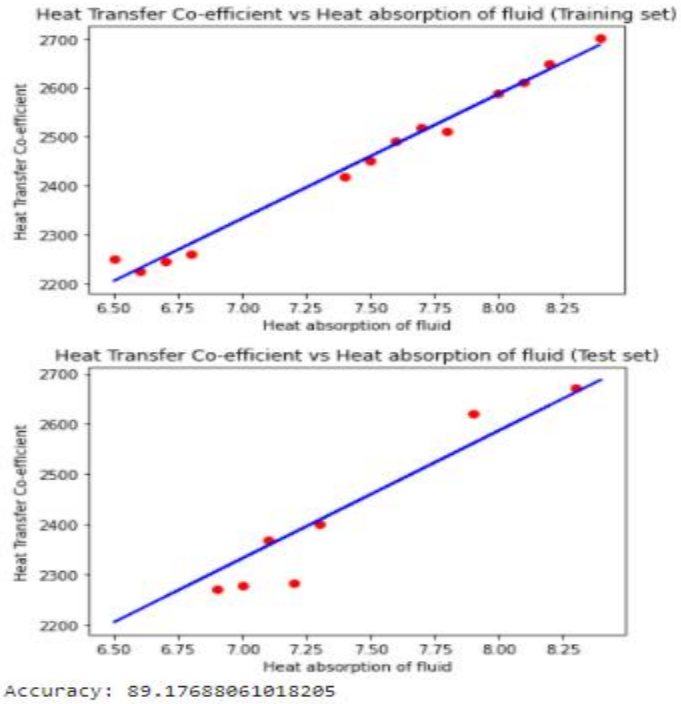

Figure 4.12: Support Vector Regression Model by using ML for 0.3% Alumina Solution

Simple Linear Regression Model by using ML for 0.3% Alumina Solution

From the model, we observe that we get a good prediction model by using the Support Vector Regression Model, and there we get the observation datasets that are so close to our predicted line.

4.1.1.5 0.4% Alumina Solution:

For 0.4% Al2O3,

Here,

m= 0.35, S= 4178J/kg-K,

$\Delta\theta$= 0.6

ΔT= 12.2

A= 0.10075 m2

Now, h1= $mS\Delta\theta/A\Delta T$

=719.7096 W/m2-K

Similarly,

h2= 619.43	h11= 680.38
h3= 611.75	h12= 707.48
h4= 625.89	h13= 690.49
h5= 633.56	h14= 749.7096
h6= 645.83	h15= 760.57
h7= 640.91	h16= 780.53
h8= 650.74	h17= 767.45

h9= 661.43

h10= 640.56

h18= 768.84

h19= 782.47

h20= 793.61

h mean= 705.2572 W/m2-K

We take the dataset for 0.4% Alumina Solution and make our predictions by using a regression model.

There we also apply other models to predict, but the regression fits most. That's why we make a detailed analysis of this. The precise result of the prediction model gives below:

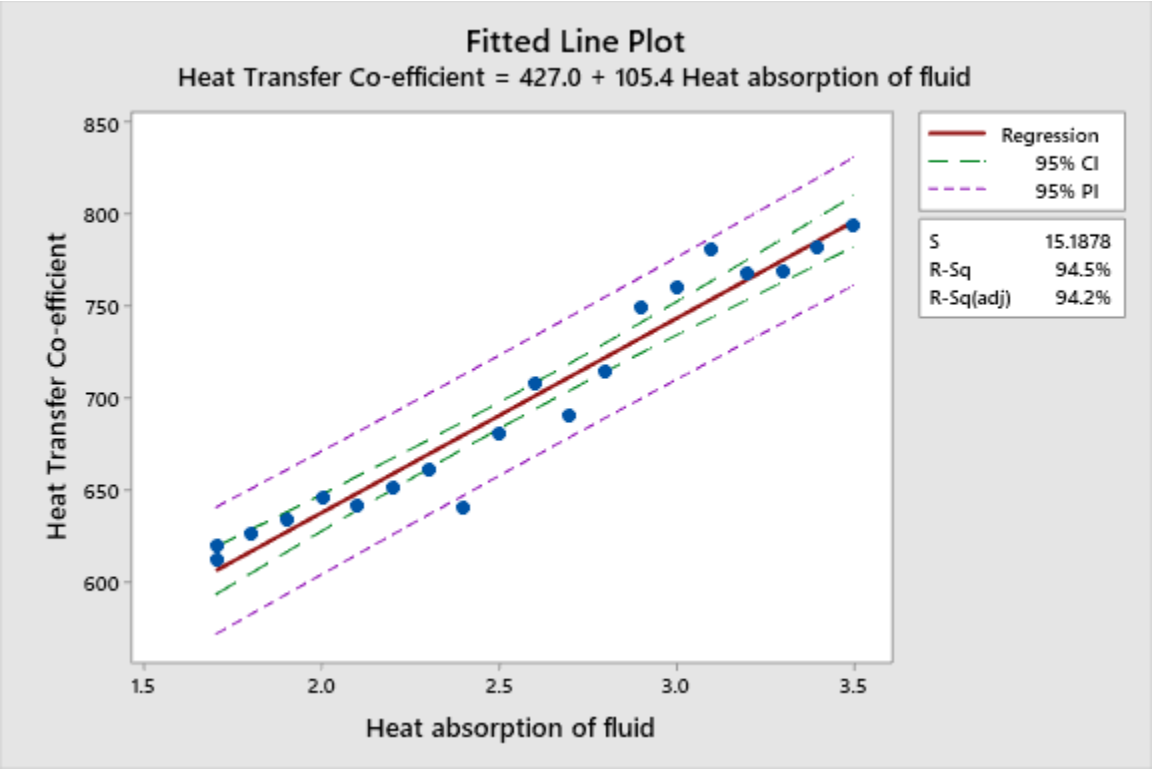

Figure 4.13: Fitted Line Plot for 0.4% Alumina Solution.

We get a fitted line plot to make our prediction using the regression model from the above figure. It gives us a relationship equation between the Heat Transfer Coefficient and the Heat absorption of fluid.

Regression Equation

Heat Transfer Co-efficient = 427.0 + 105.38 Heat absorption of fluid

Coefficients

Term	Coef	SE Coef	T-Value	P-Value	VIF
Constant	427.0	15.6	27.32	0.000	
Heat absorption of fluid	105.38	5.97	17.65	0.000	1.00

Analysis of Variance

Source	DF	Adj SS	Adj MS	F-Value	P-Value
Regression	1	71847.3	71847.3	311.47	0.000
Heat absorption of fluid	1	71847.3	71847.3	311.47	0.000
Error	18	4152.1	230.7		
Lack-of-Fit	17	4122.6	242.5	8.22	0.268
Pure Error	1	29.5	29.5		
Total	19	75999.4			

From the variance analysis result, we notice from the P-Value, which is equal to 0 & the F-value, which is larger than the F critical value that indicates Heat absorption of fluid, creates a significant impact on the regression model.

Durbin-Watson Statistic

Durbin-Watson Statistic =	1.13915

From the Durbin-Watson Statistics, we get the value equal to 1.13, which shows that the Heat Transfer Co-efficient has maintained a responsive relationship with the increasing heat absorption of fluid.

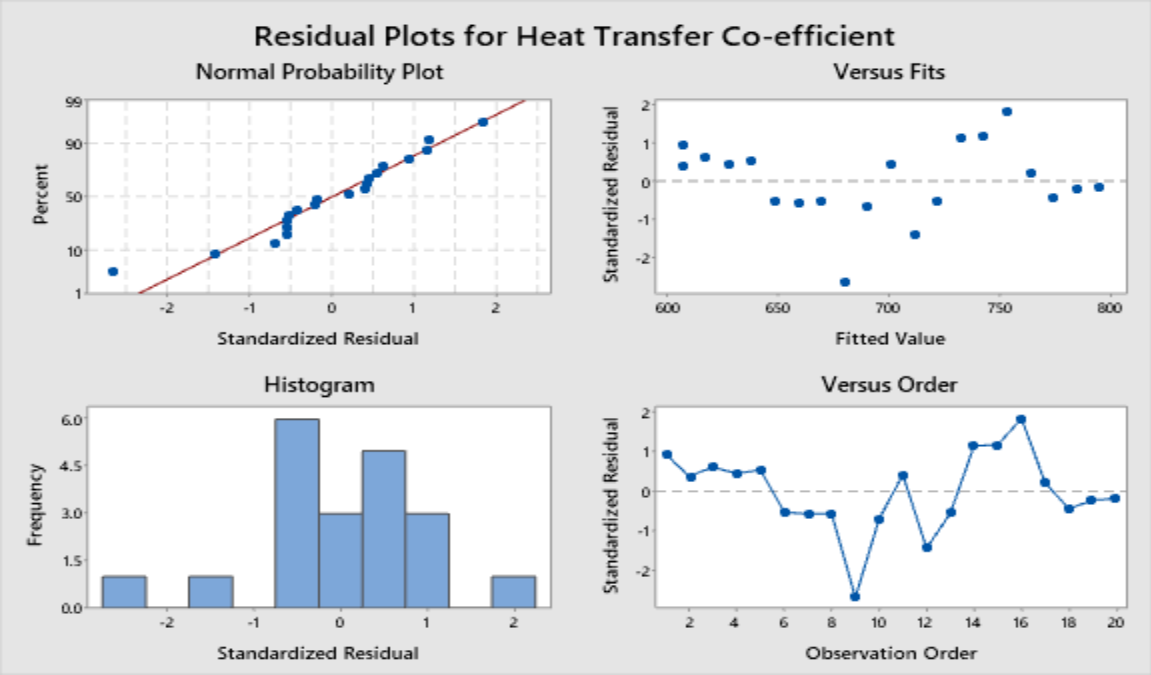

Figure 4.14: Residual Plots for 0.4% Alumina Solution

From the plots above. we get:

Fits and Diagnostics for Unusual Observations

Obs	Heat Transfer Co-efficient	Fit	Resid	Std Resid	
9	640.56	679.96	-39.40	-2.67	R

R Large residual

Model Summary

S	R-sq	R-sq(adj)	R-sq(pred)
15.1878	94.54%	94.23%	93.60%

We observe that there isn't much variation between the predicted line and the residual plot's observation data. That's why we get our satisfied R-sq value.

Then analyze more on ML algorithms and apply the Simple Linear Regression Model & Support Vector Regression to get a more accurate prediction model. For SVR, we get accuracy is 94.42% & for SLR, we get accuracy is 92.41%.

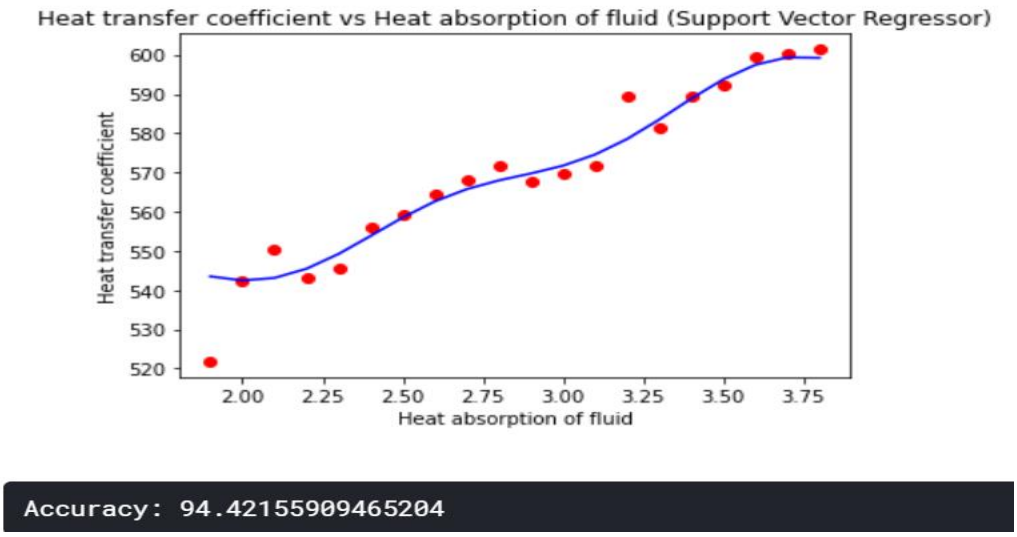

Figure 4.15: Support Vector Regression Model by using ML for 0.4% Alumina Solution

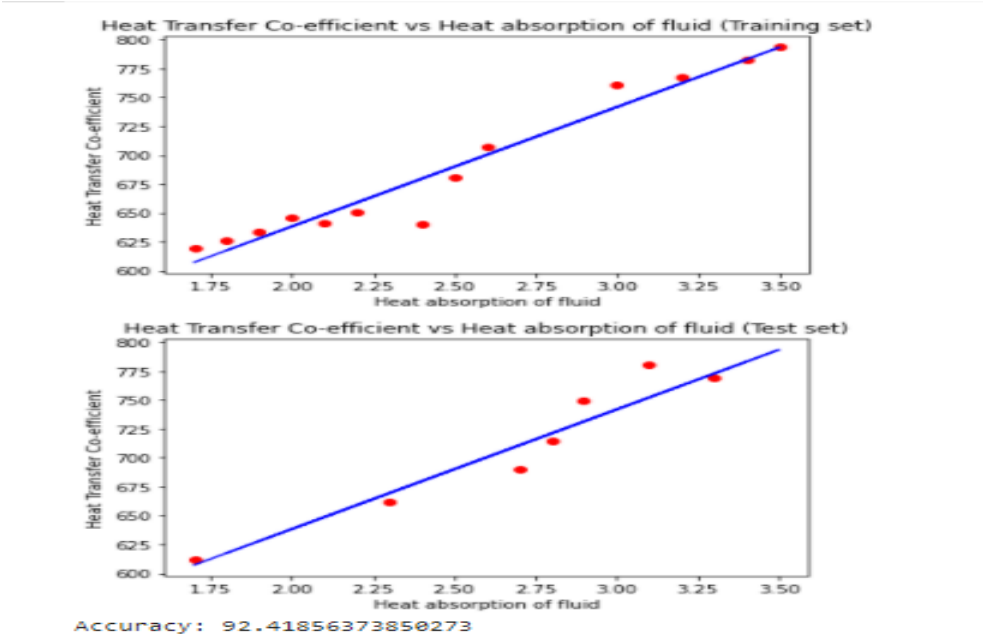

Figure 4.16: Simple Linear Regression Model by using ML for 0.4% Alumina Solution

From the model, we observe that we get a good prediction model by using the Support Vector Regression Model, and there we get the observation datasets that are so close to our predicted line.

4.1.1.6. 0.5% Alumina Solution:

For 0.5% Alumina Solution,

Here,

m= 0.35, S= 4178J/kg-K,

$\Delta\theta$= 86.2-85.7=.5

ΔT= 23.7

A= 0.10075 m2

Now, h1= $mS\Delta\theta/A\Delta T$

= 306.21 W/m2-K

Similarly,

h2= 240.78	h11= 272.98
h3= 261.45	h12= 286.65
h4= 252.91	h13= 293.91
h5= 258.42	h14= 318.42
h6= 263.59	h15= 329.48
h7= 272.19	h16= 320.58
h8= 280.56	h17= 340.45

h9= 268.89

h10= 255.74

h18= 349.57

h19= 320.75

h20= 333.03

h mean= 291.3278 W/m2-K

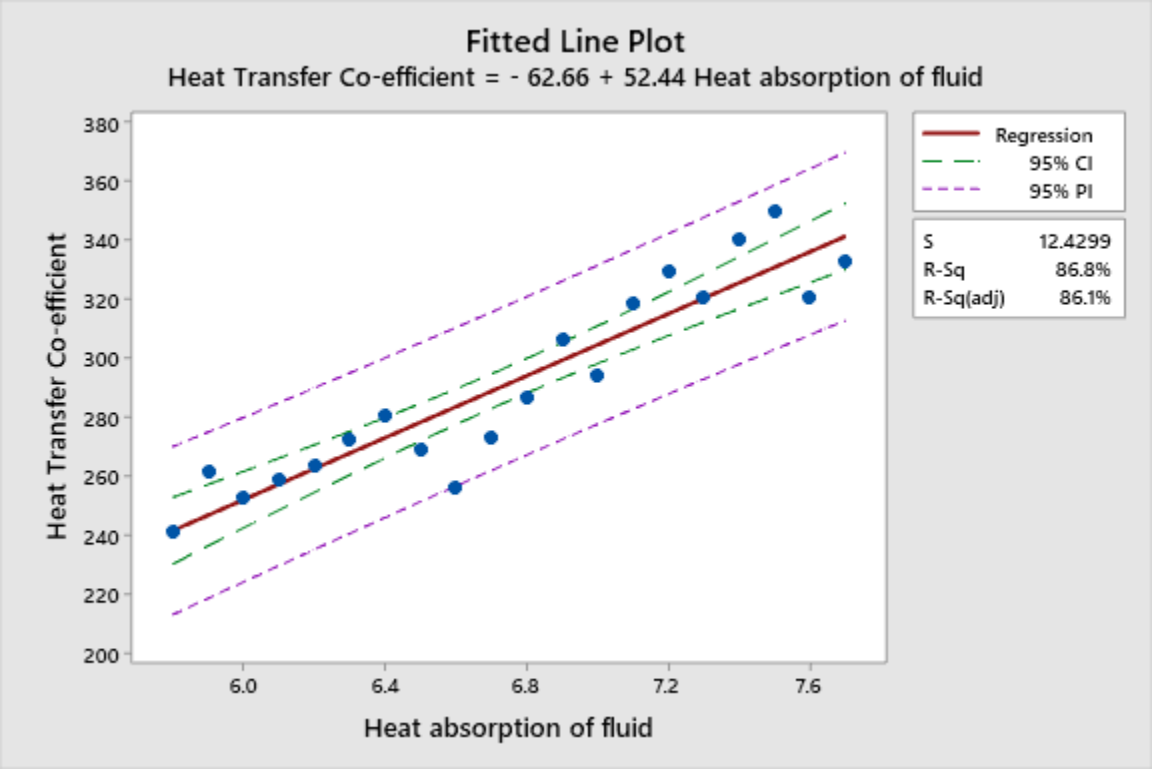

Figure4.17: Fitted Line Plot for 0.5% Alumina Solution.

From the above figure, we get a fitted line plot to make our prediction using the Regression model. It gives us a relationship equation between the Heat Transfer Coefficient and the Heat absorption of fluid.

Regression Equation

Heat Transfer Co-efficient = -62.7 + 52.44 Heat absorption of fluid

Coefficients

Term	Coef	SE Coef	T-Value	P-Value	VIF
Constant	-62.7	32.7	-1.92	0.071	
Heat absorption of fluid	52.44	4.82	10.88	0.000	1.00

Analysis of Variance

Source	DF	Adj SS	Adj MS	F-Value	P-Value
Regression	1	18289	18288.8	118.37	0.000
Heat absorption of fluid	1	18289	18288.8	118.37	0.000
Error	18	2781	154.5		
Total	19	21070			

From the variance analysis result, we notice from the P-Value, which is equal to 0 & the F-value, which is larger than the F critical value that indicates Heat absorption of fluid, creates a significant impact on the regression model.

Durbin-Watson Statistic

Durbin-Watson Statistic = 1.38247

From the Durbin-Watson Statistics, we get the value equal to 1.38, which shows that the Heat Transfer Coefficient has maintained a strong relationship with the increasing heat absorption of fluid.

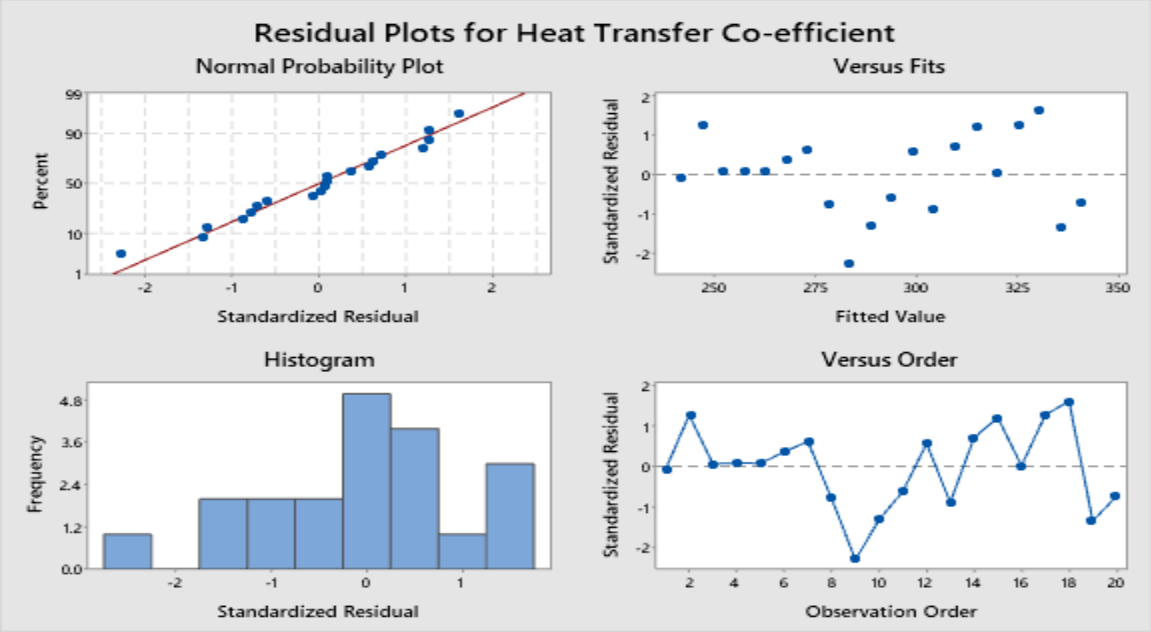

Figure 4.18: Residual Plots for 0.5% Alumina Solution

From the plots above, we get:

Fits and Diagnostics for Unusual Observations

Obs	Heat Transfer Co-efficient	Fit	Resid	Std Resid	
9	255.74	283.46	-27.72	-2.29	R

R Large residual

Model Summary

S	R-sq	R-sq(adj)	R-sq(pred)
12.4299	86.80%	86.07%	83.88%

We observe that there isn't much variation between the predicted line and the residual plot's observation data. That's why we get our satisfied R-sq value.

Then analyze more on ML algorithms and apply the Simple Linear Regression Model & Support Vector Regression to get a more accurate prediction model. For SVR, we get an accuracy of 86.33 & for SLR, and we get an accuracy of 92.42%.

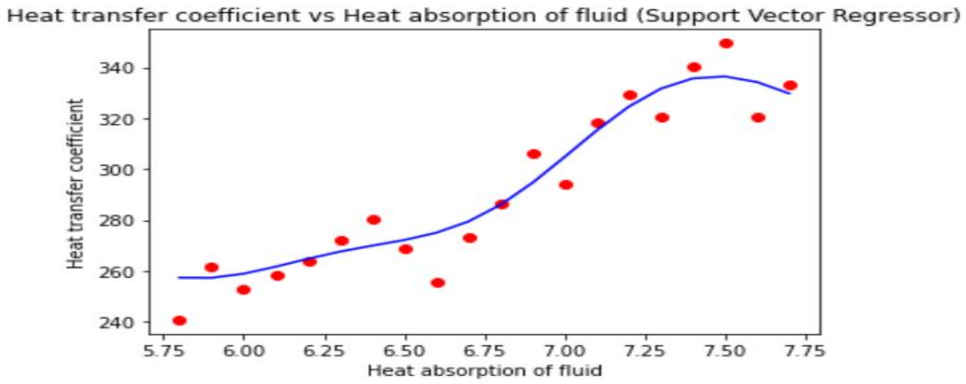

Figure 4.19: Support Vector Regression Model by using ML for 0.5% Alumina Solution

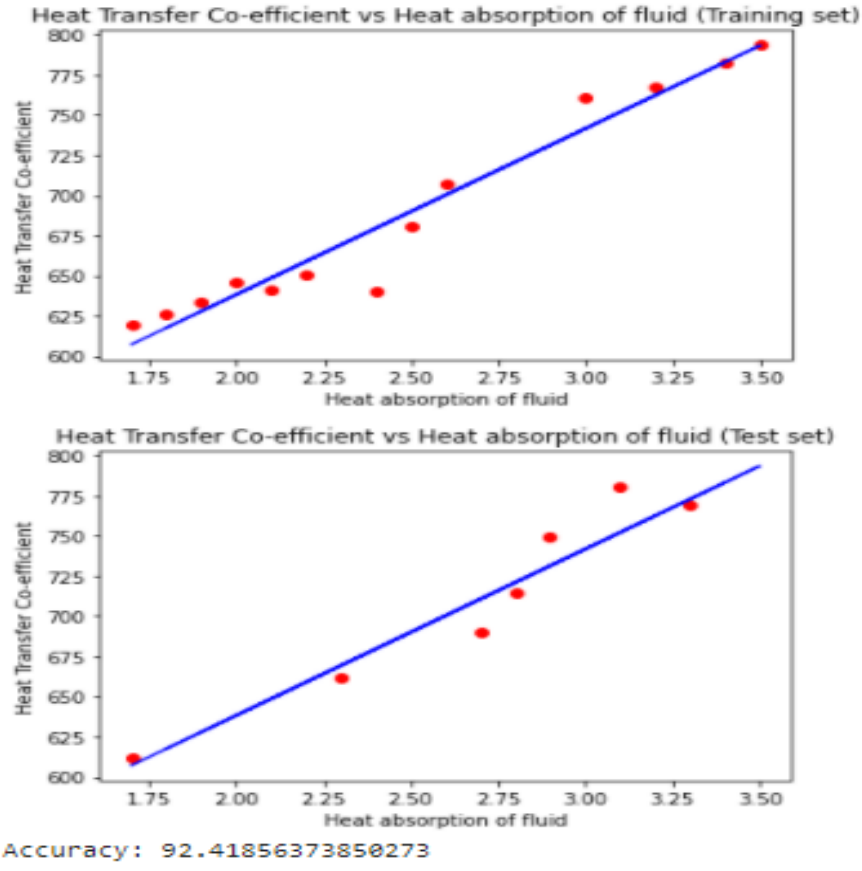

Figure 4.20: Simple Linear Regression Model by using ML for 0.5% Alumina Solution

From the model, we observe that we get a good prediction model by using the Simple Linear Regression Model, and there we get the observation datasets that are so close to our predicted line.

4.1.1.7. Heat Transfer Co-efficient of Alumina Solution:

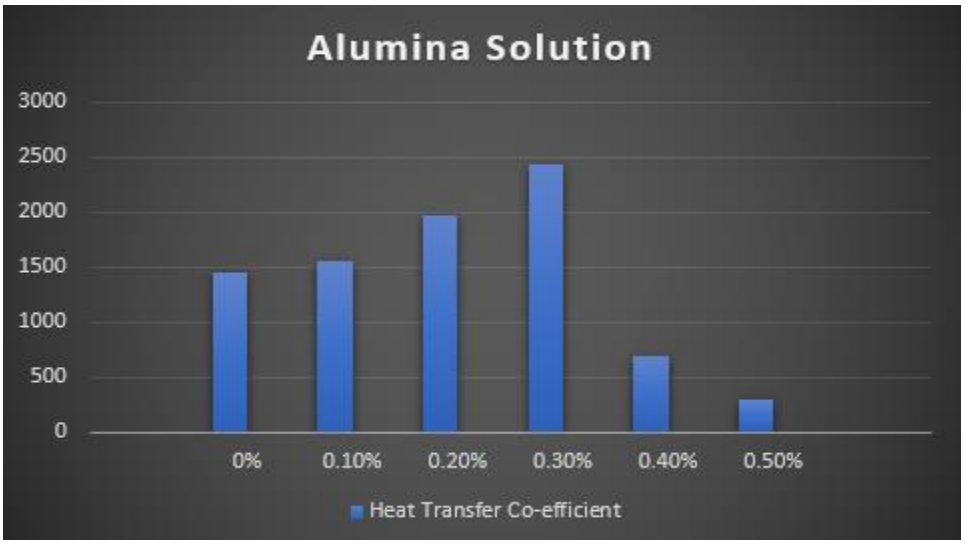

Figure 4.21: Heat Transfer Co-Efficient Bar-chart of Alumina Solution

From the above figure, we can see that as aluminum oxide nanoparticles concentration increased, the nanofluids heat transfer coefficient has also risen. Still, after a specific time, it got decreased. We found that 0.30% Alumina nanofluid gives the highest value of heat transfer co-efficient and 0.50% gives lower value, but 0.40% gives higher value than 0.50% concentration of Aluminum Oxide nanofluids.

4.1.2. Heat Transfer Coefficient Measurement of Zinc Oxide Solution:

4.1.2.1. 0.1% Zinc Oxide Solution

For 0.1% Zinc Oxide Solution,

Here,

m= 0.35, S= 4178J/kg-K,

$\Delta\theta$= 79.7-78.4= 1.3

ΔT= 5.8

A= 0.10075 m2

Now, h1= $mS\Delta\theta/A\Delta T$

= 3251.478 W/m2-K

Similarly,

h2=2700.12	h11= 3138.73
h3= 2781.38	h12= 3190.68
h4= 2812.93	h13= 3402.18
h5= 2872.47	h14= 3479.23
h6= 2903.41	h15= 3510.89
h7= 2942.64	h16= 3581.71
h8= 3121.52	h17= 3572.59
h9= 3076.49	h18= 3621.37

h10= 3099.84 h19= 3734.79

h20= 3802.41

h mean= 3231.657 W/m2-K

We take the dataset for a 0.1% Zinc Oxide Solution and make our predictions using a regression model. There we also apply other models to predict, but the regression fits most. That's why we make a detailed analysis of this. The precise result of the prediction model gives below:

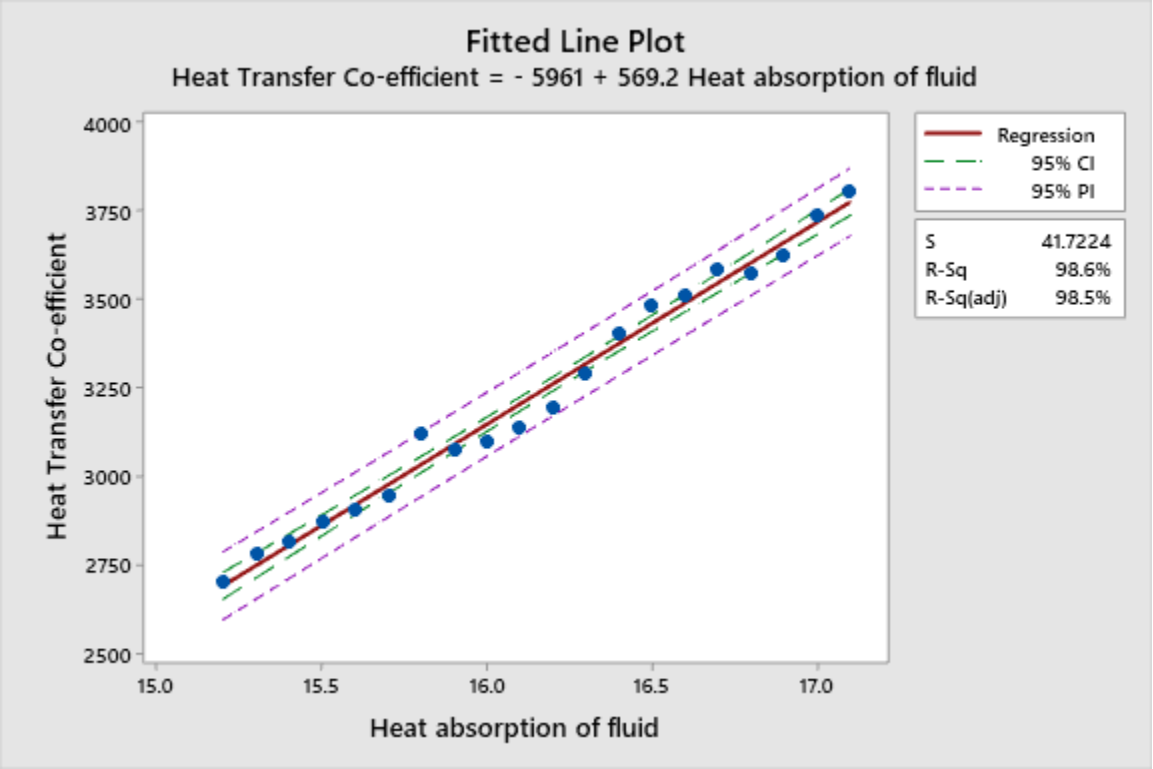

Figure 4.22: Fitted Line Plot for 0.1% Zinc Oxide Solution.

We get a fitted line plot to make our prediction using the regression model from the above figure. It gives us a relationship equation between the Heat Transfer Coefficient and the Heat absorption of fluid.

Regression Equation

Heat Transfer Co-efficient = -5961 + 569.2 Heat absorption of fluid

Coefficients

Term	Coef	SE Coef	T-Value	P-Value	VIF
Constant	-5961	261	-22.80	0.000	
Heat absorption of fluid	569.2	16.2	35.18	0.000	1.00

Analysis of Variance

Source	DF	Adj SS	Adj MS	F-Value	P-Value
Regression	1	2154509	2154509	1237.68	0.000
Heat absorption of fluid	1	2154509	2154509	1237.68	0.000
Error	18	31334	1741		
Total	19	2185842			

From the variance analysis result, we notice from the P-Value, which is equal to 0 & the F-value, which is larger than the F critical value that indicates Heat absorption of fluid, creates a significant impact on the regression model.

Durbin-Watson Statistic

Durbin-Watson Statistic = 1.36803

From the Durbin-Watson Statistics, we get the value equal to 1.36, which shows that the Heat Transfer Co-efficient has maintained a responsive relationship with the increasing heat absorption of fluid.

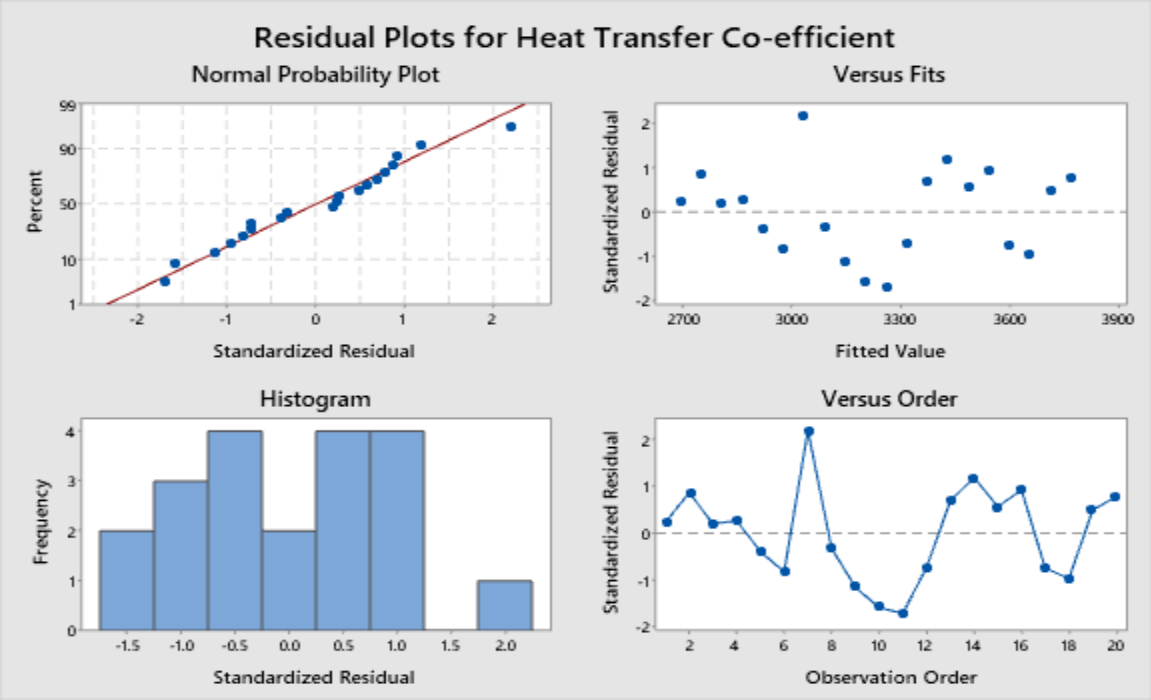

Figure 4.23: Residual Plots for 0.1% Zinc Oxide Solution

From the plots above, we get:

Fits and Diagnostics for Unusual Observations

Obs	Heat Transfer Co-efficient	Fit	Resid	Std Resid	
7	3121.5	3032.4	89.1	2.21	R

R Large residual

Model Summary

S	R-sq	R-sq(adj)	R-sq(pred)
41.7224	98.57%	98.49%	98.31%

We observe that there isn't much variation between the predicted line and the residual plot's observation data. That's why we get our satisfied R-sq value.

Then analyze more on ML algorithms and apply the Simple Linear Regression Model & Support Vector Regression to get a more accurate prediction model. For SVR, we get accuracy is 98.56% & for SLR, we get the accuracy is 96.98%.

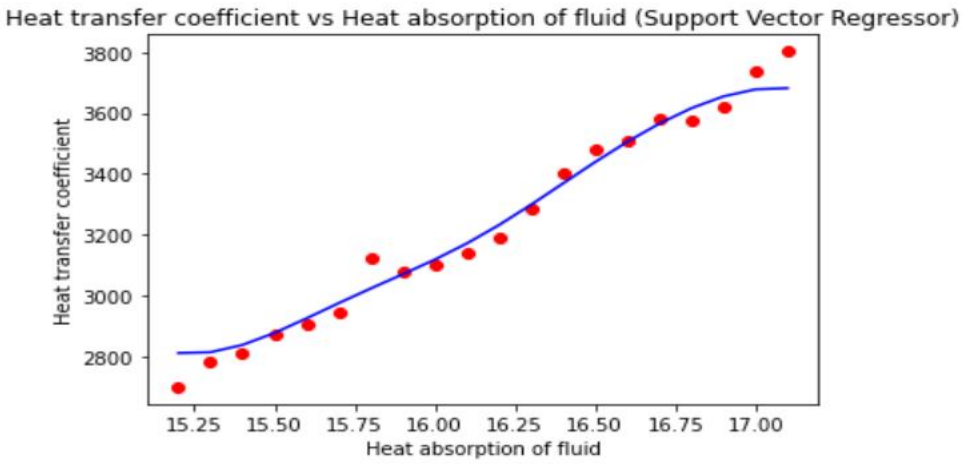


```
Accuracy: 98.56134074037215
```

Figure 4.24: Support Vector Regression Model by using ML for 0.1% Zinc Oxide Solution

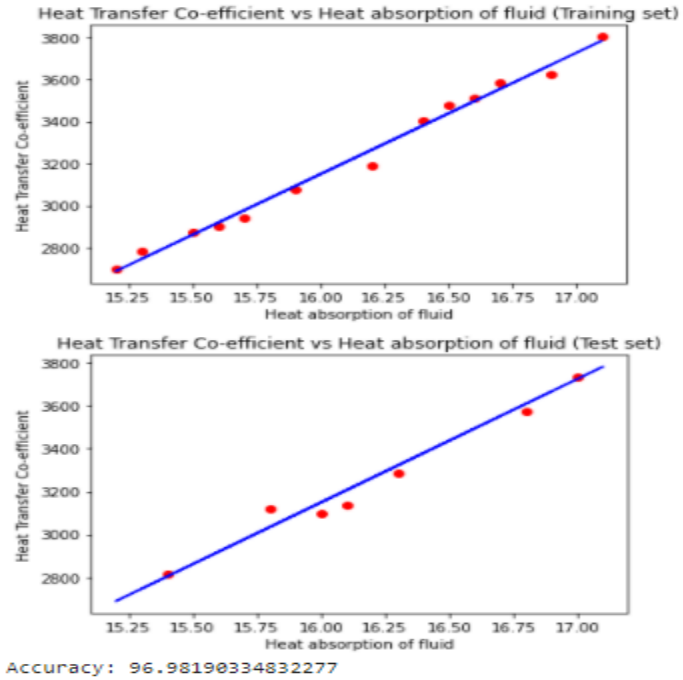

Figure 4.25: Simple Linear Regression Model by using ML for 0.1% Zinc Oxide Solution

From those models, we observe that we get a good prediction model by using Support Vector Regression. Though SLR gives a good prediction, and we get the observation datasets are so close to our predicted line in both cases, but in SVR, observation datasets are closer.

4.1.2.2 0.2% Zinc Oxide Solution:

For 0.2% Zinc Oxide Solution,

Here,

m= 0.35, S= 4178J/kg-K,

$\Delta\theta$= 74.7-73.5= 1.2

ΔT= 13.3

A= 0.10075 m2

Now, h1= $mS\Delta\theta/A\Delta T$

= 1309.55 W/m2-K

Similarly,

h2=1195.36	h11= 1275.39
h3= 1180.27	h12= 1262.53
h4= 1216.85	h13= 1354.37
h5= 1276.59	h14= 1364.71
h6= 1243.48	h15= 1352.49
h7= 1251.76	h16= 1334.63
h8= 1262.67	h17= 1398.28

h9= 1296.84

h10= 1290.42

h18= 1372.35

h19= 1465.53

h20= 1450.36

h mean=1307.164 W/m2-K

We take the dataset for a 0.2% Zinc Oxide Solution and make our predictions using a regression model. There we also apply other models to predict, but the regression fits most. That's why we make a detailed analysis of this. The exact result of the prediction model gives below:

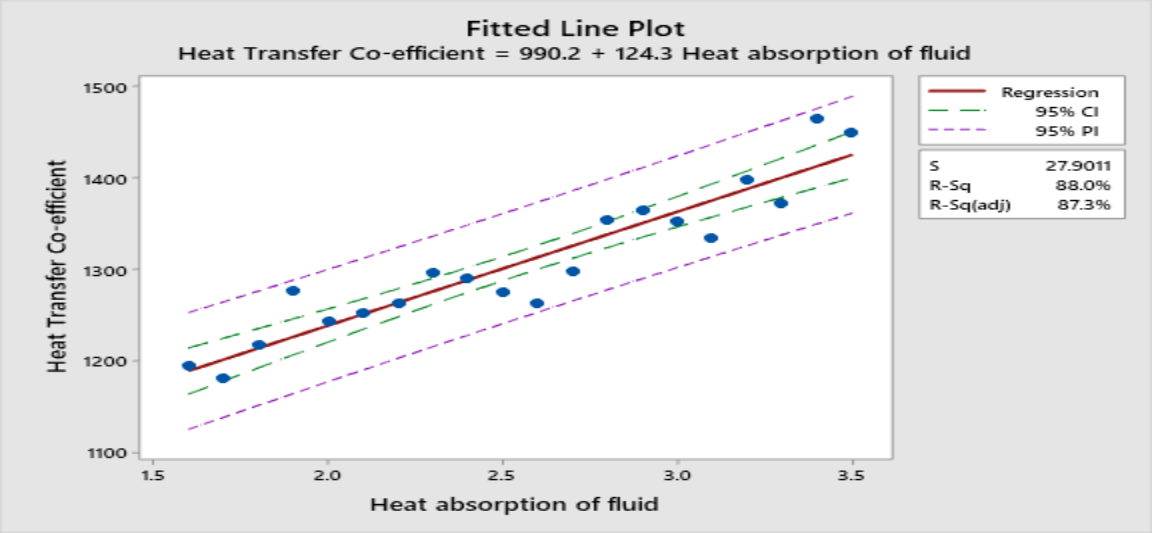

Figure 4.26: Fitted Line Plot for 0.2% Zinc Oxide Solution.

We get a fitted line plot to make our prediction using the regression model from the above figure. It gives us a relationship equation between the Heat Transfer Coefficient and the Heat absorption of fluid.

Regression Equation

Heat Transfer Co-efficient = 990.2 + 124.3 Heat absorption of fluid

Coefficients

Term	Coef	SE Coef	T-Value	P-Value	VIF
Constant	990.2	28.3	35.01	0.000	
Heat absorption of fluid	124.3	10.8	11.49	0.000	1.00

Analysis of Variance

Source	DF	Adj SS	Adj MS	F-Value	P-Value
Regression	1	102736	102736	131.97	0.000
Heat absorption of fluid	1	102736	102736	131.97	0.000
Error	18	14013	778		
Total	19	116749			

From the variance analysis result, we notice from the P-Value, which is equal to 0 & the F-value, which is larger than the F critical value that indicates Heat absorption of fluid, creates a significant impact on the regression model.

Durbin-Watson Statistic

Durbin-Watson Statistic = 1.65890

From the Durbin-Watson Statistics, we get the value equal to 1.65, which shows that the Heat Transfer Co-efficient has maintained a responsive relationship with the increasing heat absorption of fluid.

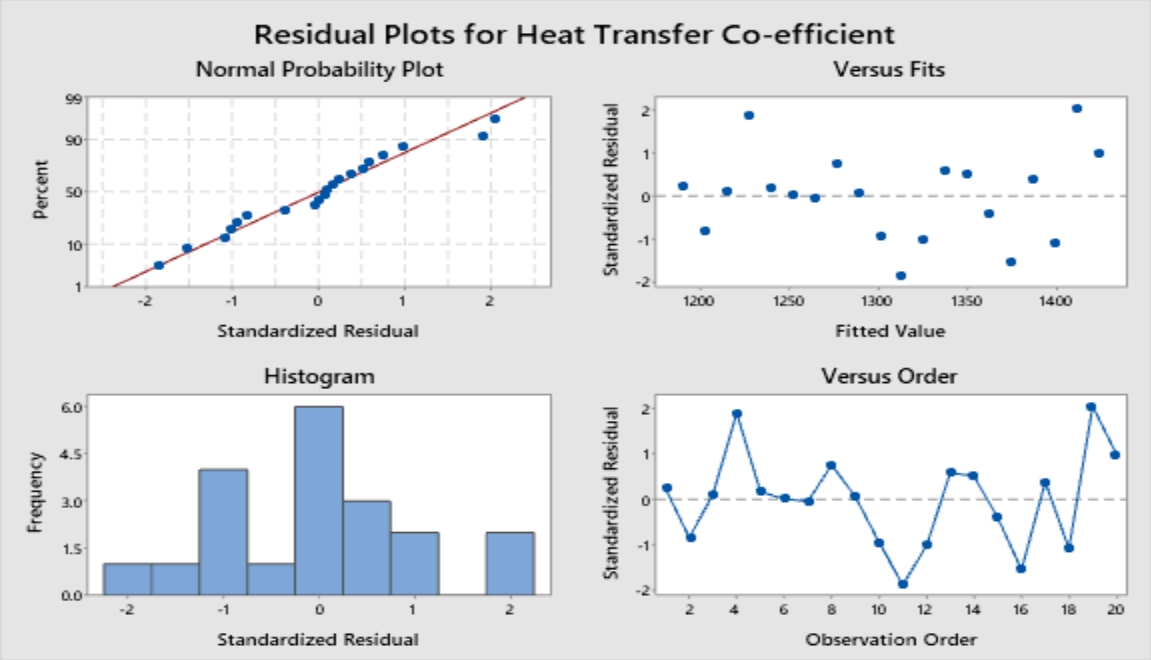

Figure 4.27: Residual Plots for 0.2% Zinc Oxide Solution

From the plots above, we get:

Fits and Diagnostics for Unusual Observations

Obs	Heat Transfer Co-efficient	Fit	Resid	Std Resid	
19	1465.53	1412.81	52.72	2.06	R

R Large residual

Model Summary

S	R-sq	R-sq(adj)	R-sq(pred)
27.9011	88.00%	87.33%	84.90%

We observe that there isn't much variation between the predicted line and the residual plot's observation data. That's why we get our satisfied R-sq value.

Then analyze more on ML algorithms and apply the Simple Linear Regression Model & Support Vector Regression to get a more accurate prediction model. For SVR, we get accuracy 87.61% & for SLR, we get accuracy of 90.43%.

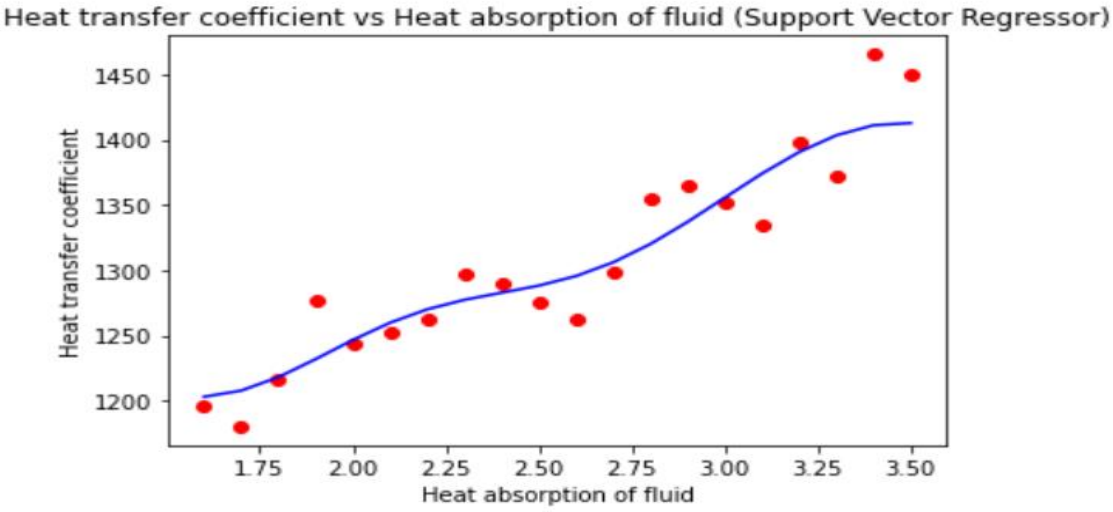

Figure 4.28: Support Vector Regression Model by using ML for 0.2% Zinc Oxide Solution

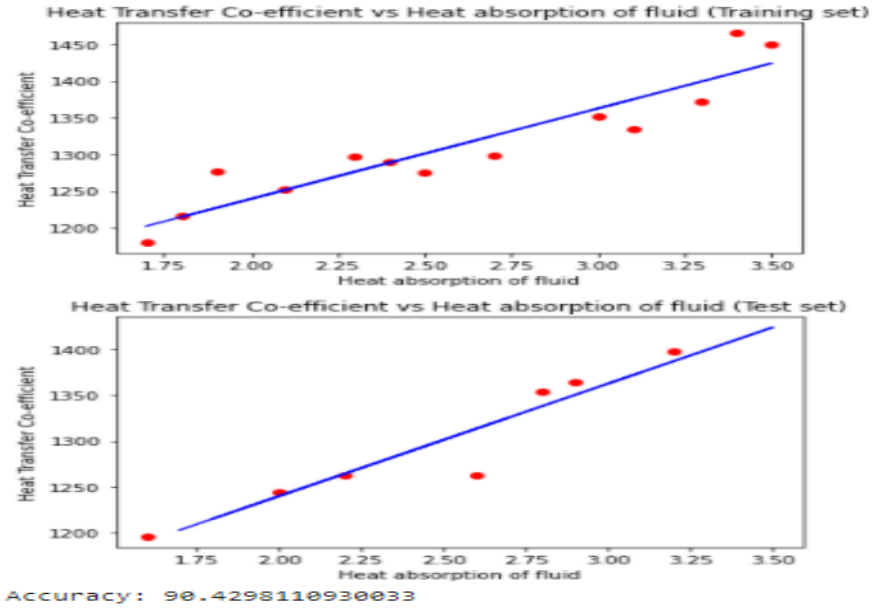

Figure 4.29: Simple Linear Regression Model by using ML for 0.2% Zinc Oxide Solution

From the model, we observe that we get a good prediction model by using the Simple Linear Regression Model, and there we get the observation datasets that are so close to our predicted line.

4.1.2.3. 0.3% Zinc Oxide Solution:

For 0.3% Zinc Oxide Solution,

Here,

m= 0.35, S= 4178J/kg-K,

$\Delta\theta$= 78.9-78.4=.5

ΔT= 15.1

A= 0.10075 m2

Now, h1= $mS\Delta\theta/A\Delta T$

= 481.02 W/m2-K

Similarly,

h2= 444.23	h11= 471.28
h3= 439.84	h12= 460.41
h4= 463.88	h13= 482.38
h5= 448.22	h14= 470.24
h6= 449.35	h15= 491.16
h7= 438.55	h16= 510.31
h8= 485.24	h17= 495.21

h9= 492.75

h10= 461.29

h18= 485.24

h19= 542.33

h20= 532.15

h mean= 474.0405 W/m2-K

We take the dataset for 0.3% Zinc Oxide Solution and make our predictions using a regression model. There we also apply other models to predict, but the regression fits most. That's why we make a detailed analysis of this. The precise result of the prediction model gives below:

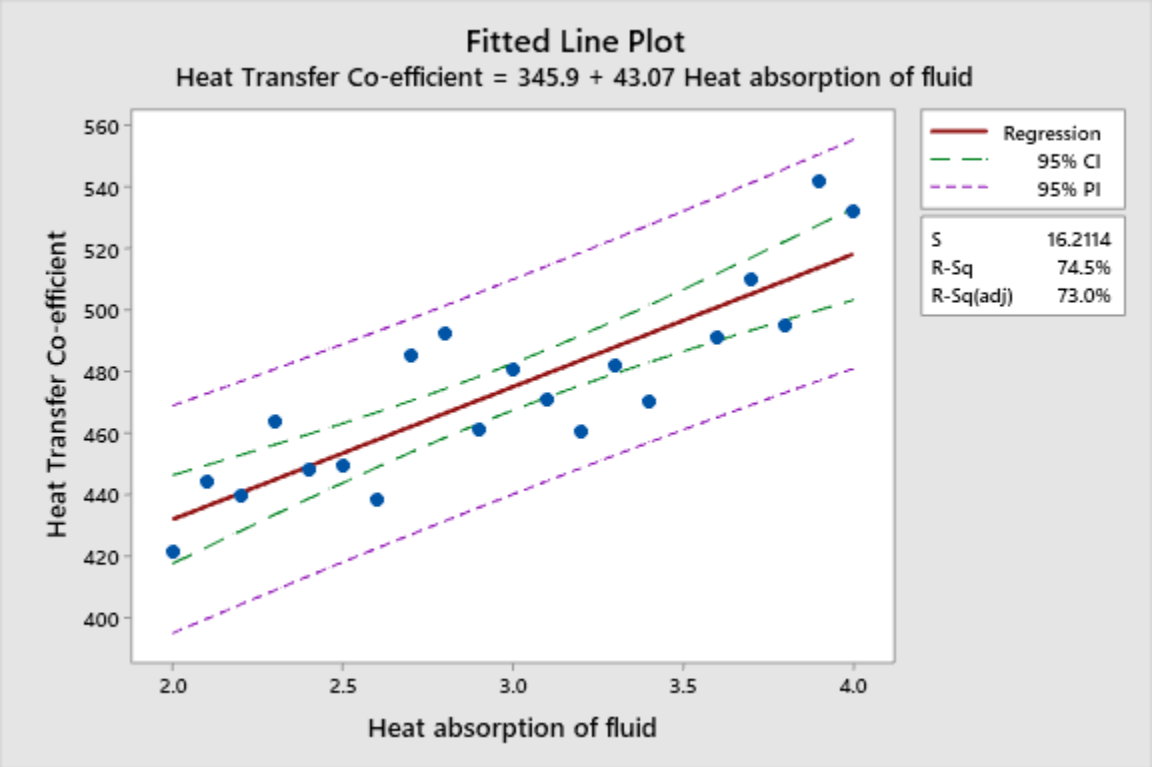

Figure 4.30: Fitted Line Plot for 0.3% Zinc Oxide Solution.

Regression Equation

Heat Transfer Co-efficient = 345.9 + 43.07 Heat absorption of fluid

Coefficients

Term	Coef	SE Coef	T-Value	P-Value	VIF
Constant	345.9	18.1	19.16	0.000	
Heat absorption of fluid	43.07	5.94	7.24	0.000	1.00

Analysis of Variance

Source	DF	Adj SS	Adj MS	F-Value	P-Value
Regression	1	13794	13794.3	52.49	0.000
Heat absorption of fluid	1	13794	13794.3	52.49	0.000
Error	18	4731	262.8		
Total	19	18525			

From the variance analysis result, we notice from the P-Value, which is equal to 0 & the F-value, which is larger than the F critical value that indicates Heat absorption of fluid, creates a significant impact on the regression model.

Durbin-Watson Statistic

Durbin-Watson Statistic = 1.80660

From the Durbin-Watson Statistics, we get the value equal to 1.81, which shows that the Heat Transfer Co-efficient has maintained a decent relationship with the increasing heat absorption of fluid.

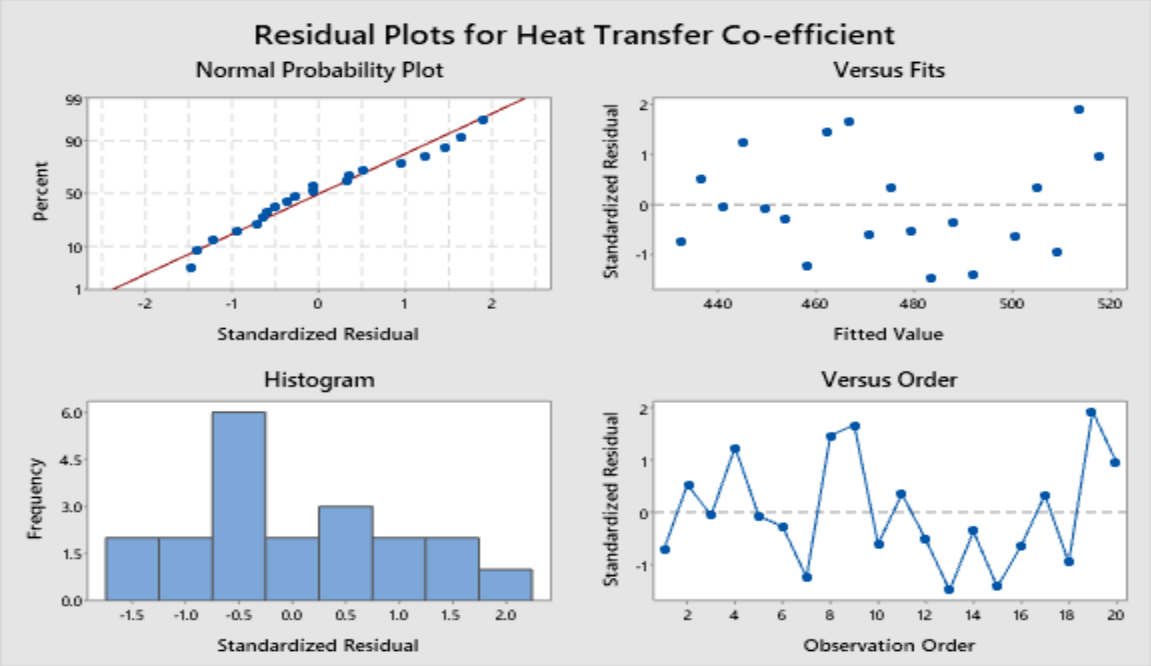

Figure 4.31: Residual Plots for 0.3% Zinc Oxide Solution

Model Summary

S	R-sq	R-sq(adj)	R-sq(pred)
16.2114	74.46%	73.05%	68.42%

We observe that there isn't much variation between the predicted line and the residual plot's observation data. That's why we get our satisfied R-sq value.

Then analyze more on ML algorithms and apply the Simple Linear Regression Model & Support Vector Regression to get a more accurate prediction model. For SVR, we get an accuracy of 97.46% & for SLR, and we get an accuracy of 86.99%.

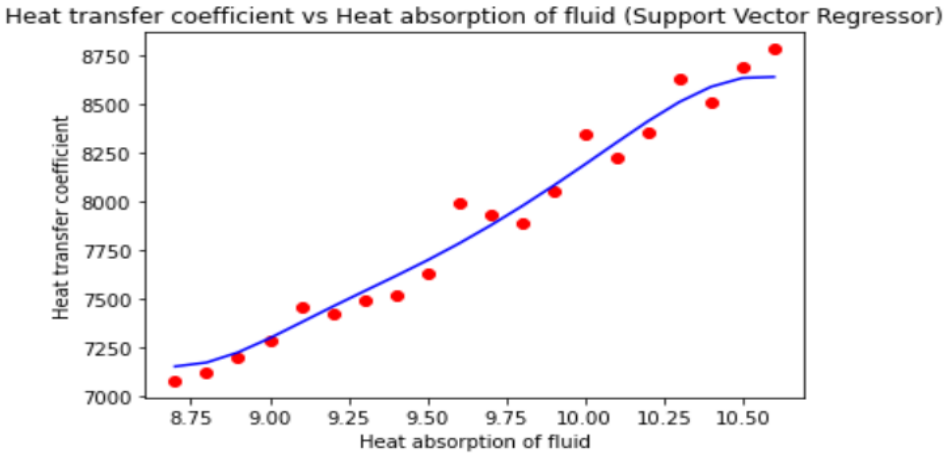


```
Accuracy: 97.45142909050121
```

Figure 4.32: Support Vector Regression Model by using ML for 0.3% Zinc Oxide Solution

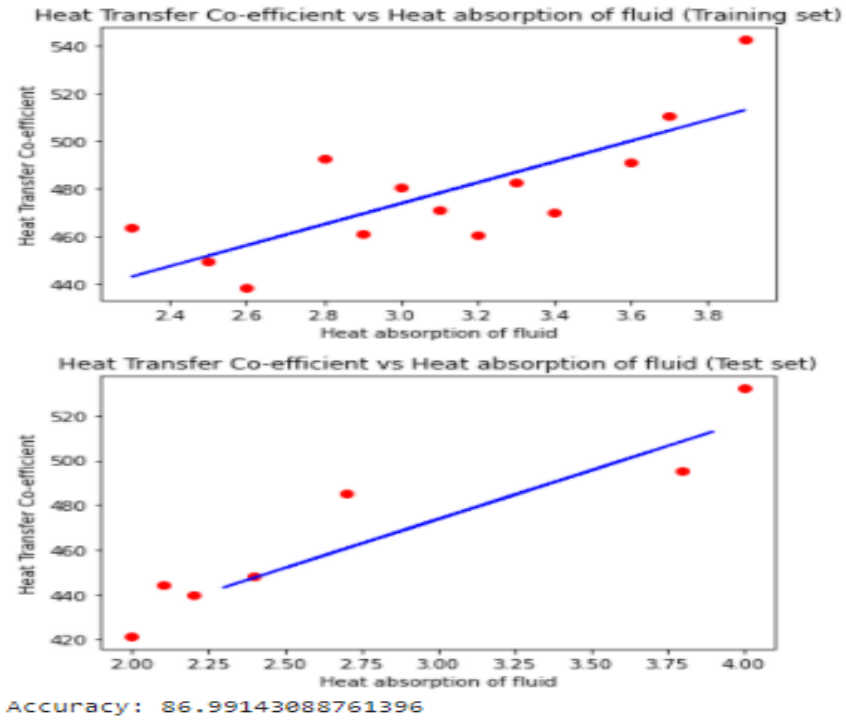

Figure 4.33: Simple Linear Regression Model by using ML for 0.3% Zinc Oxide Solution

From the model, we observe that we get a good prediction model by using the Support Vector Regression Model, and there we get the observation datasets that are so close to our predicted line.

4.1.2.4. 0.4% Zinc Oxide solution:

For 0.4% Zinc Oxide Solution,

Here,

m= 0.35, S= 4178J/kg-K,

$\Delta\theta$= 91.5-90.8= .7

ΔT= 17.9

A= 0.10075 m2

Now, h1= mSΔθ/AΔT

= 567.59 W/m2-K

Similarly,

h2= 521.84	h11= 571.67
h3= 542.46	h12= 569.57
h4= 550.33	h13= 571.86
h5= 543.31	h14= 589.31
h6= 545.43	h15= 581.49
h7= 555.98	h16= 589.43
h8= 559.13	h17= 592.25
h9= 564.49	h18= 599.59
h10= 568.15	h19= 600.41
	h20= 601.37

h mean= 569.283 W/m2-K

We take the dataset for 0.4% Zinc Oxide Solution and make our predictions using a regression model. There we also apply other models to predict, but the regression fits most. That's why we make a detailed analysis of this. The precise result of the prediction model gives below:

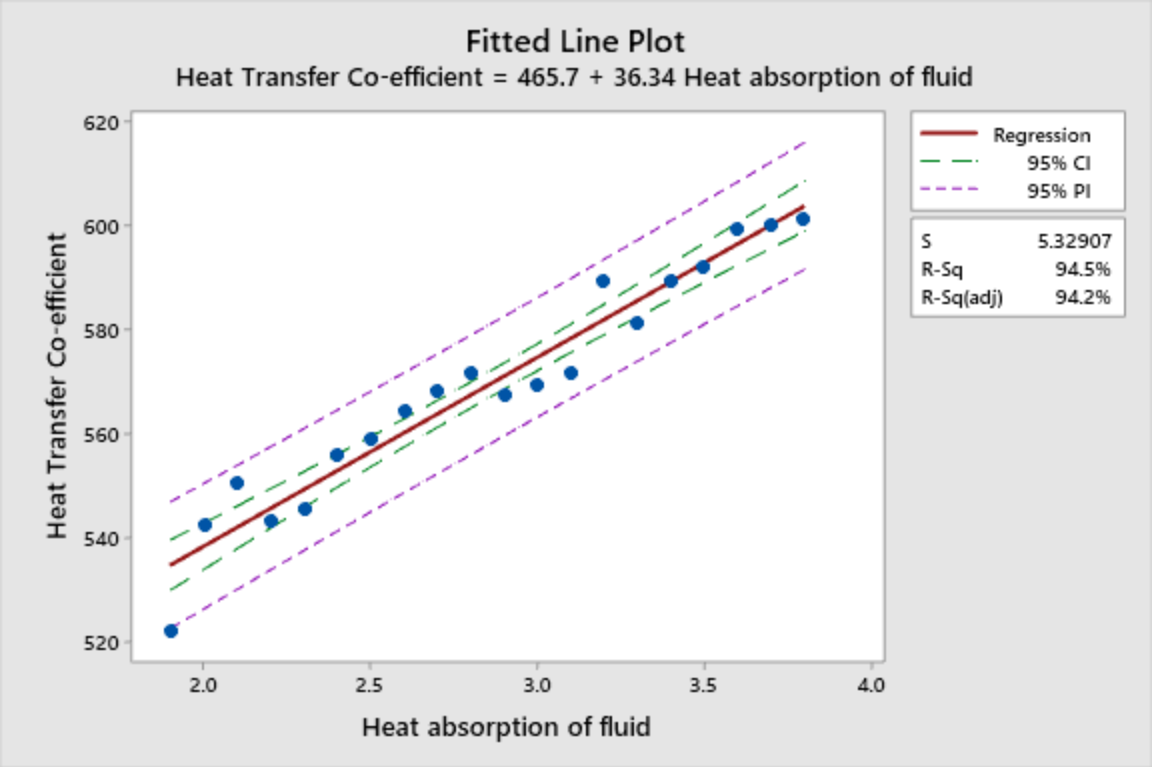

Figure 4.34: Fitted Line Plot for 0.4% Zinc Oxide Solution.

We get a fitted line plot to make our prediction using the regression model from the above figure. It gives us a relationship equation between the Heat Transfer Coefficient and the Heat absorption of fluid.

Regression Equation

Heat Transfer Co-efficient = 465.71 + 36.34 Heat absorption of fluid

Coefficients

Term	Coef	SE Coef	T-Value	P-Value	VIF
Constant	465.71	6.01	77.50	0.000	
Heat absorption of fluid	36.34	2.07	17.59	0.000	1.00

Analysis of Variance

Source	DF	Adj SS	Adj MS	F-Value	P-Value
Regression	1	8782.0	8781.96	309.23	0.000
Heat absorption of fluid	1	8782.0	8781.96	309.23	0.000
Error	18	511.2	28.40		
Total	19	9293.1			

From the variance analysis result, we notice from the P-Value, which is equal to 0 & the F-value, which is larger than the F critical value that indicates Heat absorption of fluid, creates a significant impact on the regression model.

Durbin-Watson Statistic

Durbin-Watson Statistic =	1.77521

From the Durbin-Watson Statistics, we get the value equal to 1.77, which shows that the Heat Transfer Co-efficient has maintained a decent relationship with the increasing heat absorption of fluid.

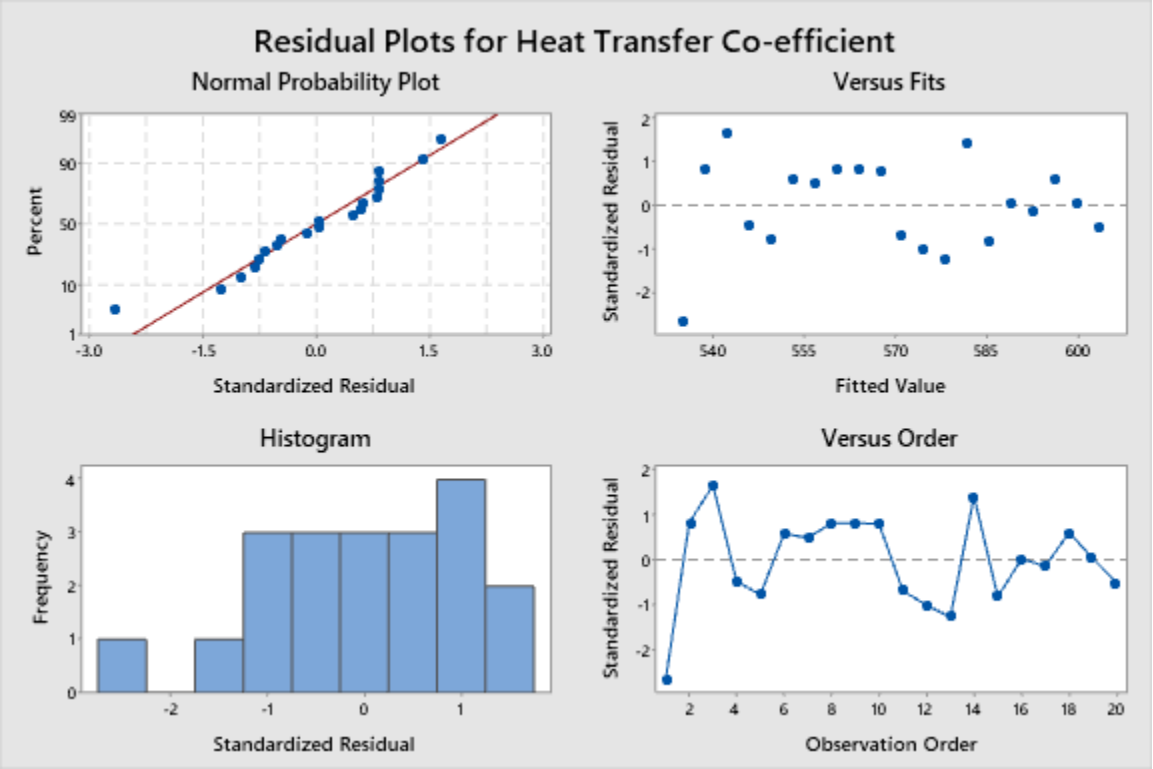

Figure 4.35: Residual Plots for 0.4% Zinc Oxide Solution

From the plots above, we get:

Fits and Diagnostics for Unusual Observations

Obs	Heat Transfer Co-efficient	Fit	Resid	Std Resid	
1	521.84	534.76	-12.92	-2.69	R

R Large residual

Model Summary

S	R-sq	R-sq(adj)	R-sq(pred)
5.32907	94.50%	94.19%	92.82%

We observe that there isn't much variation between the predicted line and the residual plot's observation data. That's why we get our satisfied R-sq value. Then analyze more on ML algorithms and apply the Simple Linear Regression Model & Support Vector Regression to get a more accurate prediction model. For SVR, we get an accuracy is 94.42% & for SLR, we get accuracy is 90.38%.

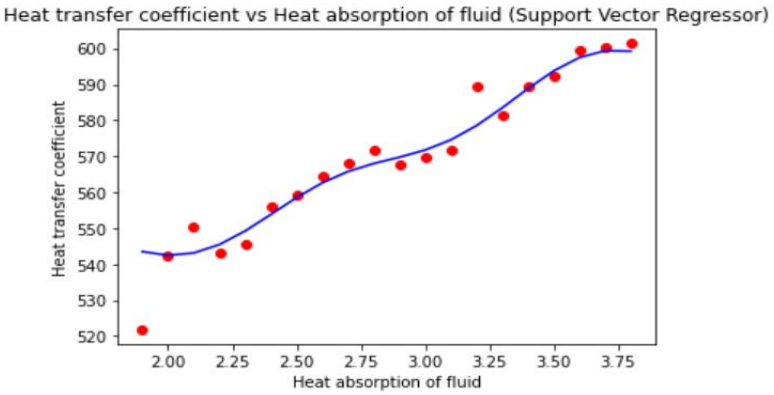


```
Accuracy: 94.42155909465204
```

Figure 4.36: Support Vector Regression Model by using ML for 0.4% Zinc Oxide Solution

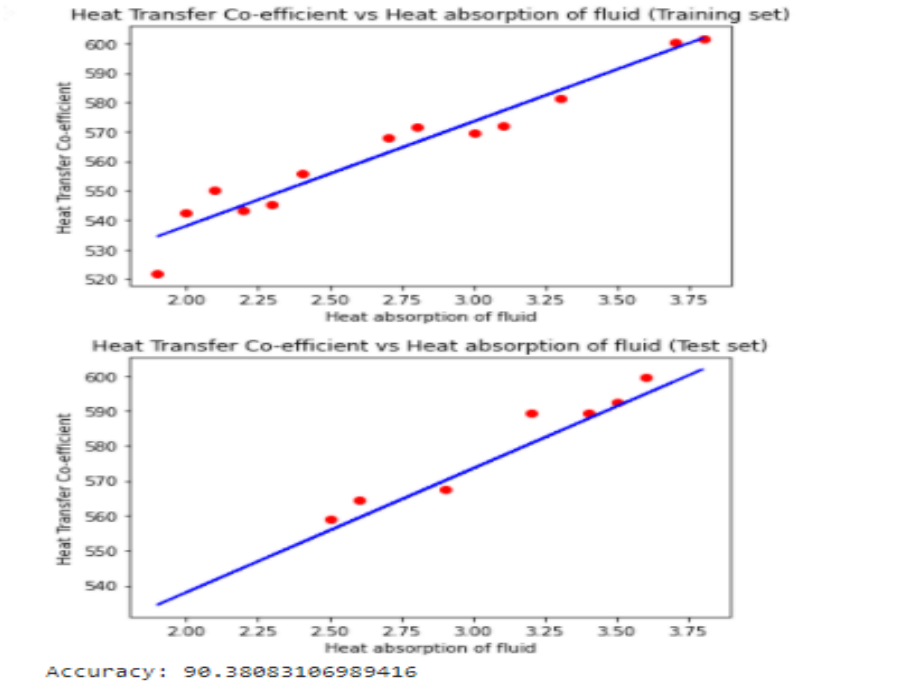

Figure 4.37: Simple Linear Regression Model by using ML for 0.4% Zinc Oxide Solution

From the model, we observe that we get a good prediction model by using the Support Vector Regression Model, and there we get the observation datasets that are so close to our predicted line.

4.1.2.5. Heat Transfer Coefficient of Zinc Oxide Solution:

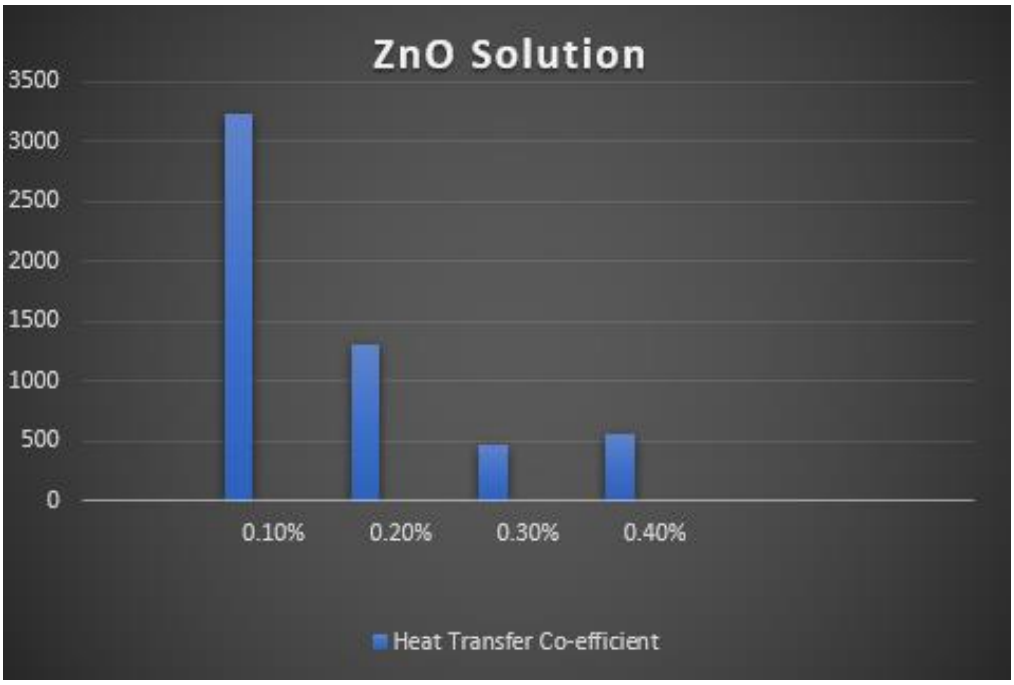

Figure 4.38: Heat Transfer Co-efficient Bar-chart of ZnO Solution

From the above figure, we can see as the concentration of Zinc Oxide nanoparticles increased, the heat transfer coefficient of nanofluids decreases, but after a particular time, it again increased. So we found that 0.10% Graphene nanofluid gives the highest value of heat transfer co-efficient and 0.30% gives lower value, but 0.40% gives higher value than 0.30% concentration of Zinc Oxide nanofluids.

4.1.3. Heat Transfer Coefficient Measurement Of Graphene Oxide Solution:

4.1.3.1. 0.1% Graphene Oxide Solution:

For 0.1% Graphene Oxide Solution,

Here,

m= 0.35, S= 4178J/kg-K,

$\Delta\theta$= 78.9-76.6= 2.3

ΔT= 7

A= 0.10075 m2

Now, h1= m$S\Delta\theta$/AΔT

= 4768.933 W/m2-K

Similarly,

h2= 4140.68	h11= 4601.52
h3= 4170.75	h12= 4668.983
h4= 4234.62	h13= 4869.34
h5= 4297.74	h14= 4951.36
h6= 4314.25	h15= 4801.38
h7= 4309.17	h16= 5089.42
h8= 4350.63	h17= 5190.45
h9= 4550.64	h18= 5221.52
h10= 4568.71	h19= 5323.94
	h20= 5420.26

h mean= 4693.299 W/m2-K

We take the dataset for 0.1% Graphene Solution and make our predictions by using a regression model.

There we also apply other models to predict, but the regression fits most. That's why we make a detailed analysis of this. The precise result of the prediction model gives below:

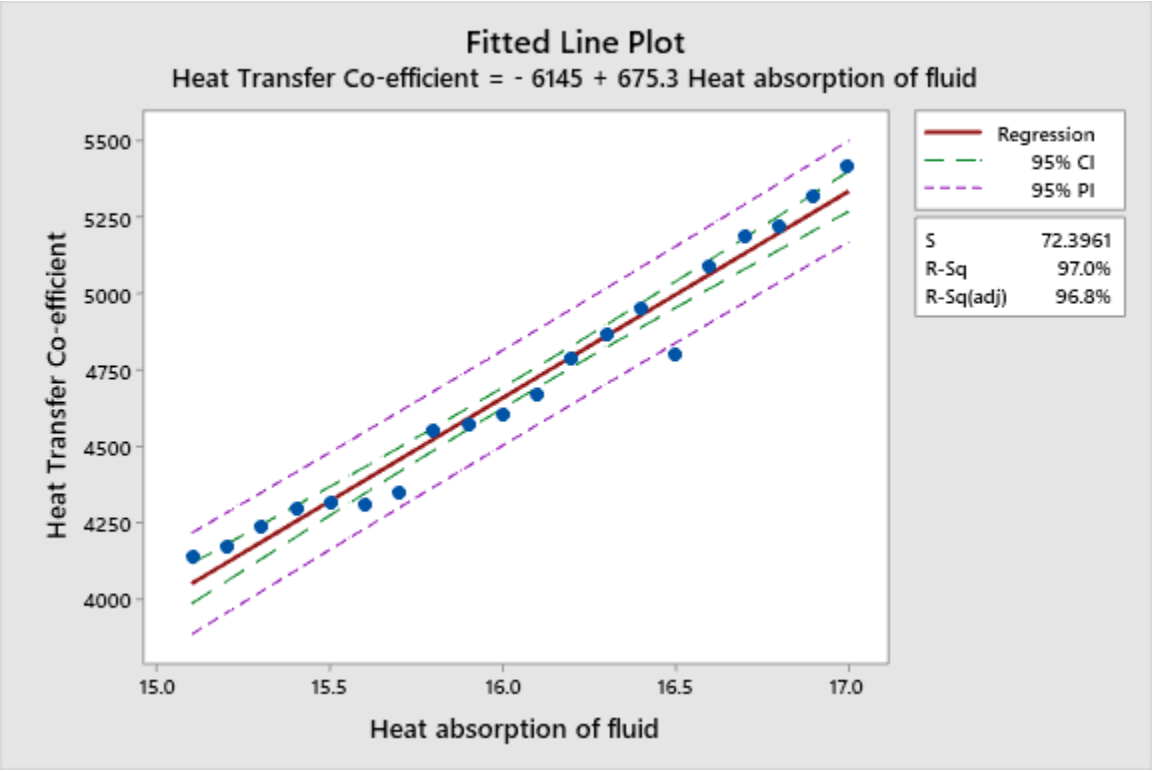

Figure 4.39: Fitted Line Plot for 0.1% Graphene Oxide Solution.

From the above figure, we get a fitted line plot to make our prediction using a Regression model, which gives us a relationship equation between the Heat Transfer Coefficient and the Heat absorption of fluid.

Regression Equation

Heat Transfer Co-efficient = -6145 + 675.3 Heat absorption of fluid

Coefficients

Term	Coef	SE Coef	T-Value	P-Value	VIF
Constant	-6145	451	-13.63	0.000	
Heat absorption of fluid	675.3	28.1	24.05	0.000	1.00

Analysis of Variance

Source	DF	Adj SS	Adj MS	F-Value	P-Value
Regression	1	3032510	3032510	578.59	0.000
Heat absorption of fluid	1	3032510	3032510	578.59	0.000
Error	18	94342	5241		
Total	19	3126852			

From the variance analysis result, we notice from the P-Value, which is equal to 0 & the F-value, which is larger than the F critical value that indicates Heat absorption of fluid, creates a significant impact on the regression model.

Durbin-Watson Statistic

Durbin-Watson Statistic = 1.42981

From the Durbin-Watson Statistics, we get the value equal to 1.42, which shows that the Heat Transfer Co-efficient has maintained a responsive relationship with the increasing heat absorption of fluid.

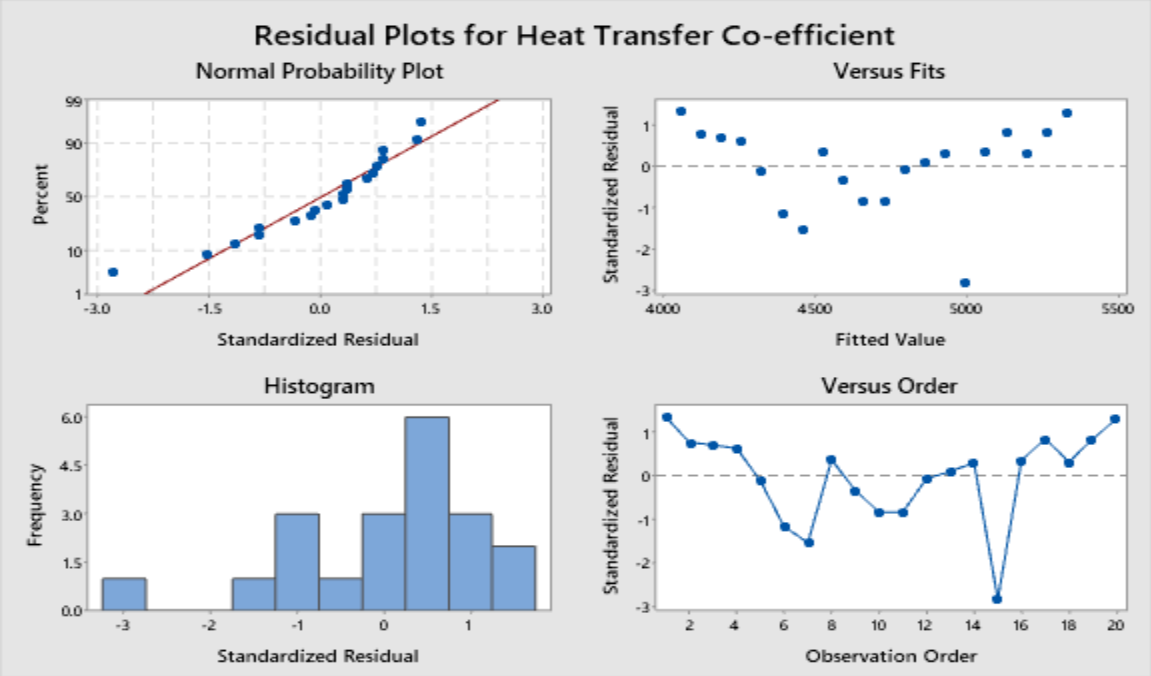

Figure 4.40: Residual Plots for 0.1% Graphene Oxide Solution

From the plots above, we get

Fits and Diagnostics for Unusual Observations

Obs	Heat Transfer Co-efficient	Fit	Resid	Std Resid	
15	4801.4	4997.2	-195.8	-2.82	R

R Large residual

Model Summary

S	R-sq	R-sq(adj)	R-sq(pred)
72.3961	96.98%	96.82%	96.23%

We observe that there isn't much variation between the predicted line and the residual plot's observation data. That's why we get our satisfied R-sq value.

Then analyze more on ML algorithms and apply the Simple Linear Regression Model & Support Vector Regression to get a more accurate prediction model. For SVR, we get accuracy is 96.96% & for SLR, we get an accuracy is 93.79%.

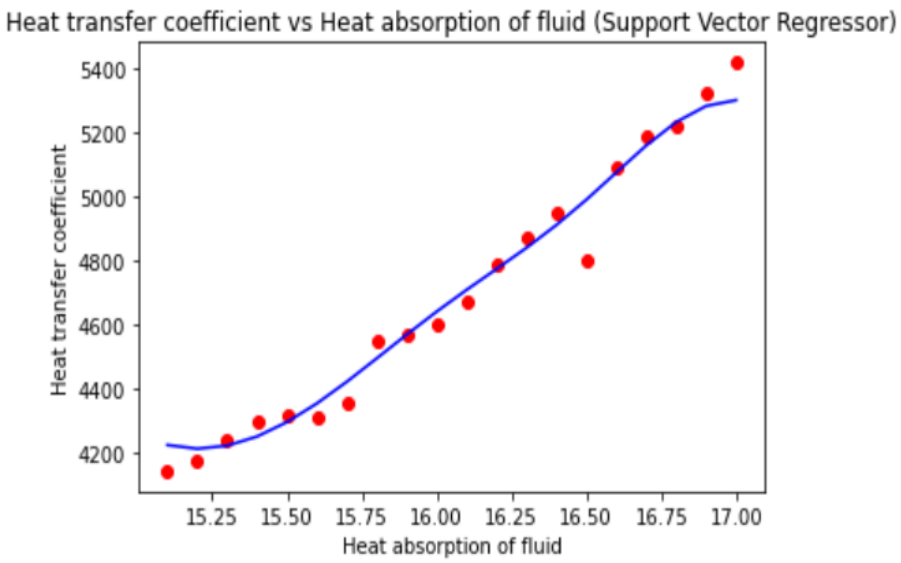


```
Accuracy: 96.95975198703474
```

Figure 4.41: Support Vector Regression Model by using ML for 0.1% Graphene Oxide Solution

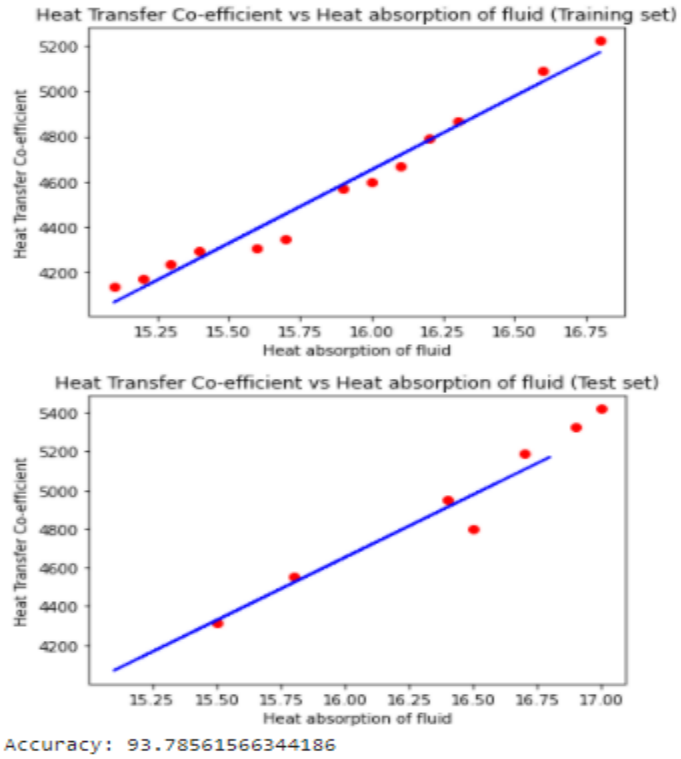

Figure 4.42: Simple Linear Regression Model by using ML for 0.1% Graphene Oxide Solution

From the model, we observe that we get a good prediction model by using the Support Vector Regression Model, and there we get the observation datasets that are so close to our predicted line.

4.1.3.2 0.3% Graphene Oxide Solution:

For 0.3% Graphene Oxide Solution,

Here,

m= 0.35, S= 4178J/kg-K,

$\Delta\theta$= 64.3-59.6= 4.7

$\Delta T = 9.8$

A= 0.10075 m2

Now, $h1 = mS\Delta\theta/A\Delta T$

= 6960.86 W/m2-K

Similarly,

h2= 7120.46	h11= 7932.14
h3= 7200.52	h12= 7890.56
h4= 7290.46	h13= 8054.45
h5= 7459.73	h14= 8345.754
h6= 7420.64	h15= 8230.56
h7= 7490.63	h16= 8360.54
h8= 7519.61	h17= 8630.48
h9= 7629.53	h18= 8512.85
h10= 7990.54	h19= 8690.63
	h20= 8785.74

h mean=7881.81.4

We take the dataset for 0.3% Graphene Solution and make our predictions by using a regression model.

There we also apply other models to predict, but the regression fits most. That's why we make a detailed analysis of this. The precise result of the prediction model gives below:

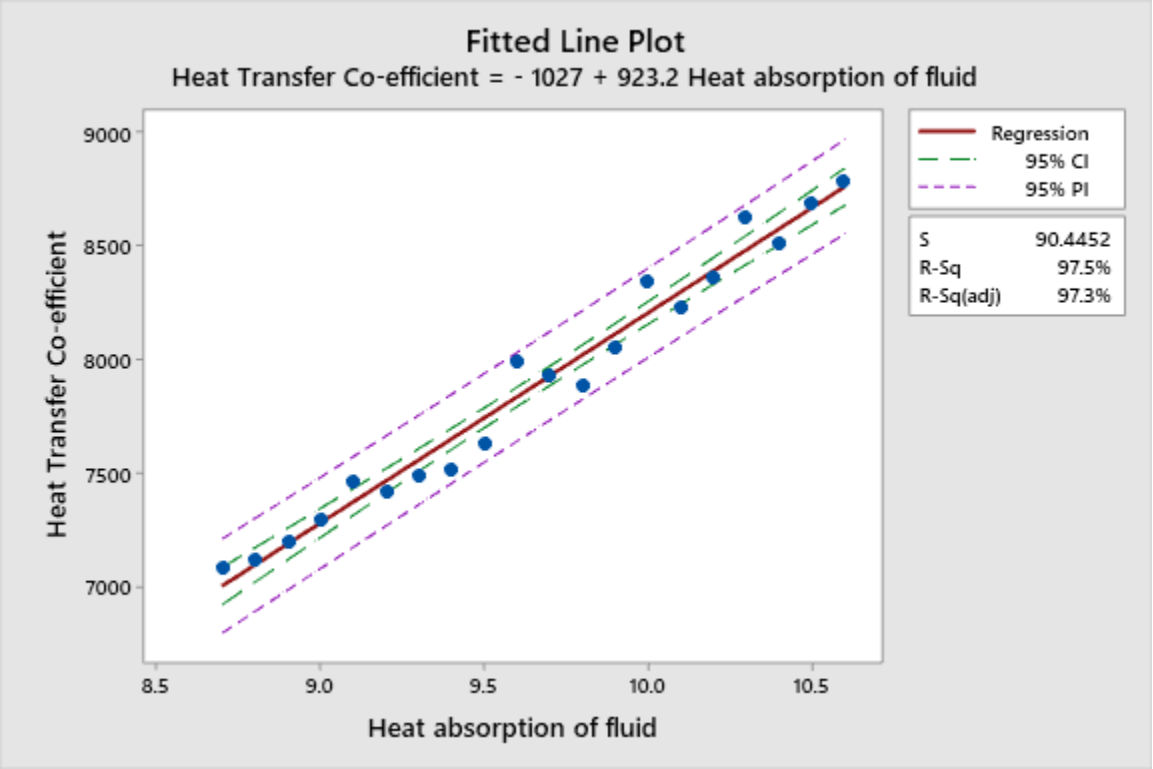

Figure 4.43: Fitted Line Plot for 0.3% Graphene Oxide Solution.

From the above figure, we get a fitted line plot to make our prediction by using a Regression model, and that gives us a relationship equation between the Heat Transfer Co-efficient and the Heat absorption of
fluid.

Regression Equation

Heat Transfer Co-efficient = -1027 + 923.2 Heat absorption of fluid

Coefficients

Term	Coef	SE Coef	T-Value	P-Value	VIF
Constant	-1027	339	-3.03	0.007	
Heat absorption of fluid	923.2	35.1	26.32	0.000	1.00

Analysis of Variance

Source	DF	Adj SS	Adj MS	F-Value	P-Value
Regression	1	5667393	5667393	692.81	0.000
Heat absorption of fluid	1	5667393	5667393	692.81	0.000
Error	18	147246	8180		
Total	19	5814639			

From the variance analysis result, we notice from the P-Value, which is equal to 0 & the F-value, which is larger than the F critical value that indicates Heat absorption of fluid, creates a significant impact on the regression model.

Durbin-Watson Statistic

Durbin-Watson Statistic = 2.14525

From the Durbin-Watson Statistics, we get the value equal to 2.15, which shows that the Heat Transfer Co-efficient has maintained a decent relationship with the increasing heat absorption of fluid.

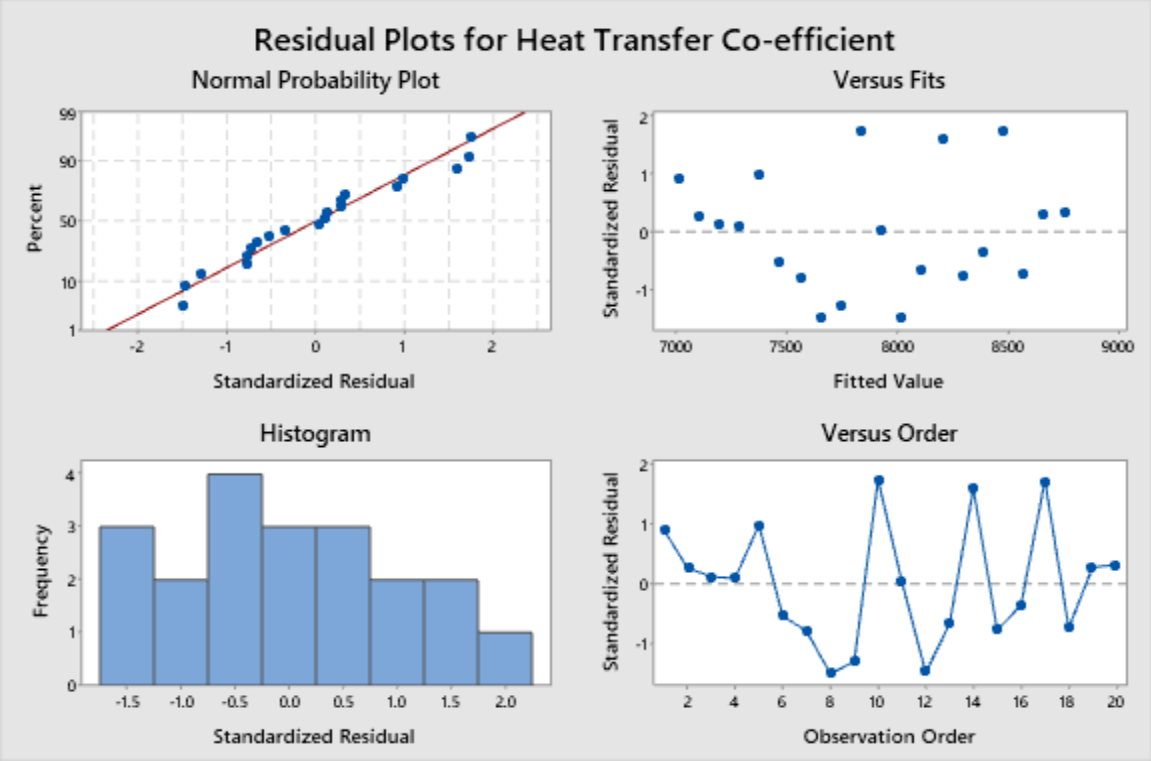

Figure 4.44: Residual Plots for 0.3% Graphene Oxide Solution

Model Summary

S	R-sq	R-sq(adj)	R-sq(pred)
90.4452	97.47%	97.33%	97.01%

We observe that there isn't much variation between the predicted line and the residual plot's observation data. That's why we get our satisfied R-sq value.

Then analyze more on ML algorithms and apply the Simple Linear Regression Model & Support Vector Regression to get a more accurate prediction model. For SVR, we get accuracy is 97.45% & for SLR, we get accuracy is 95.34%.

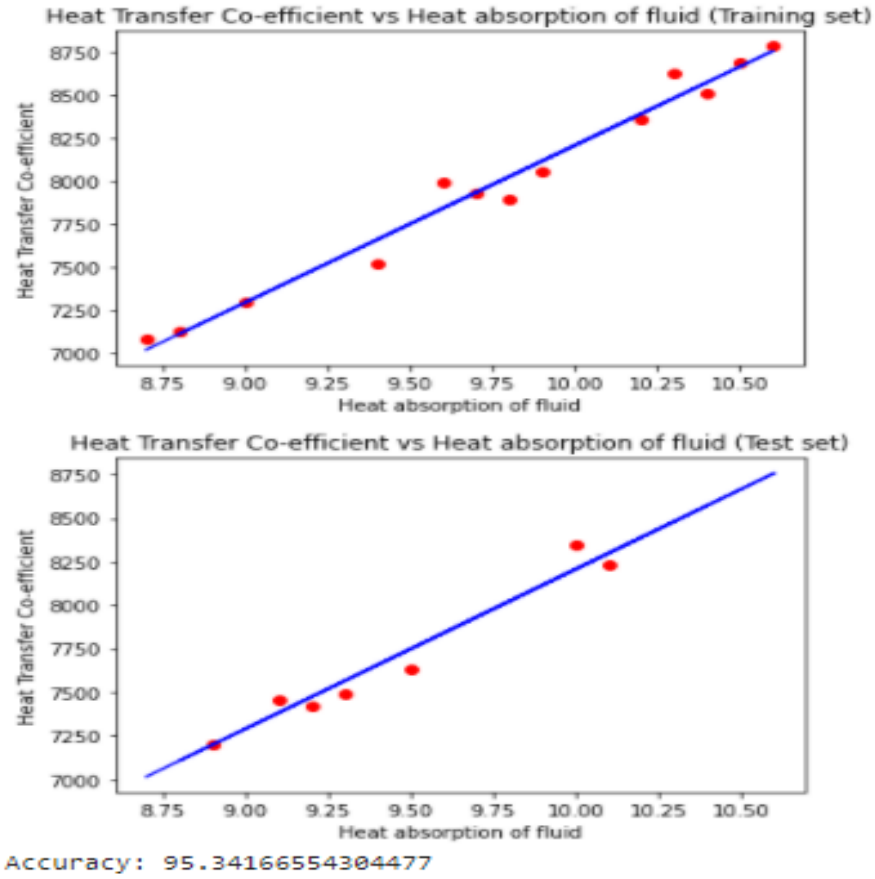

Figure 4.45: Simple Linear Regression Model by using ML for 0.3% Graphene Oxide Solution

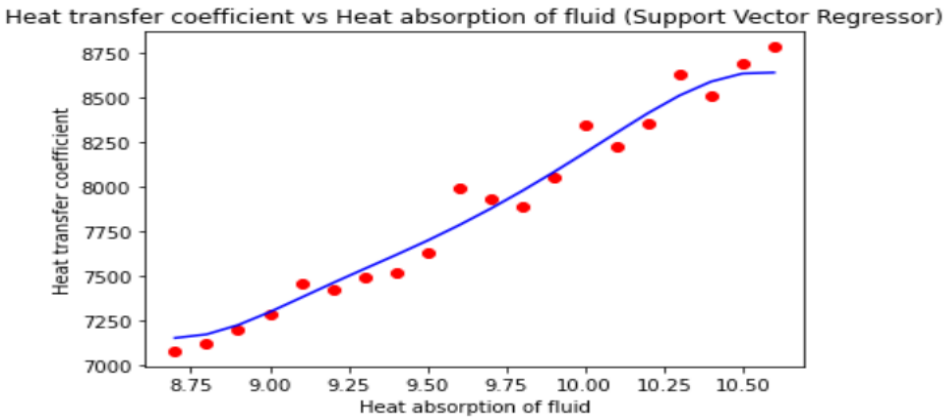


```
Accuracy: 97.45142909050121
```

Figure 4.46: Support Vector Regression Model by using ML for 0.3% Graphene Oxide Solution

From the model, we observe that we get a good prediction model by using the Support Vector Regression Model and there we get the observation datasets are so close to our predicted line.

4.1.3.3. 0.5% Graphene Oxide Solution:

For 0.5% Graphene Oxide Solution,

Here,

m= 0.35, S= 4178J/kg-K,

$\Delta\theta$= 70.7-59.4= 11.3

ΔT= 9

A= 0.10075 m2

Now, h1= m$S\Delta\theta$/AΔT

= 18223.31 W/m2-K

Similarly,

h2= 16310.52

h3= 16488.52

h4= 16531.51

h5= 17892.58

h6= 17156.56

h7= 17320.72

h8= 17542.84

h9= 17649.59

h10= 17324.65

h11= 18398.52

h12= 18521.42

h13= 18783.35

h14= 20421.47

h15= 18452.86

h16= 18990.72

h17= 20653.21

h18= 20290.32

h19= 20653.21

h20= 21500.37

h mean=18286.58

We take the dataset for 0.5% Graphene Solution and make our predictions by using a regression model. There we also apply other models to predict, but the regression fits most. That's why we make a detailed analysis of this. The exact result of the prediction model gives below:

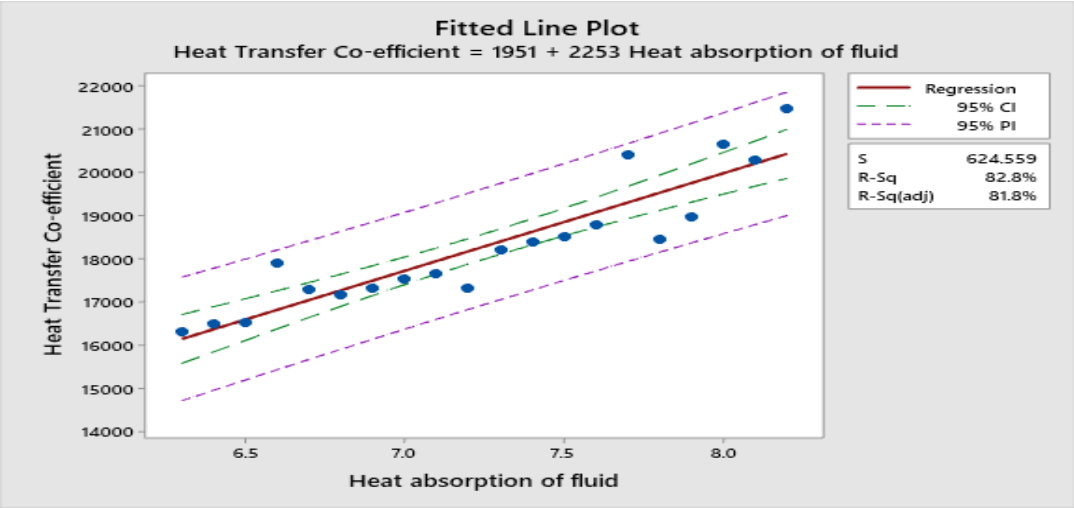

Figure 4.47: Fitted Line Plot for 0.5% Graphene Oxide Solution.

From the above figure, we get a fitted line plot to make our prediction by using a Regression model, and

that gives us a relationship equation between the Heat Transfer Coefficient and the Heat absorption of fluid.

Regression Equation

Heat Transfer Co-efficient = 1951 + 2253 Heat absorption of fluid

Coefficients

Term	Coef	SE Coef	T-Value	P-Value	VIF
Constant	1951	1761	1.11	0.283	
Heat absorption of fluid	2253	242	9.30	0.000	1.00

Analysis of Variance

Source	DF	Adj SS	Adj MS	F-Value	P-Value
Regression	1	33765927	33765927	86.56	0.000
Heat absorption of fluid	1	33765927	33765927	86.56	0.000
Error	18	7021324	390074		
Total	19	40787251			

From the result of the analysis of variance, we notice from the P-Value, which is equal to 0 & the F-value, which is larger than the F critical value that indicates Heat absorption of fluid creates a significant impact on the regression model.

Durbin-Watson Statistic

Durbin-Watson Statistic = 1.88112

From the Durbin-Watson Statistics, we get the value equal to 1.89, which shows that the Heat Transfer Co-efficient has maintained a decent relationship with the increasing heat absorption of fluid.

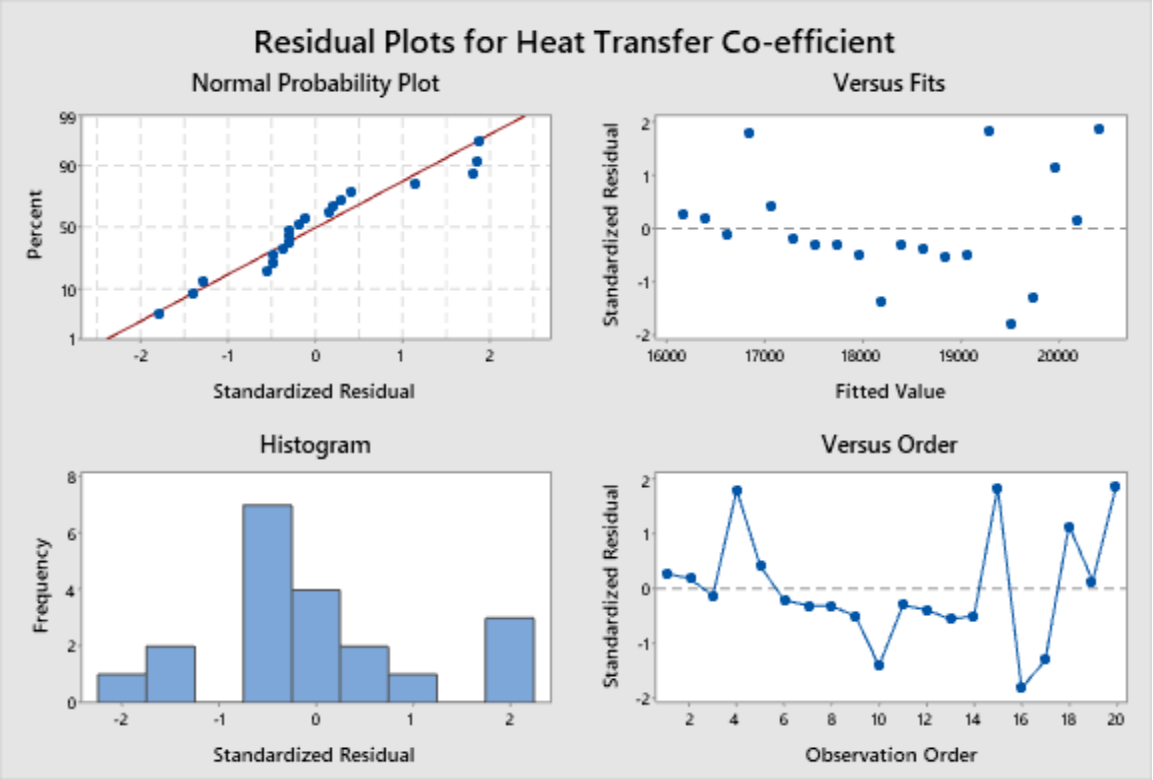

Figure4.48: Residual Plots for 0.5% Graphene Oxide Solution

Model Summary

S	R-sq	R-sq(adj)	R-sq(pred)
624.559	82.79%	81.83%	78.21%

We observe that there isn't much variation between the predicted line and the residual plot's observation data. That's why we get our satisfied R-sq value.

Then analyze more on ML algorithms and apply the Simple Linear Regression Model & Support Vector Regression to get a more accurate prediction model. For SVR, we get an accuracy is 81.97% & for SLR, we get accuracy is 88.19%

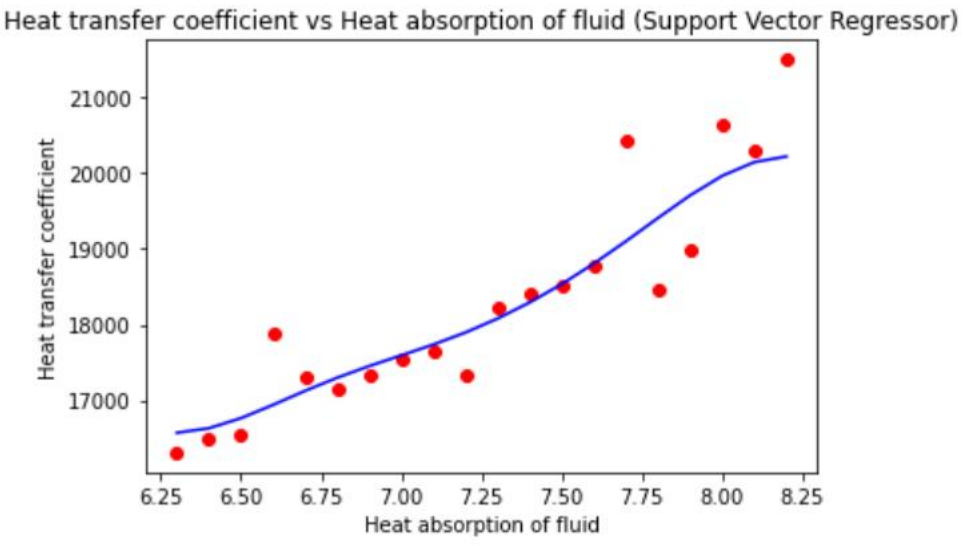


```
Accuracy: 81.97306707142515
```

Figure 4.49: Support Vector Regression Model by using ML for 0.5% Graphene Oxide Solution

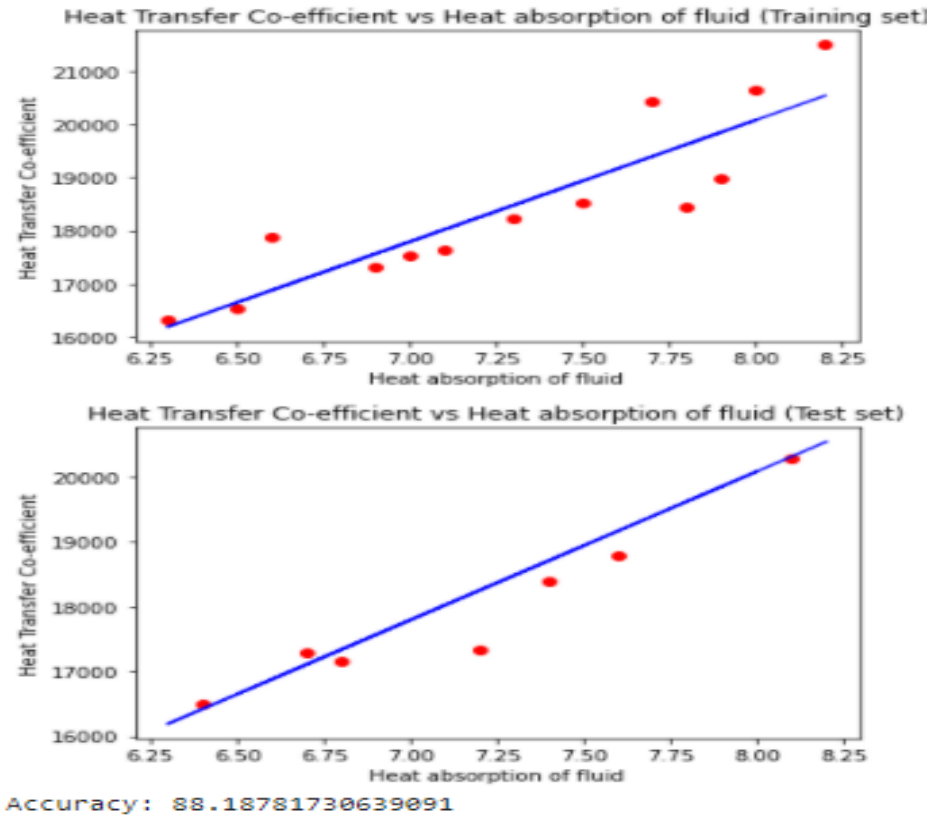

Figure 4.50: Simple Linear Regression Model by using ML for 0.5% Graphene Oxide Solution

From the model, we observe that we get a good prediction model by using the Simple Linear Regression Model, and there we get the observation datasets that are so close to our predicted line.

4.1.3.4. Heat Transfer Coefficient Of Graphene Oxide Solution:

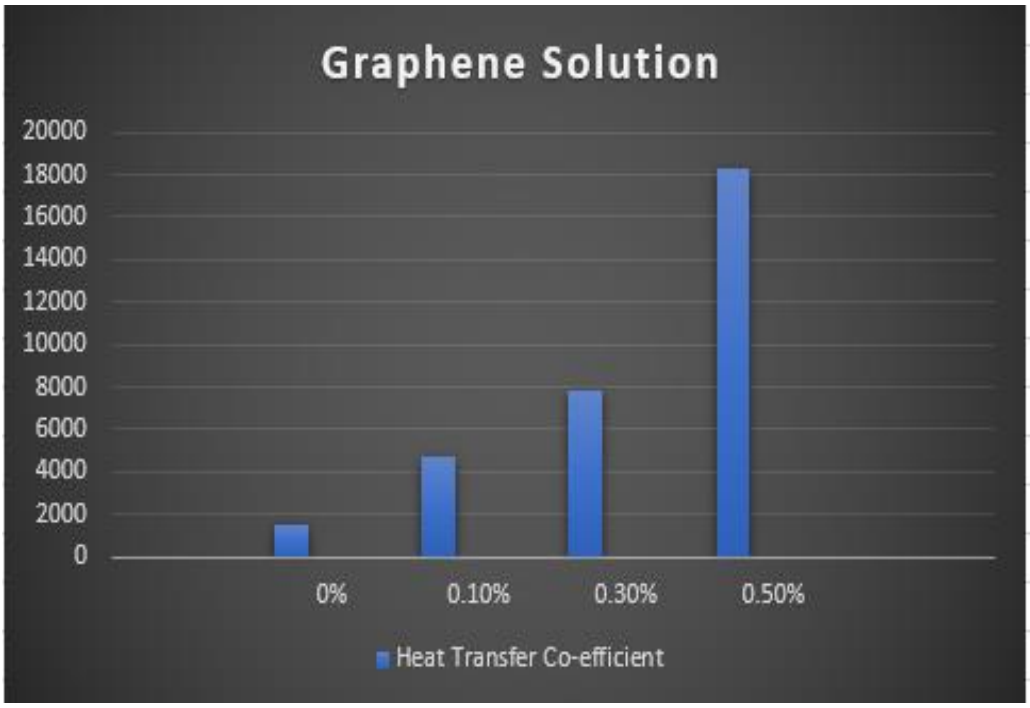

Figure 4.51: Heat Transfer Co-efficient Bar-chart of Graphene Oxide Solution

From the above figure, as the concentration of Graphene Oxide nanoparticles increased, the heat transfer coefficient of Graphene nanofluids also increases. So we found that 0.50% Graphene Oxide nanofluid gives the highest value of heat transfer co-efficient.

4.2.1. Viscosity measurement of Alumina Solution:

4.2.1.1. 0.1% Alumina Solution :

For 0.1% Alumina Solution:

We get around 200 values of viscosity in computer testing.

Viscosity, η= 0.0024 pascal-second

We take the dataset for 0.1% Alumina Solution and make our predictions by using a regression model. There we also apply other models to predict, but the regression fits most. That's why we make a detailed analysis of this. The precise result of the prediction model gives below:

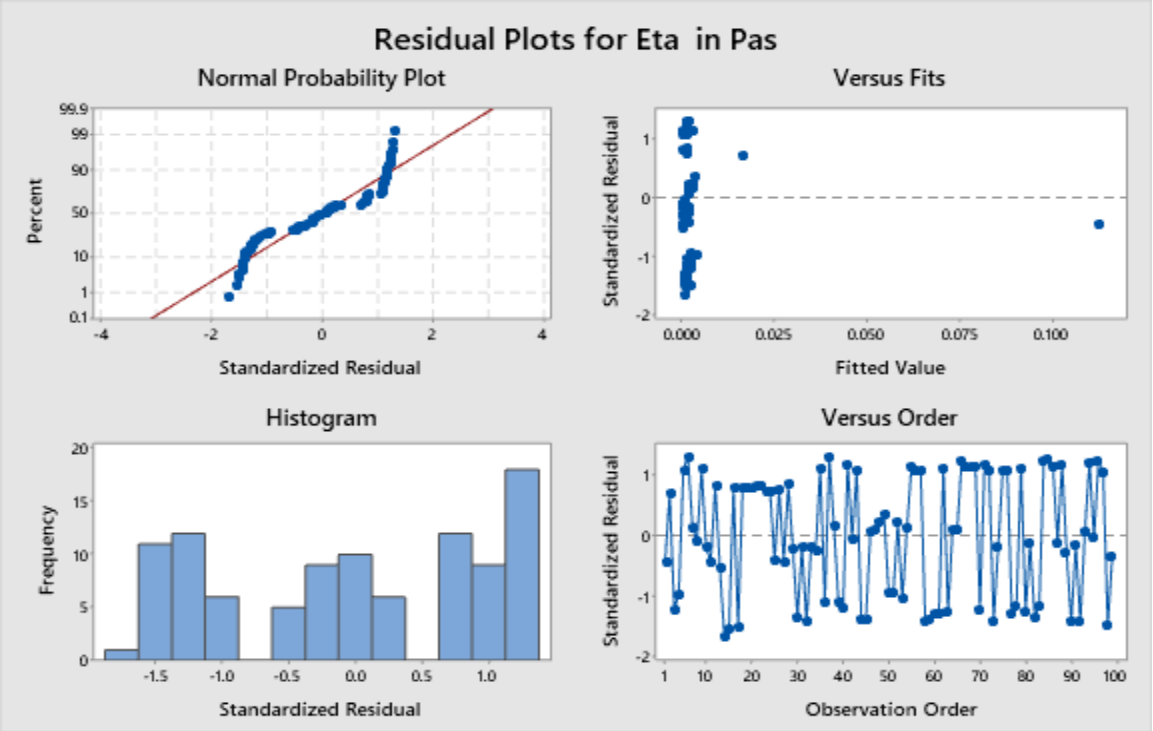

Figure 4.52: Residual Plots for 0.1% Alumina Solution

Regression Equation

Eta in = 0.000080 + 0.009989 Tau in Pa - 0.000000 t in s Pas - 0.000003 T in C

Coefficients

Term	Coef	SE Coef	T-Value	P-Value	VIF
Constant	0.000080	0.000056	1.42	0.158	
Tau in Pa	0.009989	0.000000	395441.39	0.000	1.07
t in s	-0.000000	0.000000	-1.35	0.180	1.36
T in C	-0.000003	0.000002	-1.42	0.158	1.38

Analysis of Variance

Source	DF	Adj SS	Adj MS	F-Value	P-Value
Regression	3	0.012645	0.004215	5.58396E+10	0.000
Tau in Pa	1	0.011804	0.011804	1.56374E+11	0.000
t in s	1	0.000000	0.000000	1.83	0.180
T in C	1	0.000000	0.000000	2.02	0.158
Error	95	0.000000	0.000000		
Total	98	0.012645			

From the variance analysis result, we notice from the P-Value, which is equal to 0 & the F-value, which is larger than the F critical value only for shear stress (Tau), indicating shear stress creates a significant impact on the regression model. Other factors can be considered null hypotheses as their P-value is more prominent than 0.05 and F-Value is smaller than the F critical value. We can reject the null hypothesis as it doesn't create any impact on the regression equation.

Durbin-Watson Statistic

Durbin-Watson Statistic =	1.84568

From the Durbin-Watson Statistics, we get the value equal to 1.84, which shows that the Heat Transfer Co-efficient has maintained a decent relationship with the increasing shear stress.

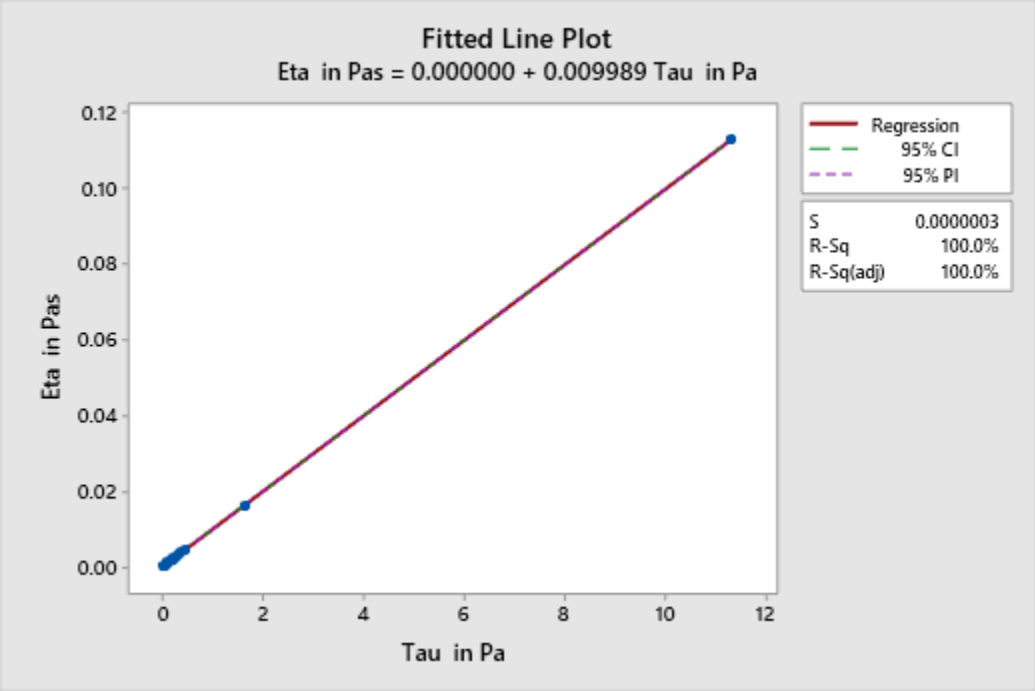

Figure 4.53: Fitted Line Plot for 0.1% Alumina Solution

The regression equation:

Viscosity = 0.000000 + 0.009989 Shear stress

Fits and Diagnostics for Unusual Observations

Obs	Eta in Pas	Fit	Resid	Std Resid	
1	0	0	-0	-0.45	X

X Unusual X

Model Summary

S	R-sq	R-sq(adj)	R-sq(pred)
0.0000003	100.00%	100.00%	100.00%

By rejecting the null hypothesis, we make a fitted line plot in between shear stress & viscosity. We observe no variation between the predicted line and the observation data from the residual plot. That's why we get our satisfied R-sq value.

4.2.1.2. 0.2% Alumina Solution:

For 0.2% Alumina Solution:

Similarly, here we get around 200 values of viscosity in computer testing.

Viscosity, η= 0.0022 pascal-second.

We take the dataset for 0.2% Alumina Solution and make our predictions by using a regression model. There we also apply other models to predict, but the regression fits most. That's why we make a detailed analysis of this. The precise result of the prediction model gives below:

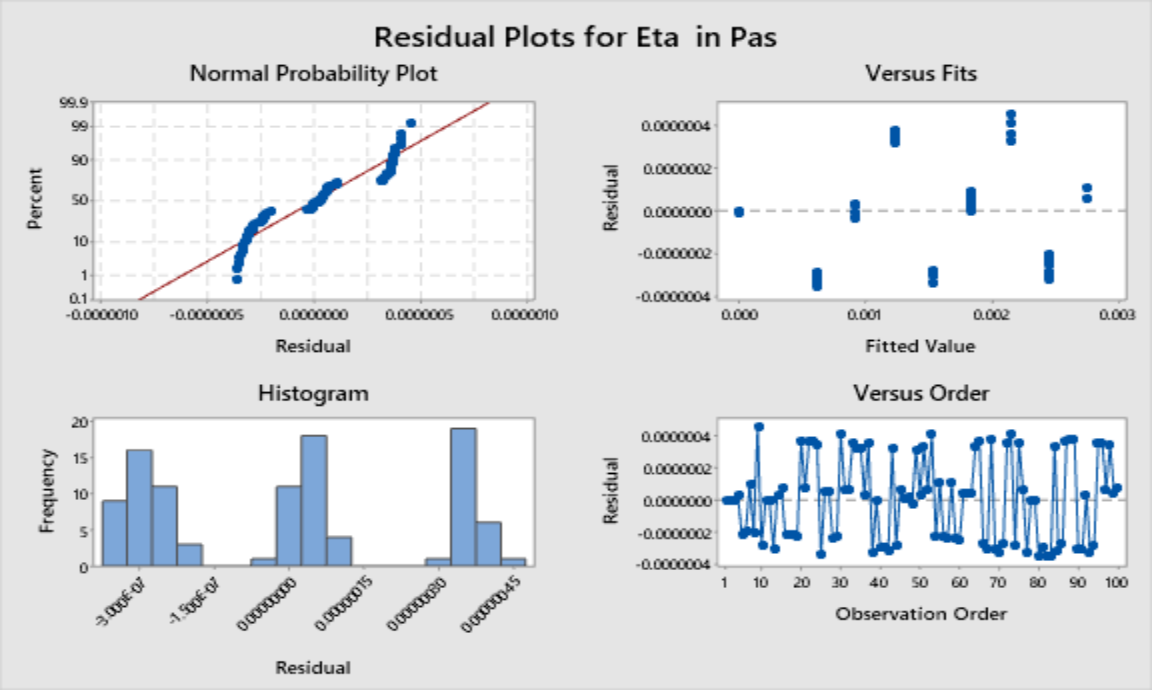

Figure4.54: Residual Plots for 0.2% Alumina Solution

Regression Equation

Eta in Pas = -0.000048 + 0.009989 Tau in Pa + 0.000002 T in C + 0.000000 t in s

Coefficients

Term	Coef	SE Coef	T-Value	P-Value	VIF
Constant	-0.000048	0.000052	-0.93	0.356	
Tau in Pa	0.009989	0.000000	24483.70	0.000	1.18
T in C	0.000002	0.000002	0.93	0.356	1.57
t in s	0.000000	0.000000	0.64	0.522	1.36

Analysis of Variance

Source	DF	Adj SS	Adj MS	F-Value	P-Value
Regression	3	0.000052	0.000017	2.35866E+08	0.000
Tau in Pa	1	0.000044	0.000044	5.99451E+08	0.000
T in C	1	0.000000	0.000000	0.86	0.356
t in s	1	0.000000	0.000000	0.41	0.522
Error	96	0.000000	0.000000		
Total	99	0.000052			

From the variance analysis result, we notice from the P-Value, which is equal to 0 & the F-value, which is larger than the F critical value only for shear stress (Tau), indicating shear stress creates a significant impact on the regression model. Other factors can be considered null hypotheses as their P-value is more prominent than 0.05 and F-Value is smaller than the F critical value. We can reject the null hypothesis as it doesn't create any impact on the regression equation.

Durbin-Watson Statistic

Durbin-Watson Statistic =	1.85014

From the Durbin-Watson Statistics, we get the value equal to 1.85, which shows that the Heat Transfer Co-efficient has maintained a decent relationship with the increasing shear stress.

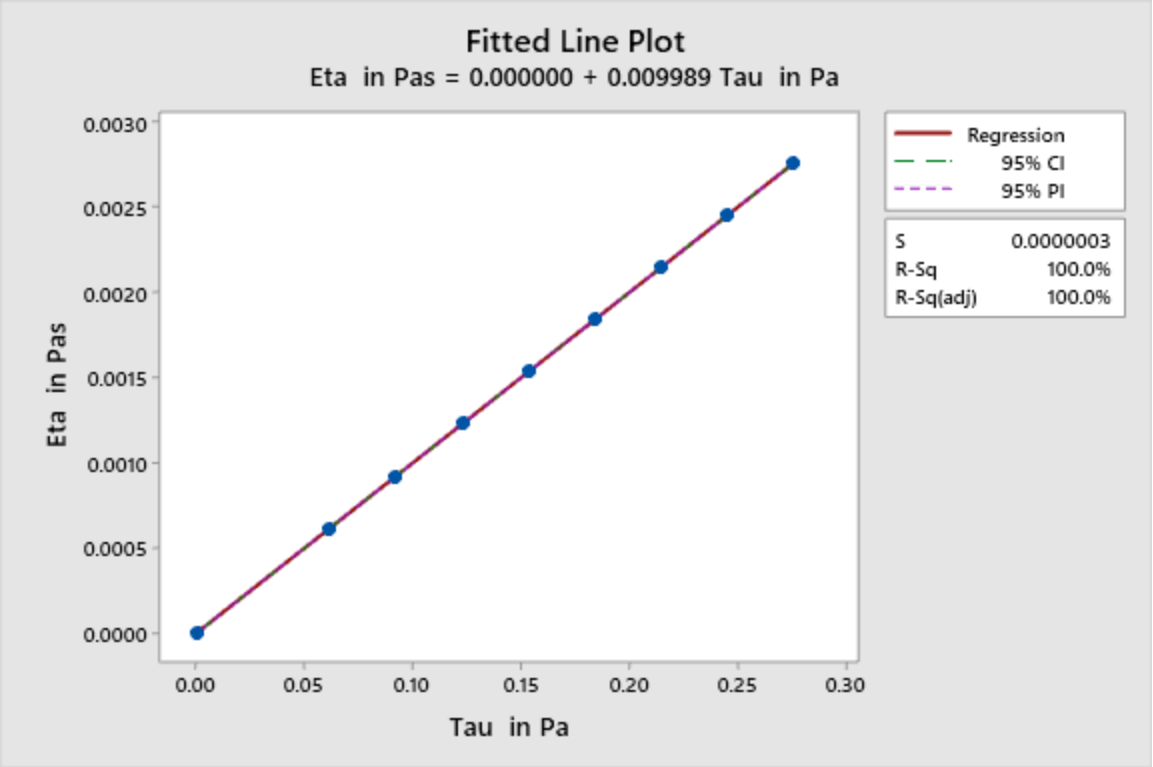

Figure 4.55: Fitted Line Plot for 0.2% Alumina Solution

The regression equation:

Viscosity = 0.000000 + 0.009989 Shear stress

Model Summary

S	R-sq	R-sq(adj)	R-sq(pred)
0.0000003	100.00%	100.00%	100.00%

By rejecting the null hypothesis, we make a fitted line plot in between shear stress & viscosity. We observe no variation between the predicted line and the observation data from the residual plot. That's why we get our satisfied R-sq value.

4.2.1.3. 0.3% Alumina Solution:

For 0.3% Alumina Solution:

We get around 200 values of viscosity in computer testing.

Viscosity, η= 0.0019 pascal-second.

We take the dataset for 0.3% Alumina Solution and make our predictions by using a regression model. There we also apply other models to predict, but the regression fits most. That's why we make a detailed analysis of this. The precise result of the prediction model gives below:

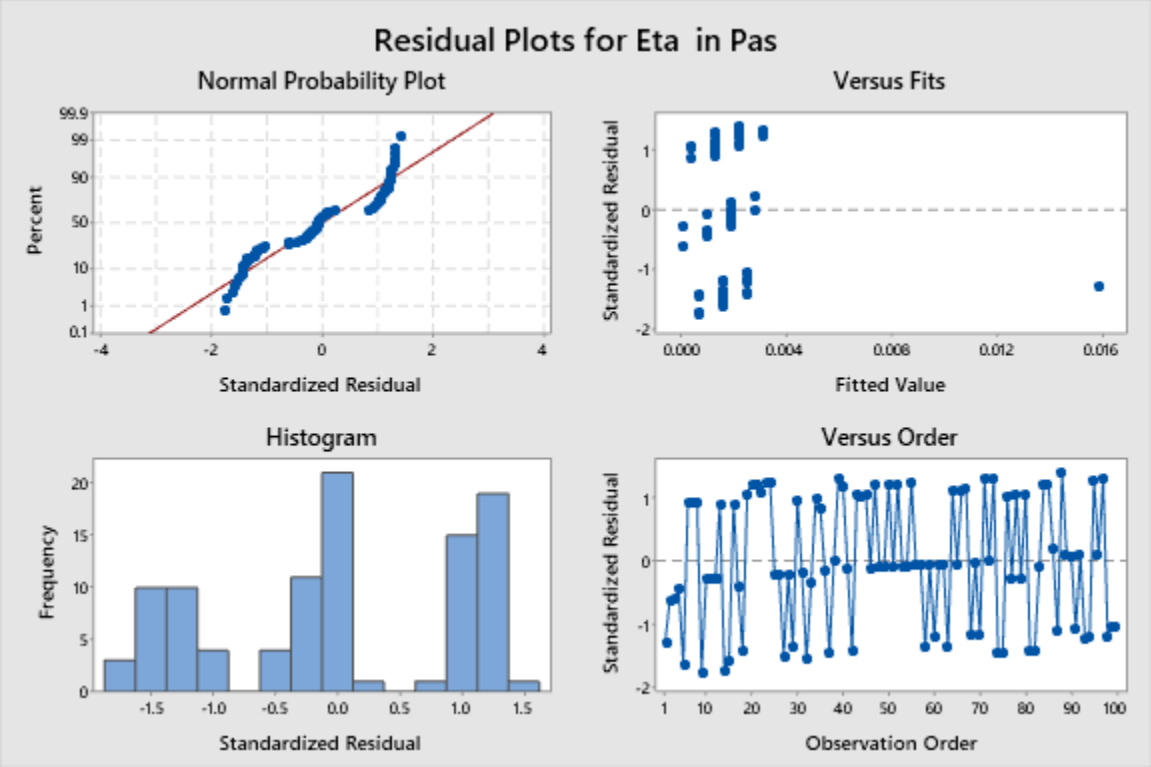

Figure 4.56: Residual Plots for 0.3% Alumina Solution

Regression Equation

Eta in Pas = 0.000004 + 0.009989 Tau in Pa - 0.000000 T in C - 0.000000 t in s

Coefficients

Term	Coef	SE Coef	T-Value	P-Value	VIF
Constant	0.000004	0.000044	0.09	0.929	
Tau in Pa	0.009989	0.000000	59069.16	0.000	1.04
T in C	0.000000	- 0.000001	-0.09	0.932	5.40
t in s	0.000000	- 0.000000	-0.64	0.524	5.34

Analysis of Variance

Source	DF	Adj SS	Adj MS	F-Value	P-Value
Regression	3	0.000255	0.000085	1.20592E+09	0.000
Tau in Pa	1	0.000246	0.000246	3.48917E+09	0.000
T in C	1	0.000000	0.000000	0.01	0.932
t in s	1	0.000000	0.000000	0.41	0.524
Error	96	0.000000	0.000000		
Total	99	0.000255			

From the variance analysis result, we notice from the P-Value, which is equal to 0 & the F-value, which is larger than the F critical value only for shear stress (Tau), indicating shear stress creates a significant impact on the regression model. Other factors can be considered null hypotheses as their P-value is more prominent than 0.05 and F-Value is smaller than the F critical value. We can reject the null hypothesis as it doesn't create any impact on the regression equation.

Durbin-Watson Statistic

Durbin-Watson Statistic =	1.90389

From the Durbin-Watson Statistics, we get the value equal to 1.90, which shows that the Heat Transfer Co-efficient has maintained a decent relationship with the increasing shear stress.

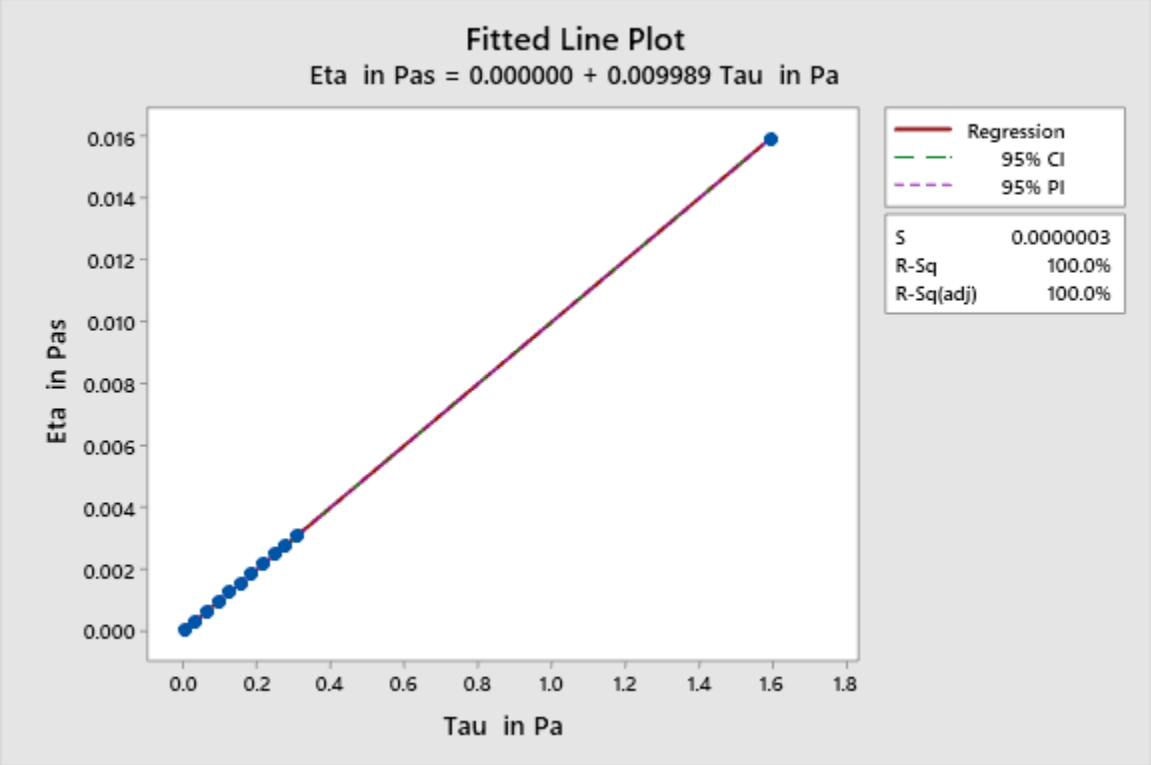

Figure 4.57: Fitted Line Plot for 0.3% Alumina Solution

The regression equation:

Viscosity = 0.000000 + 0.009989 Shear stress

Fits and Diagnostics for Unusual Observations

Obs	Eta in Pas	Fit	Resid	Std Resid
1	0.015946	0.015946	- 0.000000	-1.30 X

X Unusual X

Model Summary

S	R-sq	R-sq(adj)	R-sq(pred)
0.0000003	100.00%	100.00%	100.00%

By rejecting the null hypothesis, we make a fitted line plot in between shear stress & viscosity. We observe no variation between the predicted line and the observation data from the residual plot. That's why we get our satisfied R-sq value.

4.2.1.4. 0.5% Alumina Solution:

For 0.5% Alumina Solution:

We get around 200 values of viscosity in computer testing.

Viscosity,η= 0.0028 pascal-second.

We take the dataset for 0.5% Alumina Solution and make our predictions by using a regression model. There we also apply other models to predict, but the regression fits most.

That's why we make a detailed analysis of this. The precise result of the prediction model gives below:

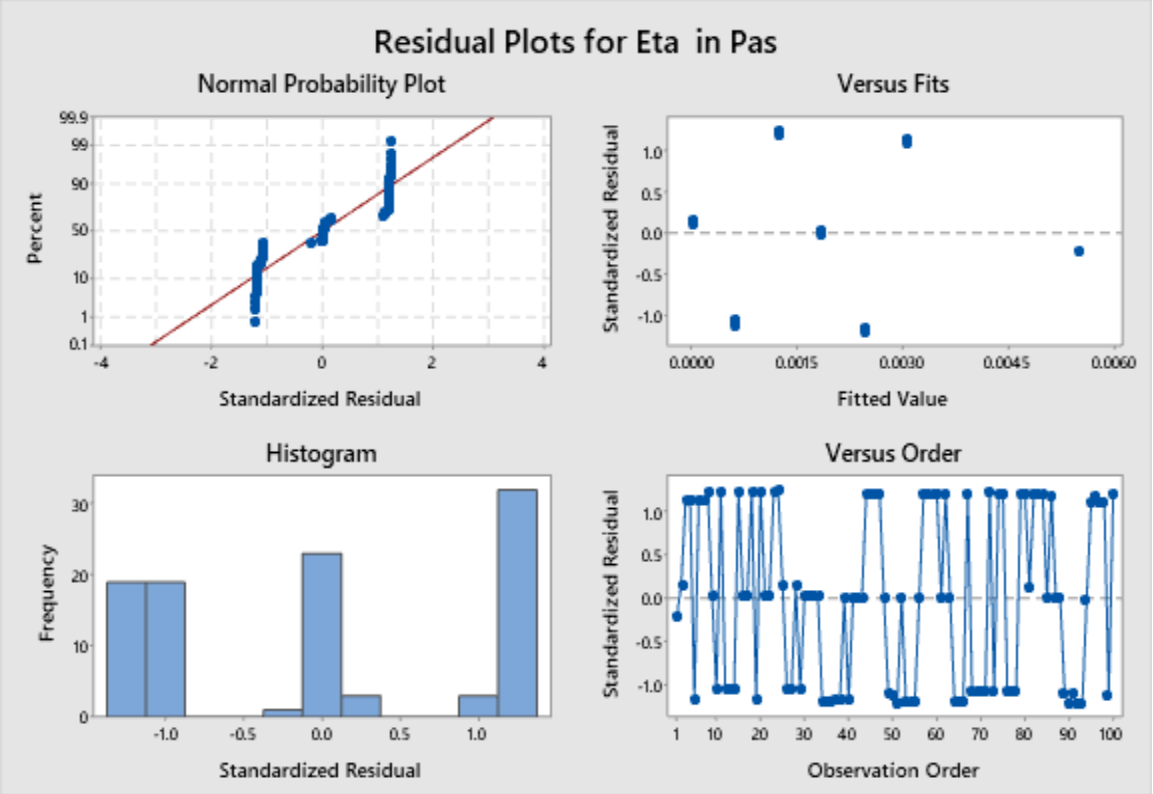

Figure 4.58: Residual Plots for 0.5% Alumina Solution

Regression Equation

Eta in = 0.000001 + 0.009989 Tau in Pa - 0.000000 T in C
Pas + 0.000000 t in s

Coefficients

Term	Coef	SE Coef	T-Value	P-Value	VIF
Constant	0.000001	0.000017	0.07	0.945	
Tau in Pa	0.009989	0.000000	27357.20	0.000	1.25
T in C	-0.000000	0.000001	-0.07	0.942	1.35
t in s	0.000000	0.000000	0.15	0.883	1.10

Analysis of Variance

Source	DF	Adj SS	Adj MS	F-Value	P-Value
Regression	3	0.000078	0.000026	3.10622E+08	0.000
Tau in Pa	1	0.000063	0.000063	7.48417E+08	0.000
T in C	1	0.000000	0.000000	0.01	0.942
t in s	1	0.000000	0.000000	0.02	0.883
Error	96	0.000000	0.000000		
Total	99	0.000078			

From the variance analysis result, we notice from the P-Value, which is equal to 0 & the F-value, which is larger than the F critical value only for shear stress (Tau), indicating shear stress creates a significant impact on the regression model. Other factors can be considered null hypotheses as their P-value is more prominent than 0.05 and F-Value is smaller than the F critical value. We can reject the null hypothesis as it doesn't create any impact on the regression equation.

Durbin-Watson Statistic

Durbin-Watson Statistic = 1.35286

From the Durbin-Watson Statistics, we get the value equal to 1.35, which shows that the Heat Transfer Co-efficient has maintained a decent relationship with the increasing shear stress.

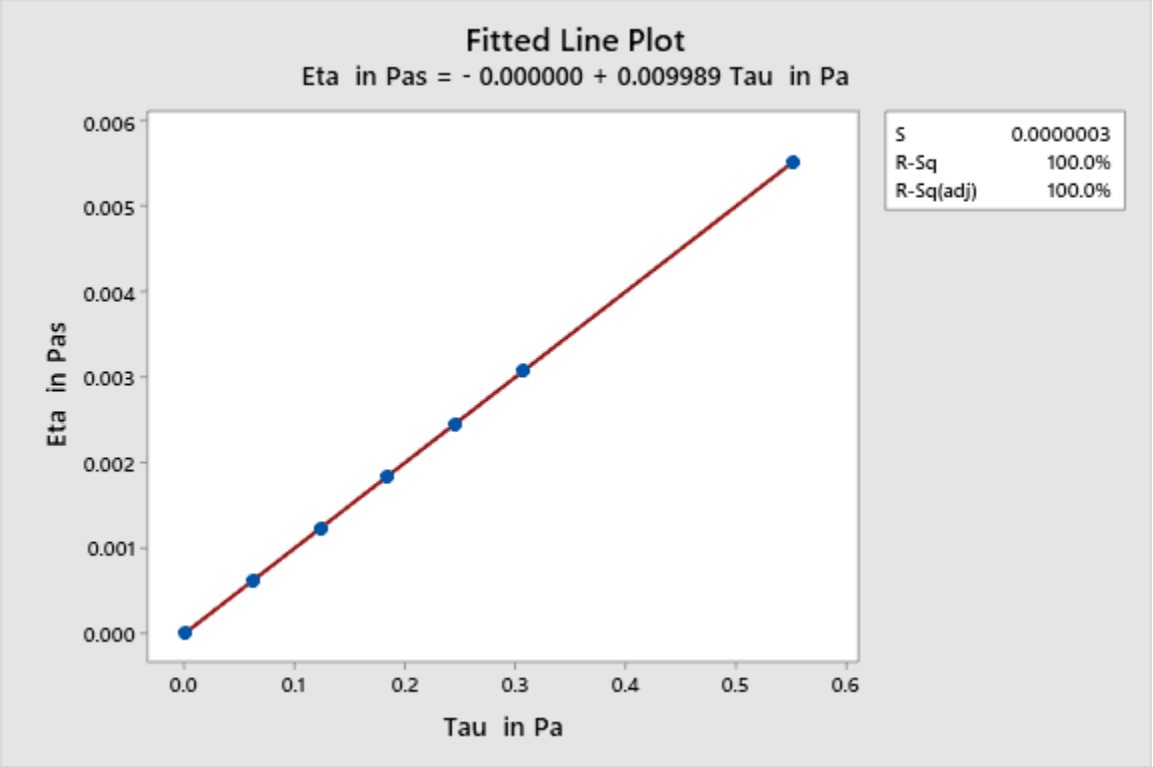

Figure 4.59: Fitted Line Plot for 0.5% Alumina Solution

The regression equation:

Viscosity= - 0.000000 + 0.009989 Shear stress

Fits and Diagnostics for Unusual Observations

Obs	Eta in Pas	Fit	Resid	Std Resid
1	0.005520	0.005520	- 0.000000	-0.21 X

X Unusual X

Model Summary

S	R-sq	R-sq(adj)	R-sq(pred)
0.0000003	100.00%	100.00%	100.00%

By rejecting the null hypothesis, we make a fitted line plot in between shear stress & viscosity. We observe no variation between the predicted line and the observation data from the residual plot. That's why we get our satisfied R-sq value.

4.2.1.4. Viscosity Properties of Alumina Solution:

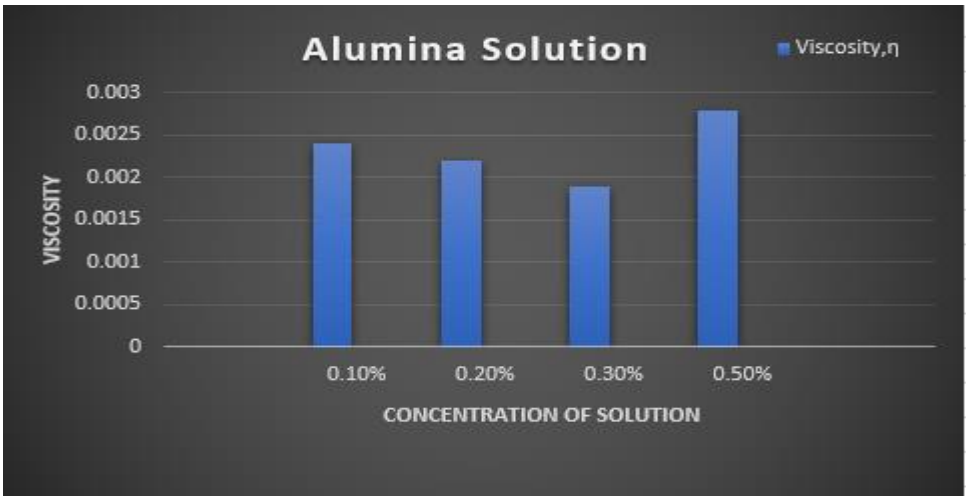

Figure4.60: Viscosity Bar-chart of Alumina Solution

From the above figure, we can see that as aluminum oxide nanoparticles' concentration increased, nanofluids' viscosity decreases, but after a particular time, it grew. So, we found that 0.50% Alumina nanofluid gives the highest value of heat transfer co-efficient and 0.30% gives lower value, but 0.50% gives higher value than all concentrations of Aluminum Oxide nanofluids.

4.2.2. Viscosity measurement of Zinc Oxide Solution:

4.2.2.1. 0.1% Zinc Solution:

For 0.1% Zinc Oxide Solution:

We get around 200 values of viscosity in computer testing.

Viscosity, η= 0.001358 pascal-second.

We take the dataset for a 0.1% Zinc Oxide Solution and make our predictions using a regression model. There we also apply other models to predict, but the regression fits most. That's why we make a detailed analysis of this. The precise result of the prediction model gives below:

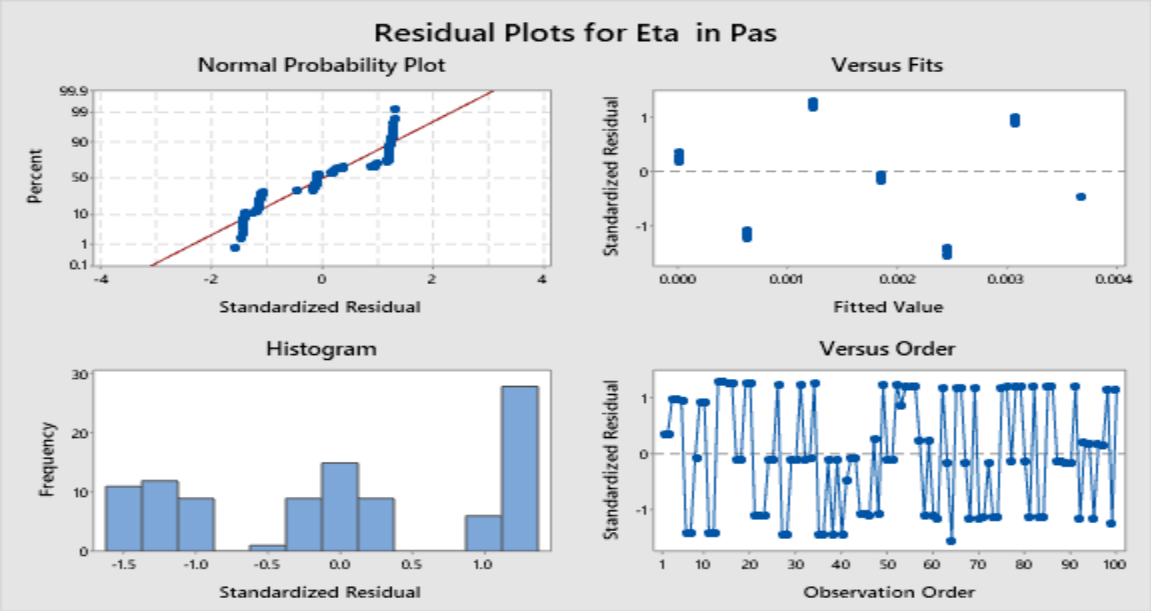

Figure 4.61: Residual Plots for 0.1% Zinc Oxide Solution

Regression Equation

Eta in Pas = 0.000006 + 0.009990 Tau in Pa - 0.000000 T in C + 0.000000 t in s

Coefficients

Term	Coef	SE Coef	T-Value	P-Value	VIF
Constant	0.000006	0.000036	0.16	0.874	
Tau in Pa	0.009990	0.000000	27709.51	0.000	1.23
T in C	- 0.000000	0.000001	-0.16	0.872	1.54
t in s	0.000000	0.000000	0.37	0.709	1.81

Analysis of Variance

Source	DF	Adj SS	Adj MS	F-Value	P-Value
Regression	3	0.000070	0.000023	3.13837E+08	0.000
Tau in Pa	1	0.000057	0.000057	7.67817E+08	0.000
T in C	1	0.000000	0.000000	0.03	0.872
t in s	1	0.000000	0.000000	0.14	0.709
Error	96	0.000000	0.000000		
Total	99	0.000070			

From the variance analysis result, we notice from the P-Value, which is equal to 0 & the F-value, which is larger than the F critical value only for shear stress (Tau), indicating shear stress creates a significant impact on the regression model. Other factors can be considered null hypotheses as their P-value is more prominent than 0.05 and F-Value is smaller than the F critical value. We can reject the null hypothesis as it doesn't create any impact on the regression equation.

Durbin-Watson Statistic

Durbin-Watson Statistic =	1.75664

From the Durbin-Watson Statistics, we get the value equal to 1.76, which shows that the Heat Transfer Co-efficient has maintained a decent relationship with the increasing shear stress.

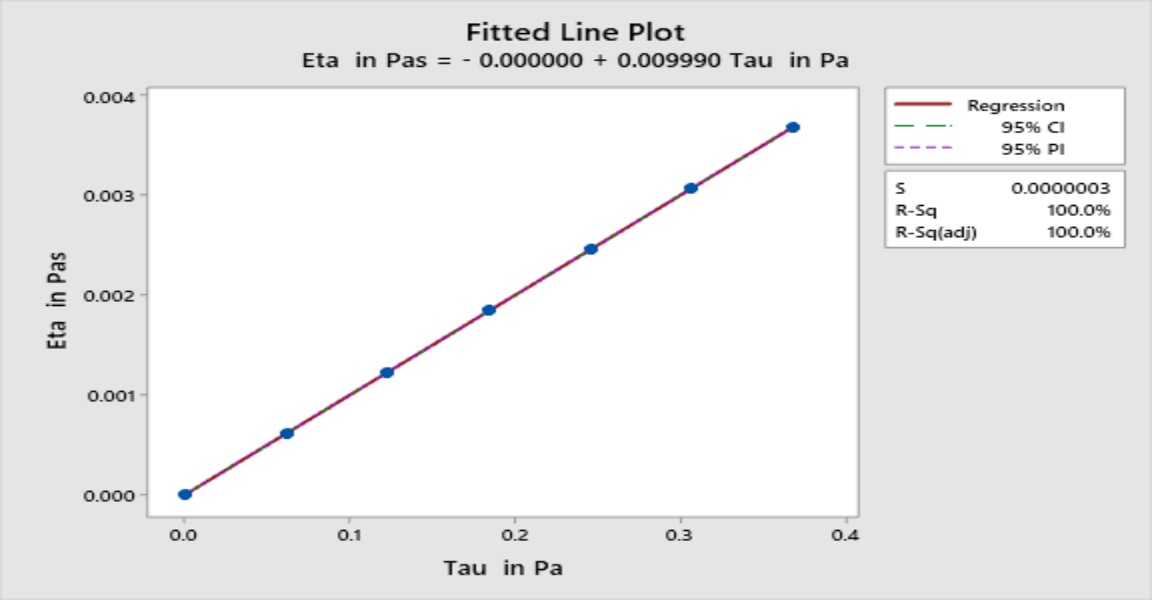

Figure 4.62: Fitted Line Plot for 0.1% Zinc Oxide Solution

The regression equation is

Viscosity = - 0.000000 + 0.009990 Shear Stress

Fits and Diagnostics for Unusual Observations

Obs	Eta in Pas	Fit	Resid	Std Resid	
1	0.000000	- 0.000000	0.000000	0.37	X
2	0.000000	- 0.000000	0.000000	0.37	X

X Unusual X

Model Summary

S	R-sq	R-sq(adj)	R-sq(pred)
0.0000003	100.00%	100.00%	100.00%

By rejecting the null hypothesis, we make a fitted line plot in between shear stress & viscosity. We observe no variation between the predicted line and the observation data from the residual plot. That's why we get our satisfied R-sq value.

4.2.2.2. 0.2% Zinc Solution:

For 0.2% Zinc Oxide Solution:

We get around 200 values of viscosity in computer testing.

Viscosity,η= 0.001668 pascal-second.

We take the dataset for a 0.2% Zinc Oxide Solution and make our predictions using a regression model. There we also apply other models to predict, but the regression fits most. That's why we make a detailed analysis of this. The precise result of the prediction model gives below:

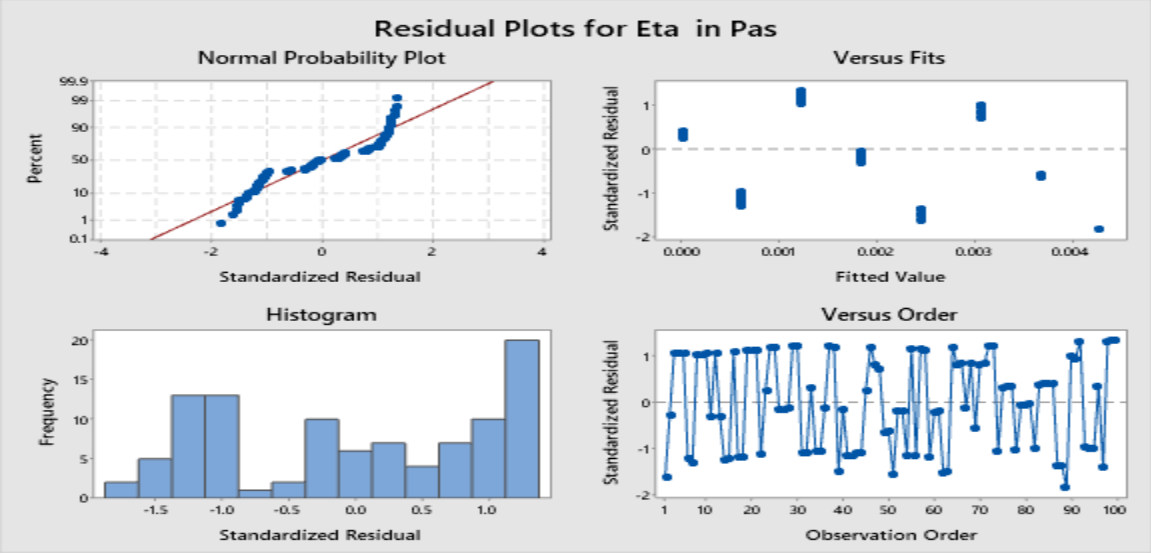

Figure 4.63: Residual Plots for 0.2% Zinc Oxide Solution

Regression Equation

Eta in Pas = -0.000027 + 0.009990 Tau in Pa + 0.000001 T in C - 0.000000 t in s

Coefficients

Term	Coef	SE Coef	T-Value	P-Value	VIF
Constant	-0.000027	0.000057	-0.48	0.634	
Tau in Pa	0.009990	0.000000	35131.91	0.000	1.04
T in C	0.000001	0.000002	0.48	0.634	1.91
t in s	-0.000000	0.000000	-0.23	0.817	1.93

Analysis of Variance

Source	DF	Adj SS	Adj MS	F-Value	P-Value
Regression	3	0.000098	0.000033	4.27888E+08	0.000
Tau in Pa	1	0.000094	0.000094	1.23425E+09	0.000
T in C	1	0.000000	0.000000	0.23	0.634
t in s	1	0.000000	0.000000	0.05	0.817
Error	96	0.000000	0.000000		
Total	99	0.000098			

From the variance analysis result, we notice from the P-Value, which is equal to 0 & the F-value, which is larger than the F critical value only for shear stress (Tau), indicating shear stress creates a significant impact on the regression model. Other factors can be considered null hypotheses as their P-value is larger than 0.05 and F-Value is smaller than the F critical value. We can reject the null hypothesis as it doesn't create any impact on the regression equation.

Durbin-Watson Statistic

Durbin-Watson Statistic =	1.59085

From the Durbin-Watson Statistics, we get the value equal to 1.59, which shows that the Heat Transfer Co-efficient has maintained a decent relationship with the increasing shear stress.

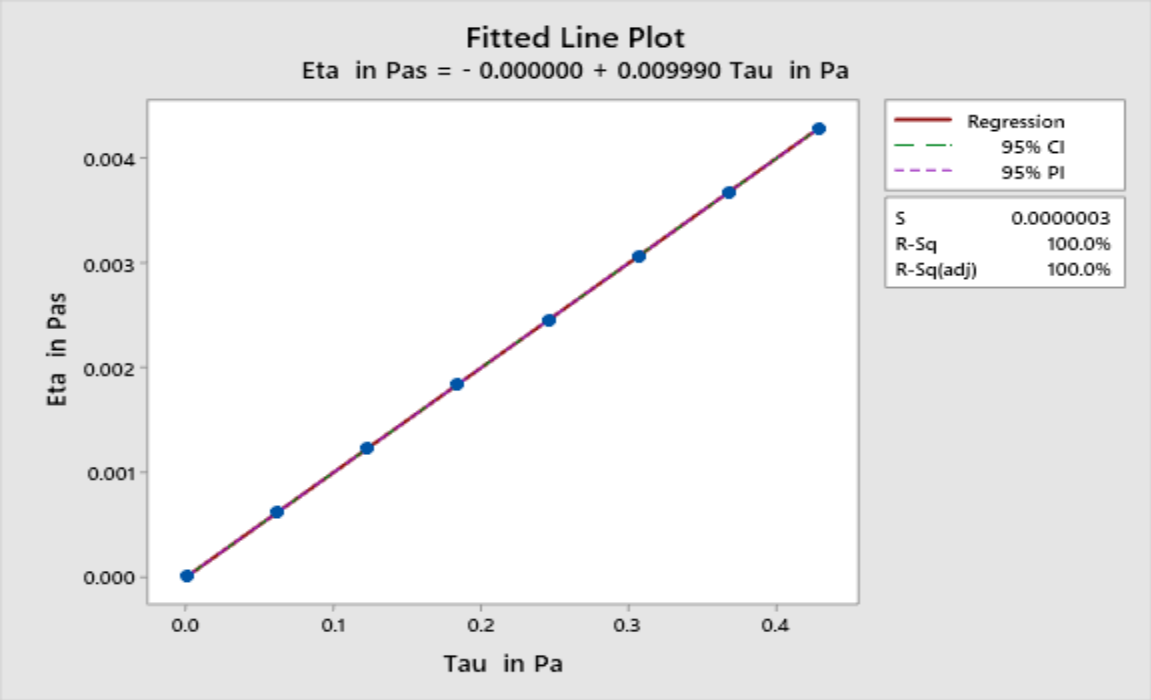

Figure 4.64: Fitted Line Plot for 0.2% Zinc Oxide Solution

The regression equation:

Viscosity = - 0.000000 + 0.009990 Shear Stress

Fits and Diagnostics for Unusual Observations

Obs	Eta in Pas	Fit	Resid	Std Resid
89	0.004293	0.004293	- 0.000000	-1.84 X

X Unusual X

Model Summary

S	R-sq	R-sq(adj)	R-sq(pred)
0.0000003	100.00%	100.00%	100.00%

By rejecting the null hypothesis, we make a fitted line plot in between shear stress & viscosity. We observe no variation between the predicted line and the observation data from the residual plot. That's why we get our satisfied R-sq value.

4.2.2.3. 0.3% Zinc Solution:

For 0.3% Zinc Oxide Solution:

We get around 200 values of viscosity in computer testing.

Viscosity,η= 0.002106 pascal-second.

We take the dataset for 0.3% Zinc Oxide Solution and make our predictions using a regression model. There we also apply other models to predict, but the regression fits most. That's why we make a detailed analysis of this. The precise result of the prediction model gives below:

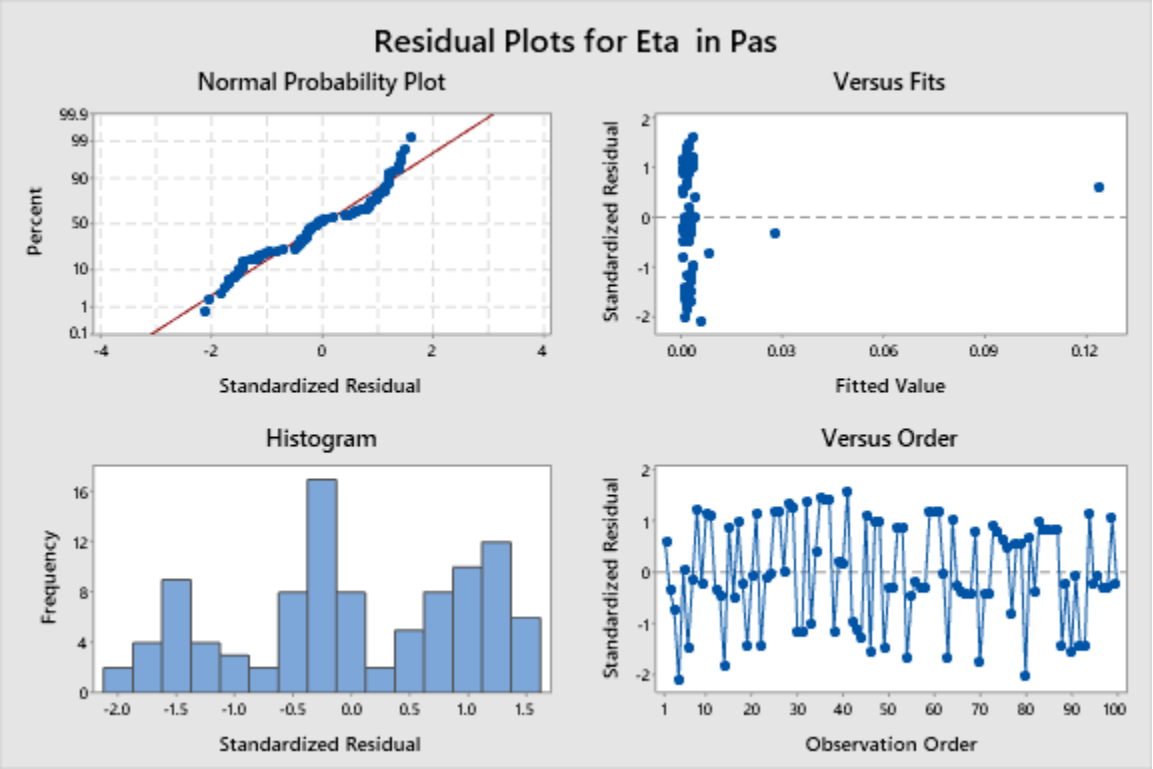

Figure 4.65: Residual Plots for 0.3% Zinc Oxide Solution

Regression Equation

Eta in Pas = -0.000067 + 0.009989 Tau in Pa + 0.000002 T in C + 0.000000 t in s

Coefficients

Term	Coef	SE Coef	T-Value	P-Value	VIF
Constant	- 0.000030	0.000067	-2.19	0.031	
Tau in Pa	0.009989	0.000000	468550.65	0.000	1.08
T in C	0.000002	0.000001	2.19	0.031	1.14
t in s	0.000000	0.000000	0.91	0.368	1.17

Analysis of Variance

Source	DF	Adj SS	Adj MS	F-Value	P-Value
Regression	3	0.015685	0.005228	7.92422E+10	0.000
Tau in Pa	1	0.014485	0.014485	2.19540E+11	0.000
T in C	1	0.000000	0.000000	4.80	0.031
t in s	1	0.000000	0.000000	0.82	0.368
Error	96	0.000000	0.000000		
Total	99	0.015685			

From the variance analysis result, we notice from the P-Value, which is equal to 0 & the F-value, which is larger than the F critical value only for shear stress (Tau), indicating shear stress creates a significant impact on the regression model. Other factors can be considered null hypotheses as their P-value is larger than 0.05 and F-Value is smaller than the F critical value. We can reject the null hypothesis as it doesn't create any impact on the regression equation.

Durbin-Watson Statistic

Durbin-Watson Statistic = 2.04113

From the Durbin-Watson Statistics, we get the value equal to 2.04, which shows that the Heat Transfer Co-efficient has maintained a decent relationship with the increasing shear stress.

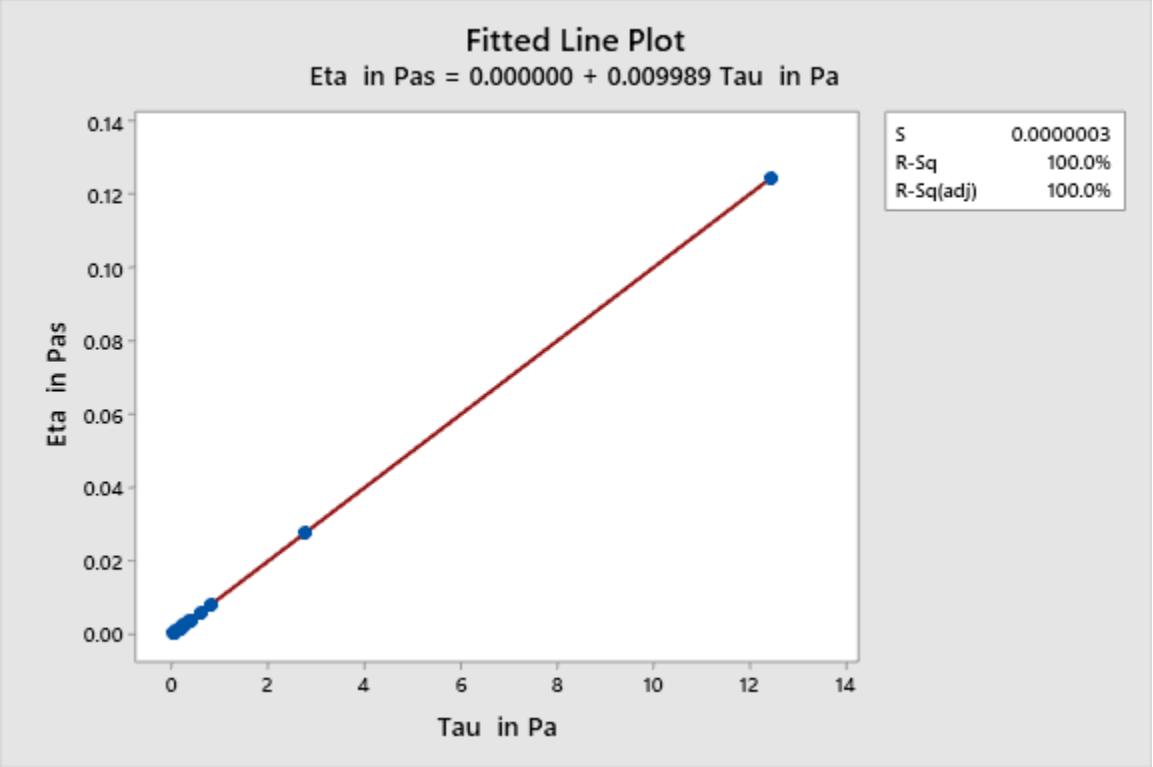

Figure 4.66: Fitted Line Plot for 0.3% Zinc Oxide Solution

The regression equation is

Viscosity = 0.000000 + 0.009989 Shear Stress

Fits and Diagnostics for Unusual Observations

Obs	Eta in Pas	Fit	Resid	Std Resid	
1	0.124502	0.124502	0.000000	0.60	X
4	0.005826	0.005827	-0.000001	-2.12	R
80	0.000613	0.000614	-0.000001	-2.04	R

Model Summary

S	R-sq	R-sq(adj)	R-sq(pred)
0.0000003	100.00%	100.00%	100.00%

By rejecting the null hypothesis, we make a fitted line plot in between shear stress & viscosity. We observe no variation between the predicted line and the observation data from the residual plot. That's why we get our satisfied R-sq value.

4.2.2.4. 0.4% Zinc Solution:

For 0.4% Zinc Oxide Solution:

We get around 200 values of viscosity in computer testing.

Viscosity,η= 0.00176026 pascal-second.

We take the dataset for 0.4% Zinc Oxide Solution and make our predictions using a regression model. There we also apply other models to predict, but the regression fits most. That's why we make a detailed analysis of this. The precise result of the prediction model gives below:

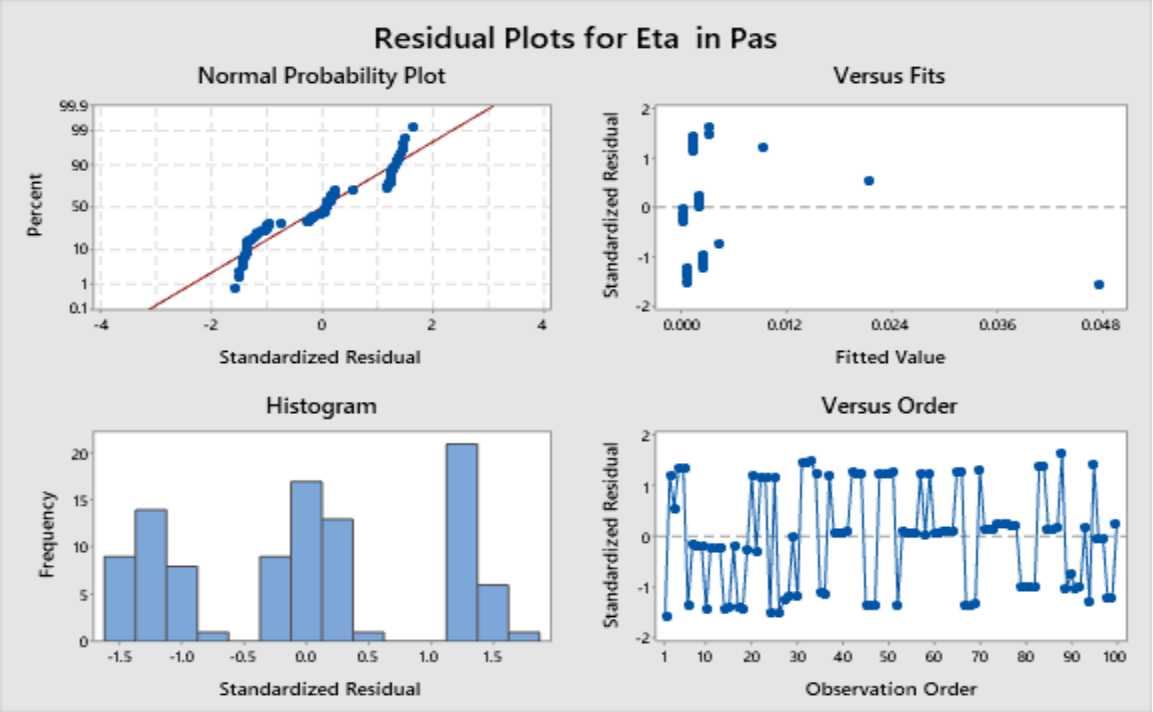

Figure 4.67: Residual Plots for 0.1% Zinc Oxide Solution

Regression Equation

Eta in Pas = 0.000014 + 0.009989 Tau in Pa - 0.000000 T in C - 0.000000 t in s

Coefficients

Term	Coef	SE Coef	T-Value	P-Value	VIF
Constant	0.000014	0.000029	0.49	0.623	
Tau in Pa	0.009989	0.000000	186021.01	0.000	1.09
T in C	-0.000001	0.000000	-0.49	0.625	1.34
t in s	-0.000000	0.000000	-0.25	0.806	1.37

Analysis of Variance

Source	DF	Adj SS	Adj MS	F-Value	P-Value
Regression	3	0.002635	0.000878	1.26243E+10	0.000
Tau in Pa	1	0.002407	0.002407	3.46038E+10	0.000
T in C	1	0.000000	0.000000	0.24	0.625
t in s	1	0.000000	0.000000	0.06	0.806
Error	96	0.000000	0.000000		
Total	99	0.002635			

From the variance analysis result, we notice from the P-Value, which is equal to 0 & the F-value, which is larger than the F critical value only for shear stress (Tau), indicating shear stress creates a significant impact on the regression model. Other factors can be considered null hypotheses as their P-value is larger than 0.05 and F-Value is smaller than the F critical value. We can reject the null hypothesis as it doesn't create any impact on the regression equation.

Durbin-Watson Statistic

Durbin-Watson Statistic =	1.56386

From the Durbin-Watson Statistics, we get the value equal to 1.56, which shows that the Heat Transfer Co-efficient has maintained a decent relationship with the increasing shear stress.

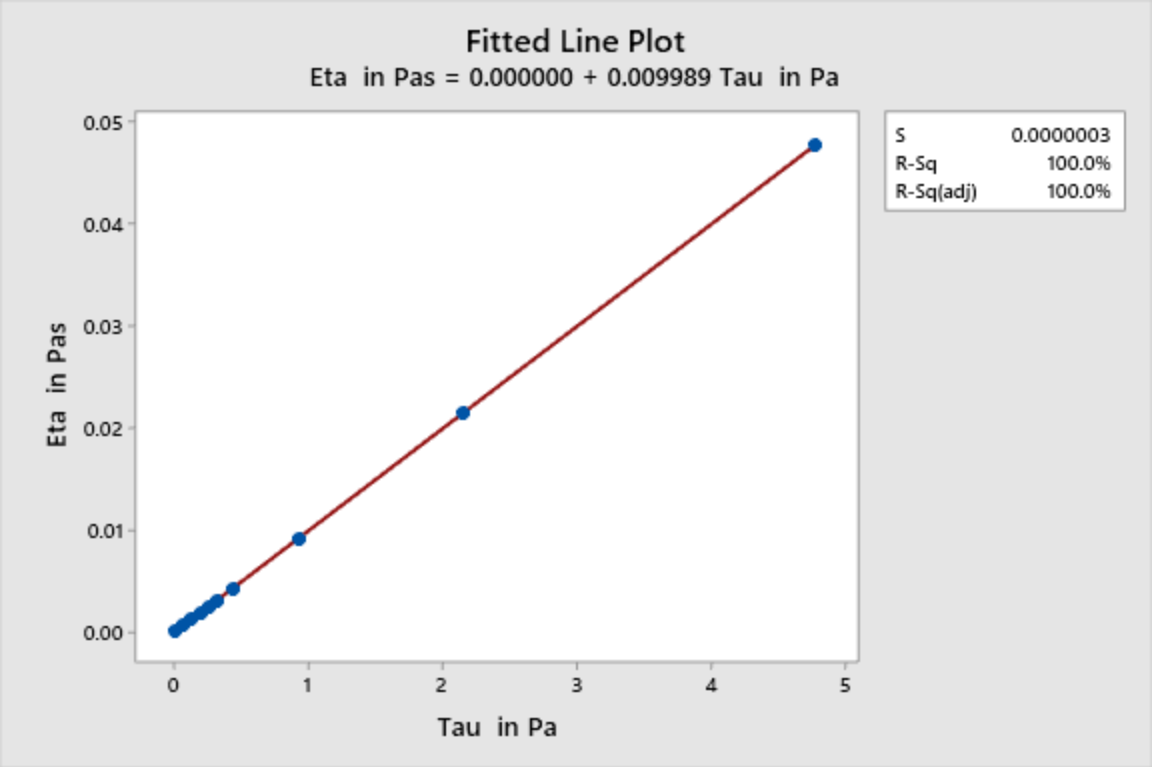

Figure 4.68: Fitted Line Plot for 0.4% Zinc Oxide Solution

The regression equation is

Viscosity = 0.000000 + 0.009989 Shear Stress

Fits and Diagnostics for Unusual Observations

Obs	Eta in Pas	Fit	Resid	Std Resid
1	0.047838	0.047838	-0.000000	-1.57 X
3	0.021466	0.021466	0.000000	0.55 X

X Unusual X

Model Summary

S	R-sq	R-sq(adj)	R-sq(pred)
0.0000003	100.00%	100.00%	100.00%

By rejecting the null hypothesis, we make a fitted line plot in between shear stress & viscosity. We observe no variation between the predicted line and the observation data from the residual plot. That's why we get our satisfied R-sq value.

4.2.2.5. Viscosity Properties of Zinc Oxide Solution:

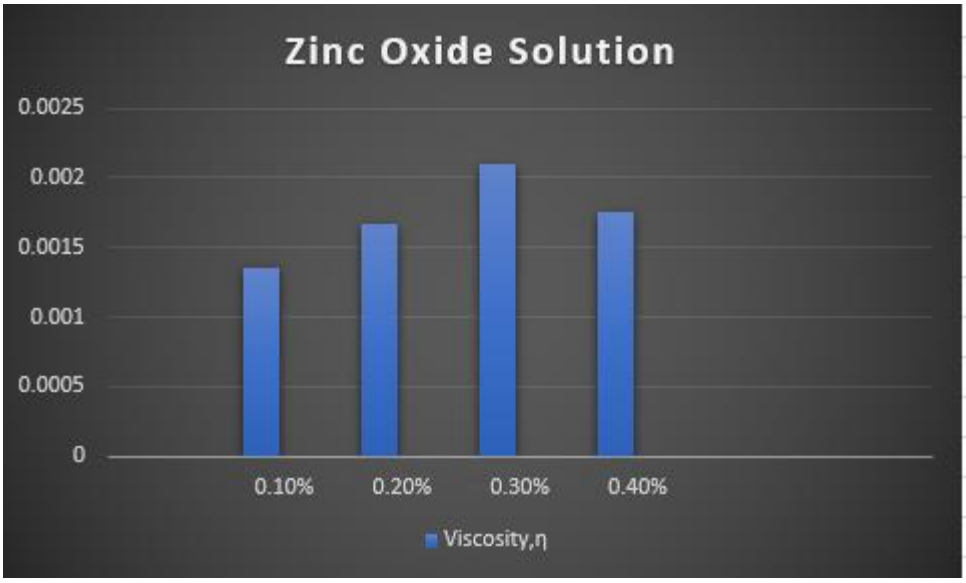

Figure 4.69: Viscosity Bar-chart of ZnO Solution

From the above figure, we can see that as the concentration of Zinc Oxide nanoparticles increased, nanofluids' viscosity also increases, but after a particular time, it again decreased. Increasing the thickness of the fluid boundary layer leads to a decrease in the heat transfer coefficient. So, we

found that 0.30% Graphene nanofluid gives the highest value of viscosity and 0.10% gives lower value, but 0.40% gives a lower value than the 0.30% concentration of Zinc Oxide nanofluids.

4.2.3. Viscosity measurement of Graphene Oxide Solution:

4.2.3.1. 0.1% Graphene Oxide Solution:

For 0.1% Graphene Oxide Solution:

We get around 200 values of viscosity in computer testing.

Viscosity,η= 0.00084 pascal-second

We take the dataset for 0.1% Graphene Solution and make our predictions by using a regression model. There we also apply other models to predict, but the regression fits most. That's why we make a detailed analysis of this. The precise result of the prediction model gives below:

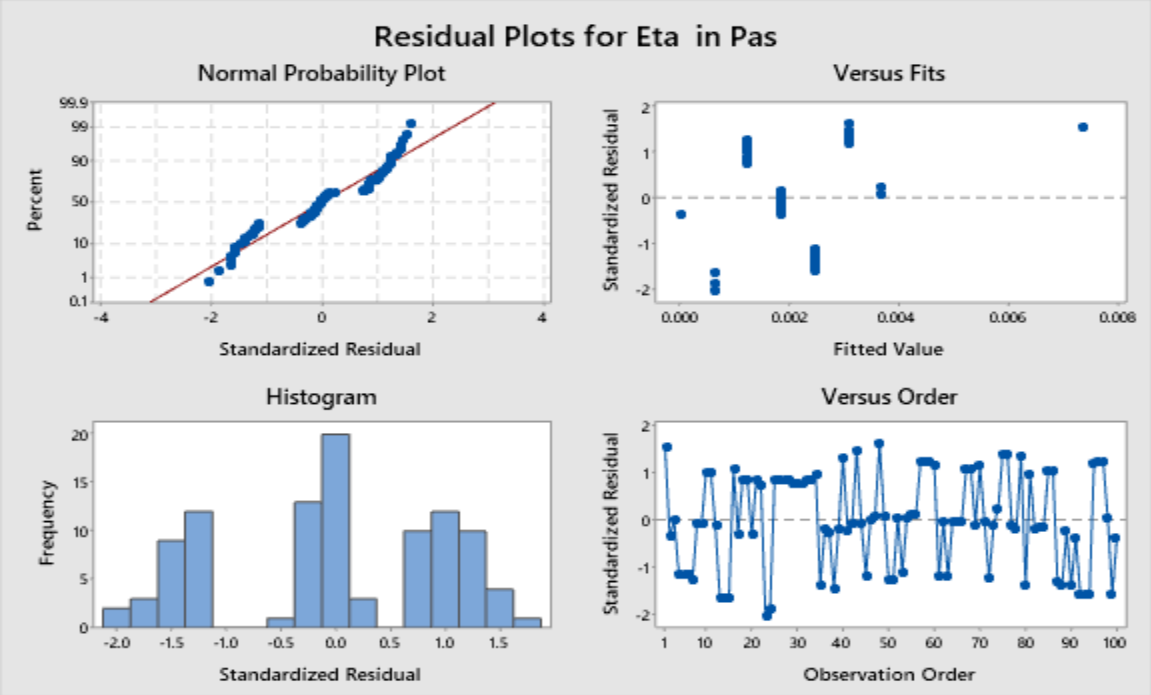

Figure 4.70: Residual Plots for 0.1% Graphene Oxide Solution

Regression Equation

Eta in Pas = 0.000059 + 0.009989 Tau in Pa - 0.000002 T in C + 0.000000 t in s

Coefficients

Term	Coef	SE Coef	T-Value	P-Value	VIF
Constant	0.000059	0.000040	1.47	0.145	
Tau in Pa	0.009989	0.000000	32719.97	0.000	1.11
T in C	-0.000002	0.000001	-1.47	0.146	1.08
t in s	0.000000	0.000000	0.43	0.666	1.09

Analysis of Variance

Source	DF	Adj SS	Adj MS	F-Value	P-Value
Regression	3	0.000079	0.000026	3.95711E+08	0.000
Tau in Pa	1	0.000071	0.000071	1.07060E+09	0.000
T in C	1	0.000000	0.000000	2.15	0.146
t in s	1	0.000000	0.000000	0.19	0.666
Error	96	0.000000	0.000000		
Total	99	0.000079			

From the variance analysis result, we notice from the P-Value, which is equal to 0 & the F-value, which is larger than the F critical value only for shear stress (Tau), indicating shear stress creates a significant impact on the regression model. Other

factors can be considered null hypotheses as their P-value is larger than 0.05 and F-Value is smaller than the F critical value. We can reject the null hypothesis as it doesn't create any impact on the regression equation.

Durbin-Watson Statistic

Durbin-Watson Statistic = 1.40142

From the Durbin-Watson Statistics, we get the value equal to 1.84, which shows that the Heat Transfer Co-efficient has maintained a decent relationship with the increasing shear stress.

The regression equation is in between shear stress & viscosity: viscosity = 0.000000 + 0.009989 shear stress

Fits and Diagnostics for Unusual Observations

Obs	Eta in Pas	Fit	Resid	Std Resid	
1	0.007360	0.007360	0.000000	1.56	X
23	0.000613	0.000614	-0.000001	-2.06	R

R Large residual

X Unusual X

Model Summary

S	R-sq	R-sq(adj)	R-sq(pred)
0.0000003	100.00%	100.00%	100.00%

We observe no variation between the predicted line and the observation data from the residual plot. That's why we get our satisfied R-sq value.

4.2.3.2. 0.3% Graphene Oxide Solution:

For 0.3% Graphene Oxide Solution:

We get around 200 values of viscosity in computer testing.

Viscosity,η= 0.00079 pascal-second

We take the dataset for 0.3% Graphene Solution and make our predictions by using a regression model. There we also apply other models to predict, but the regression fits most. That's why we make a detailed analysis of this. The precise result of the prediction model gives below:

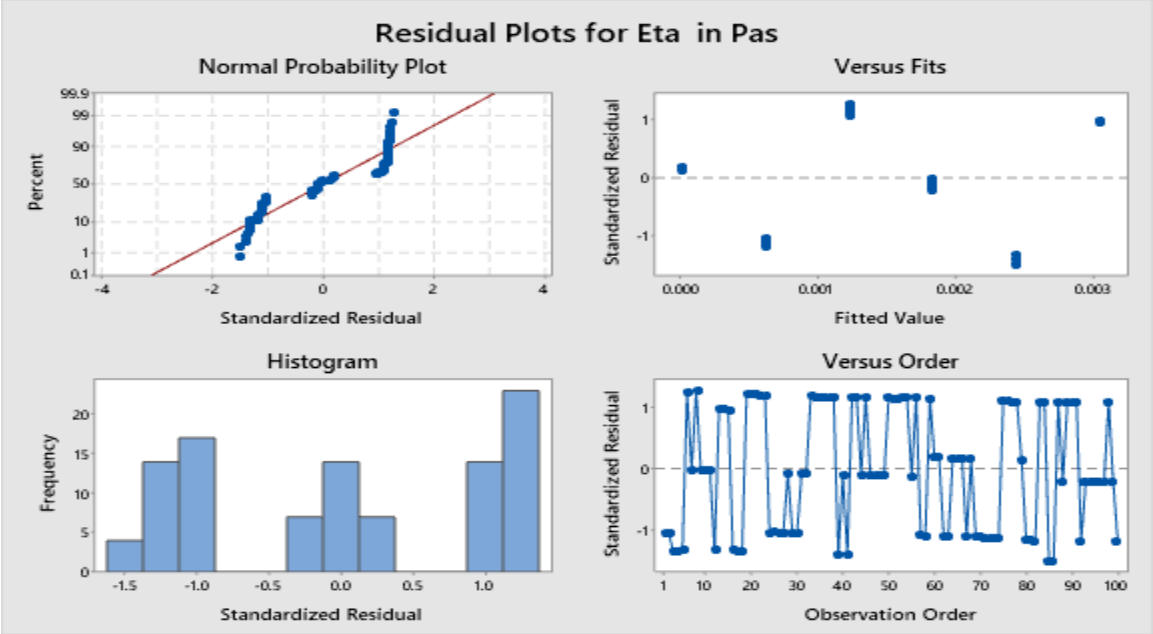

Figure 4.71: Residual Plots for 0.3% Graphene Oxide Solution

Regression Equation

Eta in Pas = 0.000004 + 0.009990 Tau in Pa - 0.000000 T in C + 0.000000 t in s

Coefficients

Term	Coef	SE Coef	T-Value	P-Value	VIF
Constant	0.000004	0.000050	0.09	0.931	
Tau in Pa	0.009990	0.000000	23973.88	0.000	1.13
T in C	-0.000000	0.000002	-0.09	0.930	1.35
t in s	0.000000	0.000000	0.44	0.660	1.38

Analysis of Variance

Source	DF	Adj SS	Adj MS	F-Value	P-Value
Regression	3	0.000053	0.000018	2.16964E+08	0.000
Tau in Pa	1	0.000047	0.000047	5.74747E+08	0.000
T in C	1	0.000000	0.000000	0.01	0.930
t in s	1	0.000000	0.000000	0.19	0.660
Error	96	0.000000	0.000000		
Total	99	0.000053			

From the variance analysis result, we notice from the P-Value, which is equal to 0 & the F-value, which is larger than the F critical value only for shear stress (Tau), indicating shear stress creates a significant impact on the regression model. Other factors can be considered null hypotheses as their P-value is larger than 0.05 and F-Value is smaller than the F critical value. We can reject the null hypothesis as it doesn't create any impact on the regression equation.

Durbin-Watson Statistic

Durbin-Watson Statistic =	1.26547

From the Durbin-Watson Statistics, we get the value equal to 1.27, which shows that the Heat Transfer Co-efficient has maintained a decent relationship with the increasing shear stress.

The regression equation is in between shear stress & viscosity:
viscosity= - 0.000000 + 0.009990 shear stress

Model Summary

S	R-sq	R-sq(adj)	R-sq(pred)
0.0000003	100.00%	100.00%	100.00%

We observe no variation between the predicted line and the observation data from the residual plot. That's why we get our satisfied R-sq value.

4.2.3.3. 0.5% Graphene Oxide Solution:

For 0.5% Graphene Oxide Solution:

We get around 200 values of viscosity in computer testing.

Viscosity,η= 0.00072 pascal-second

We take the dataset for 0.5% Graphene Oxide Solution and make our predictions by using a regression model. There we also apply other models to predict, but the regression fits most. That's why we make a detailed analysis of this. The precise result of the prediction model gives below:

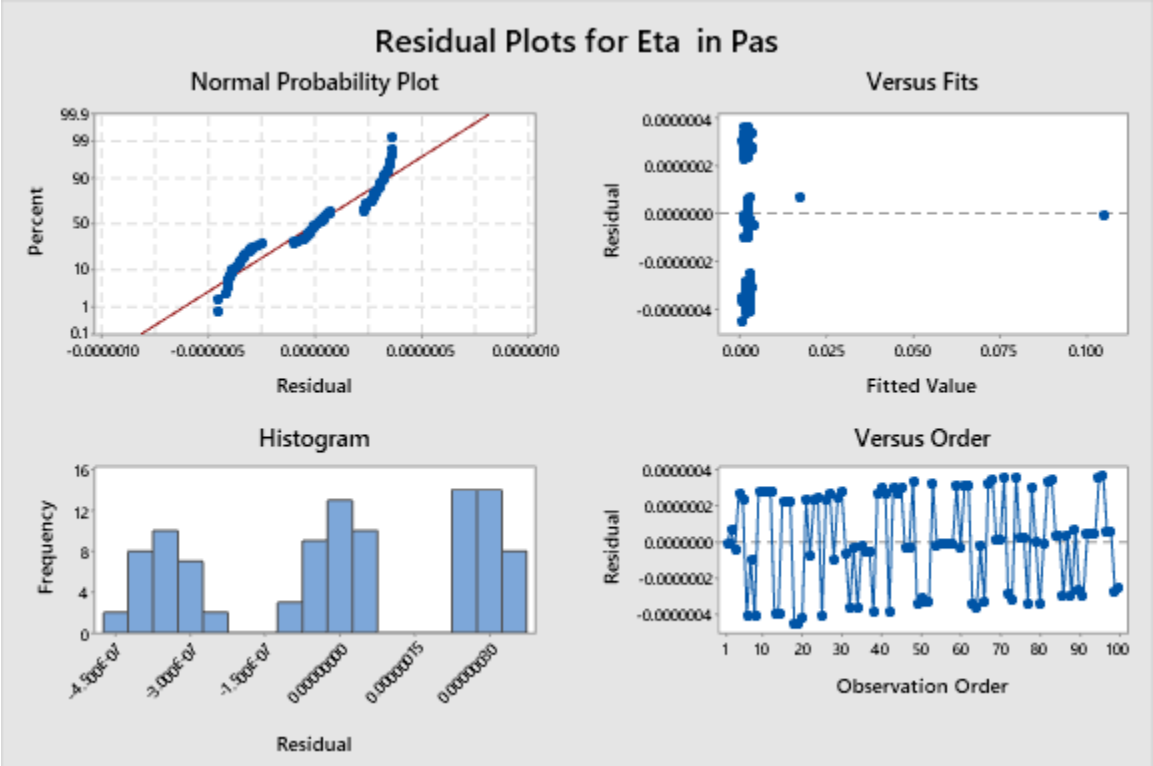

Figure4.72: Residual Plots for 0.5% Graphene Oxide Solution

Regression Equation

Eta in Pas = -0.000006 + 0.009989 Tau in Pa + 0.000000 T in C - 0.000000 t in s

Coefficients

Term	Coef	SE Coef	T-Value	P-Value	VIF
Constant	-0.000006	0.000048	-0.12	0.903	
Tau in Pa	0.009989	0.000000	378031.75	0.000	1.05
T in C	0.000000	0.000002	0.13	0.900	1.51
t in s	-0.000000	0.000000	-1.42	0.158	1.57

Analysis of Variance

Source	DF	Adj SS	Adj MS	F-Value	P-Value
Regression	3	0.010890	0.003630	5.01616E+10	0.000
Tau in Pa	1	0.010342	0.010342	1.42908E+11	0.000
T in C	1	0.000000	0.000000	0.02	0.900
t in s	1	0.000000	0.000000	2.02	0.158
Error	96	0.000000	0.000000		
Total	99	0.010890			

From the variance analysis result, we notice from the P-Value, which is equal to 0 & the F-value, which is larger than the F critical value only for shear stress (Tau), indicating shear stress creates

a significant impact on the regression model. Other factors can be considered null hypotheses as their P-value is larger than 0.05 and F-Value is smaller than the F critical value. We can reject the null hypothesis as it doesn't create any impact on the regression equation.

Durbin-Watson Statistic

Durbin-Watson Statistic =	1.79212

From the Durbin-Watson Statistics, we get the value equal to 1.35, which shows that the Heat Transfer Co-efficient has maintained a decent relationship with the increasing shear stress.

The regression equation is in between shear stress & viscosity: viscosity = 0.000000 + 0.009989 shear stress

Fits and Diagnostics for Unusual Observations

Obs	Eta in Pas	Fit	Resid	Std Resid	
1	0.105490	0.105490	-0.000000	-0.23	X

X Unusual X

Model Summary

S	R-sq	R-sq(adj)	R-sq(pred)
0.0000003	100.00%	100.00%	100.00%

We observe no variation between the predicted line and the observation data from the residual plot. That's why we get our satisfied R-sq value.

4.2.3.4. Viscosity Properties of Graphene Solution:

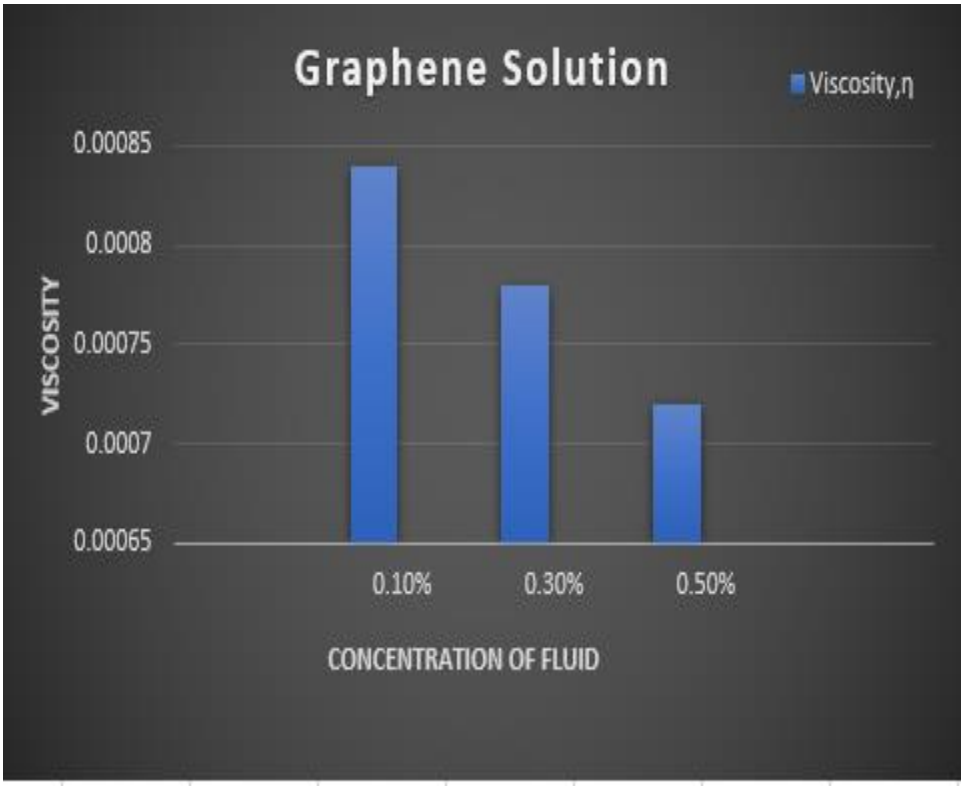

Figure 4.73: Viscosity Bar-chart of Graphene Oxide Solution

From the above figure, as Graphene Oxide nanoparticles' concentration increased, Graphene Oxide nanofluids' viscosity also decreases. So, we found that 0.10% Graphene nanofluid gives the highest value of viscosity. This leads to a decrease in the thickness of the fluid boundary layer, leading to an increase in the heat transfer coefficient.

4.3. Overall result in Heat Transfer Co-efficient:

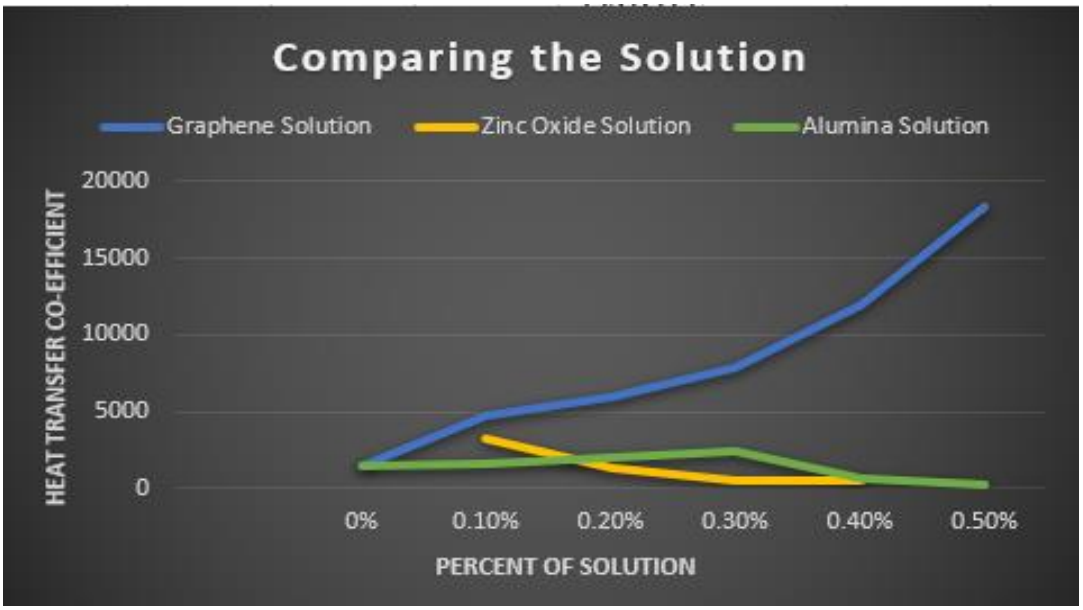

Figure4.74: Overall result in Heat Transfer Co-efficient

From the above figure, we observe that the concentration of Zinc Oxide nanoparticles increased, the heat transfer coefficient of nanofluids decreases, but after a particular time, it again increased. Only 0.1% nanofluid of Zinc Oxide gives a good performance. Other concentrations weren't satisfactory.

The concentration of Aluminum Oxide nanoparticles increased, the heat transfer coefficient of nanofluids has risen, but after a particular time, it decreased. And we found that 0.30% Alumina nanofluid gives the highest value of heat transfer coefficient, the higher than 0.30% Alumina Nanofluid gives a lower value.

When the concentration of nanoparticles increased, the overall heat transfer coefficient values of Graphene also increased. Graphene Oxide shows the best deals among all nanoparticles. So, Graphene Oxide enhances heat transfer more than Alumina and Zinc Oxide.

4.4. Limitations:

1. We could not attain the base fluid to a 100 degree because while carrying from oven to device, it got decreased from 100 degrees.

2. The reservoir shell was not thoroughly heating resistive.

3. The fluid could not come out properly from the outlet.

4. Also, we use the same sample several times, that contamination might happen.

5. Again, the prepared nanofluids were not in 100 percent disperse condition.

CHAPTER 5

Conclusion

Here we can conclude from our result and discussion that nanofluid increases the heat transfer rate and viscosity decreases compare than water or other fluid.

- Al2O3 primarily increases its heat coefficient with the increase of its concentration, after an optimum concentration the heat coefficient decreases with the increase of its concentration. For alumina 0.2% and 0.3 % Alumina gives the best heat coefficient.
- ZnO decreases the heat coefficient with the increase of its concentration. 0.1% ZnO gives the best heat coefficient.
- GO gives the superior heat coefficient. It increases its heat coefficient with the increase of its concentration. 0.5 % gives the best heat coefficient which is the best among the all of our experimental nanofluid sample.

References

Abu-Nada, E., Masoud, Z., & Hijazi, A. (2008). Natural convection heat transfer enhancement in horizontal concentric annuli using nanofluids. *International Communications in Heat and Mass Transfer*, *35*(5), 657-665.

Ahmed, M. A., Shuaib, N. H., & Yusoff, M. Z. (2012). Numerical investigations on the heat transfer enhancement in a wavy channel using nanofluid. *International Journal of Heat and Mass Transfer*, *55*(21-22), 5891-5898.

Hassan, M., Marin, M., Alsharif, A., & Ellahi, R. (2018). Convective heat transfer flow of nanofluid in a porous medium over wavy surface. *Physics Letters A*, *382*(38), 2749-2753.

He, Y., Jin, Y., Chen, H., Ding, Y., Cang, D., & Lu, H. (2007). Heat transfer and flow behaviour of aqueous suspensions of TiO2 nanoparticles (nanofluids) flowing upward through a vertical pipe. *International journal of heat and mass transfer*, *50*(11-12), 2272-2281.

Lotfi, R., Rashidi, A. M., & Amrollahi, A. (2012). Experimental study on the heat transfer enhancement of MWNT-water nanofluid in a shell and tube heat exchanger. *International communications in heat and mass transfer*, *39*(1), 108-111.

Murshed, S. M. S., Leong, K. C., & Yang, C. (2005). Enhanced thermal conductivity of TiO2—water based nanofluids. *International Journal of thermal sciences*, *44*(4), 367-373.

Park, S. S., & Kim, N. J. (2014). A study on the characteristics of carbon nanofluid for heat transfer enhancement of heat pipe. *Renewable energy*, *65*, 123-129.

Sheikholeslami, M., Bandpy, M. G., Ellahi, R., & Zeeshan, A. (2014). Simulation of MHD CuO–water nanofluid flow and convective heat transfer considering Lorentz forces. *Journal of Magnetism and Magnetic Materials*, *369*, 69-80.

Sheikholeslami, M., & Sadoughi, M. K. (2018). Simulation of CuO-water nanofluid heat transfer enhancement in presence of melting surface. *International Journal of Heat and Mass Transfer*, *116*, 909-919.

Heris, S. Z., Etemad, S. G., & Esfahany, M. N. (2006). Experimental investigation of oxide nanofluids laminar flow convective heat transfer. *International communications in heat and mass transfer*, *33*(4), 529-535.

Kumar, R. R., Sridhar, K., & Narasimha, M. (2014). Heat transfer performance in heat pipe using Al2O3-DI water nanofluid. *International Journal of Material and Mechanical Engineering*, *3*, 1-5.

Qi, C., He, Y., Hu, Y., Jiang, B., Luan, T., & Ding, Y. (2013). Experimental study on boiling heat transfer of α-Al2O3-water nanofluid. *Nanoscience and Nanotechnology Letters*, *5*(8), 895-901.

Hong, Y., Wu, W., Hu, J., Zhang, M., Voevodin, A. A., Chow, L., & Su, M. (2011). Controlling supercooling of encapsulated phase change nanoparticles for enhanced heat transfer. *Chemical Physics Letters*, *504*(4-6), 180-184.

Meenakshi, K. S., Sudhan, P. J., Nadu, T., & Nadu, T. (2015). Preparation and characterization of copper oxide-water based nanofluids by one step method for heat transfer applications. *Chem Sci Trans*, *4*, 127-132.

Senthilraja, S., & Vijayakumar, K. C. K. (2013). Analysis of heat transfer coefficient of CuO/water nanofluid using double pipe heat exchanger. *International Journal of Engineering Research and Technology*, *6*(5), 675-680.

Jesumathy, S., Udayakumar, M., & Suresh, S. (2012). Experimental study of enhanced heat transfer by addition of CuO nanoparticle. *Heat and Mass Transfer*, *48*(6), 965-978.

Manimaran, R., Palaniradja, K., Alagumurthi, N., Sendhilnathan, S., & Hussain, J. (2014). Preparation and characterization of copper oxide nanofluid for heat transfer applications. *Applied Nanoscience*, *4*(2), 163-167.

Mosavian, M. H., Heris, S. Z., Etemad, S. G., & Esfahany, M. N. (2010). Heat transfer enhancement by application of nano-powder. *Journal of nanoparticle Research*, *12*(7), 2611-2619.

Nguyen, C. T., Roy, G., Gauthier, C., & Galanis, N. (2007). Heat transfer enhancement using Al2O3–water nanofluid for an electronic liquid cooling system. *Applied Thermal Engineering*, *27*(8-9), 1501-1506.

Nguyen, C. T., Desgranges, F., Galanis, N., Roy, G., Maré, T., Boucher, S., & Mintsa, H. A. (2008). Viscosity data for Al2O3–water nanofluid—hysteresis: is heat transfer enhancement using nanofluids reliable?. *International journal of thermal sciences*, *47*(2), 103-111.

Noie, S. H., Heris, S. Z., Kahani, M., & Nowee, S. M. (2009). Heat transfer enhancement using Al2O3/water nanofluid in a two-phase closed thermosyphon. *International Journal of Heat and Fluid Flow*, *30*(4), 700-705.

Zamzamian, A., Oskouie, S. N., Doosthoseini, A., Joneidi, A., & Pazouki, M. (2011). Experimental investigation of forced convective heat transfer coefficient in nanofluids of Al2O3/EG and CuO/EG in a double pipe and plate heat exchangers under turbulent flow. *Experimental Thermal and Fluid Science*, *35*(3), 495-502.

Yang, L., Mao, M., Huang, J. N., & Ji, W. (2019). Enhancing the thermal conductivity of SAE 50 engine oil by adding zinc oxide nano-powder: an experimental study. *Powder Technology*, *356*, 335-341.

NawazishMehdia, S., Hussain, M. M., Basha, S. K., & Samad, M. A. (2018). Heat enhancement of heat exchanger using aluminium oxide (Al2O3), copper oxide (CuO) nano fluids with different concentrations. *Materials Today: Proceedings*, *5*(2), 6481-6488.

Bhattad, A., Sarkar, J., & Ghosh, P. (2020). Hydrothermal performance of different alumina hybrid nanofluid types in plate heat exchanger. *Journal of Thermal Analysis and Calorimetry*, *139*(6), 3777-3787.

Kumar, M. S., Vasu, V., & Gopal, A. V. (2016). Thermal conductivity and rheological studies for Cu–Zn hybrid nanofluids with various basefluids. *Journal of the Taiwan Institute of Chemical Engineers*, *66*, 321-327.

Salari, E., Peyghambarzadeh, M., Sarafraz, M., & Hormozi, F. (2016). Boiling heat transfer of alumina nano-fluids: role of nanoparticle deposition on the boiling heat transfer coefficient.

Joseph, A., Mohan, S., Kumar, C. S., Mathew, A., Thomas, S., Vishnu, B. R., & Sivapirakasam, S. P. (2019). An experimental investigation on pool boiling heat transfer enhancement using sol-gel derived nano-CuO porous coating. *Experimental Thermal and Fluid Science, 103, 37-50.*

Jesumathy, S., Udayakumar, M., & Suresh, S. (2012). Experimental study of enhanced heat transfer by addition of CuO nanoparticle. *Heat and Mass Transfer*, *48*(6), 965-978.

Luna, I. Z., Chowdhury, A. S., Gafur, M. A., & Khan, R. A. (2015). Measurement of forced convective heat transfer coefficient of low volume fraction CuO-PVA nanofluids under laminar flow condition. *American J. of Nanomaterials*, *3*(2), 64-67.

Luna, I. Z., Chowdhury, S., Gafur, M. A., Khan, N., & Khan, R. A. (2015). Preparation and characterization of CuO-PVA nanofluids for heat transfer applications. *Journal of Chemical Engineering and Chemistry Research*, *2*(5), 607-615.